

SOUTHWEST RESEARCH INSTITUTE

POST OFFICE DRAWER 28510 • 6220 CULEBRA ROAD • SAN ANTONIO, TEXAS, USA 78284 • (512) 684-5111 • TELEX 244846

August 15, 1987

TO: Mr. Craig A. Harvey, Project Officer
Emission Control Technology Division
Environmental Protection Agency
2565 Plymouth Road
Ann Arbor, Michigan 48105

FROM: E. Robert Fanick and Charles T. Hare
Department of Emissions Research
Southwest Research Institute
6220 Culebra Road
San Antonio, Texas 78284

SUBJECT: Final Report for Work Assignment No. B-8, Contract 68-03-3353,
"Catalyst Evaluation (Cert. FY 87)," SwRI Project 03-1193-008

This work assignment was intended to evaluate the condition of catalysts removed from in-use vehicles. The catalysts were removed by EPA from 1983 Model Year In-Use Technology Assessment (IUTA) vehicles, and one low-mileage in-use vehicle. Eleven catalysts were analyzed under this work assignment. The catalysts represented monolith technology. Catalysts used by several different manufacturers were included in the evaluation. The catalysts were either three-way or three-way plus oxidation catalysts, with dual biscuits.

This letter report, along with the included data, is intended to be the final report of the results from the catalyst evaluation testing. It includes all the results from the laboratory analyses by whole converter x-ray, BET surface area, x-ray fluorescence (XRF), proton induced x-ray emission (PIXE), and x-ray diffraction (XRD). Only a brief discussion of the analytical procedure, and no discussion of the trends observed in the evaluation of each catalyst, is included. A total of 11 converters (4 whole and 7 partial samples) were examined. A list of the converters evaluated in the program is presented in Table 1. Only two of the converters underwent whole catalyst x-ray; two had been x-rayed in a previous work assignment (A254/0037 and A254/0191). Of the eleven converters, two underwent XRF, XRD, and PIXE of the rear biscuit, and nine received all of the analytical procedures. Only the rear biscuits were analyzed by XRF. A detailed description of the laboratory analytical procedures is presented in the final reports for Work Assignments No. 10 and 17 of Contract 68-03-3162, with the exception of PIXE.

L Laboratory Analysis

The laboratory analysis of the catalyst samples consisted of whole converter x-ray, BET surface area, x-ray fluorescence (XRF), PIXE, and x-ray diffraction (XRD). The catalyst samples were examined as follows:

1. Only whole converters were examined by whole converter x-ray radiographs.



SAN ANTONIO, TEXAS
DALLAS, TEXAS • DETROIT, MICHIGAN • HOUSTON, TEXAS • WASHINGTON, DC

TABLE 1. LIST OF CATALYSTS FOR EVALUATION

<u>Converter Number</u>	<u>Manufacturer</u>	<u>Engine Family</u>	<u>Type of Catalyst</u>
A221/0198	Chrysler	DCR2.2V2HAC3	Dual biscuit 3W-OX
A221/0310	Chrysler	DCR2.2V2HAC3	Dual biscuit 3W-OX
A280/0005L	Chrysler	ECR2.2V2HAC4	Dual biscuit 3W-OX
A220/0400	GM	D4G3.8V2NEA3	Dual biscuit 3W-OX
A230/0649	GM	D1G2.0V2XAJ4	Dual biscuit 3W
A230/0734	GM	D1G2.0V2XAJ4	Dual biscuit 3W
A246/0092	GM	D1G3.8V2NDA4	Dual biscuit 3W-OX
A240/0007	Ford	DFM1.6V2GDK6	Dual biscuit 3W-OX
A240/0270	Ford	DFM1.6V2GDK6	Dual biscuit 3W-OX
A254/0037	Toyota	DTY2.4V5FBB2	Dual biscuit 3W-OX
A254/0191	Toyota	DTY2.4V5FBB2	Dual biscuit 3W-OX

2. The whole converters were visually inspected, weighed with and without any heat shields, and then carefully cut to expose the catalyst material. All catalyst samples were visually inspected and weighed.
3. Each converter was disassembled in a manner to expose the catalyst material with a minimum of disturbance.
 - a. In step one, the catalyst was sectioned into quarter pieces. The upstream biscuit of the catalytic converter was sectioned as pictured in Figure 1. Each quarter has a length "L" the same as the length of the original uncut biscuit, but a height and width half of the original height and width ($1/2H$ and $1/2W$).
 - b. In step two, one of the quarter sections was further sectioned into three pieces as shown in Figure 1. The front piece had a length of 0.5 inch, the rear piece had a length of 1.0 inch, and the middle piece had a length of "L - 1.5 inches." From the center of the middle piece, a 0.5-inch sample was taken. Each of these three 0.5-inch samples underwent surface area analysis. The opposite quarter was submitted in its entirety for (XRD) analysis. Samples were scraped from an area no larger than 0.25 cubic inches along the center line of the catalyst. One sample each was taken 1 inch from the front and rear faces, and the third sample was taken at the midpoint of the length of the substrate and 0.5 inch from the outside surface.
 - c. Two of the quarter sections shown in Figure 1 were not subjected to any immediate analysis when a whole catalyst was supplied. These samples were kept as additional material for future analysis. Partial catalyst samples were sectioned starting with step two.
 - d. The downstream biscuit was sectioned by cutting the substrate into quarters similar to the upstream substrate. One sample each was taken 0.5 inch from the front face and the rear face as shown in Figure 2. Each of these two pieces underwent BET surface area analysis. The remaining middle section was submitted for XRD. The XRD samples from the B biscuit were scraped from an area no larger than 0.25 cubic inch along the center line and 1.0 inch from the front face. This was the only sample for XRD from the B biscuit. The entire quarter section positioned diagonally from the section used for BET surface area analysis was used for PIXE analysis. The remaining two quarter sections from the four whole converters (when provided) did not undergo analysis at this time, but were saved for future work.

A. Sample Identification

For the purpose of identifying the converters analyzed in this program, each converter was designated with the seven or eight digit EPA identification code. Once the converters were opened, the upstream biscuit was labeled "A," and the downstream biscuit was labeled "B." Each quarter section from the A biscuit was designated according to its location within the can (UL-upper left, UR-upper right, LL-lower left, LR-lower right). The samples for BET surface area and PIXE were

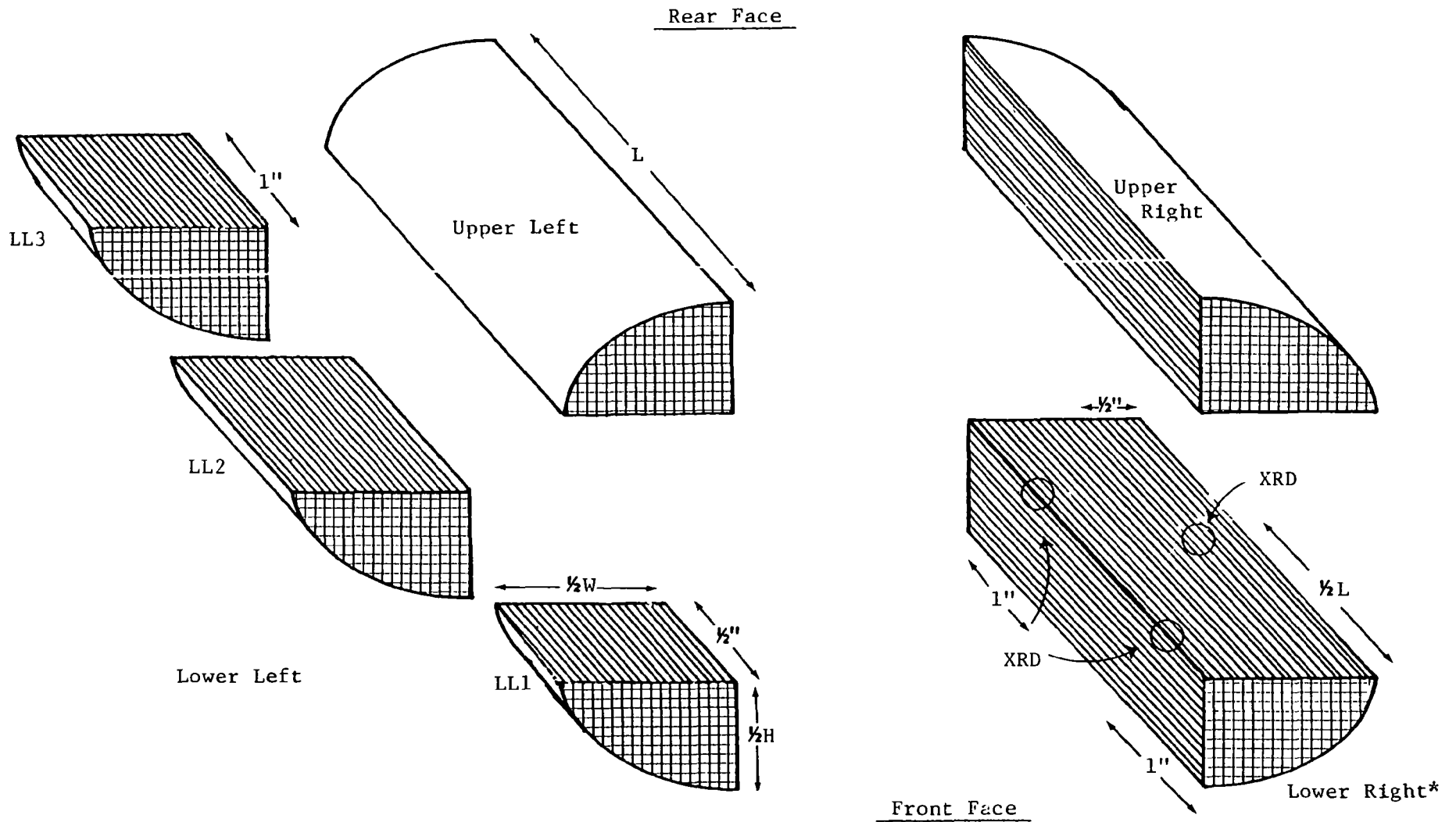


FIGURE 1. SAMPLE SECTIONS AND SAMPLE LOCATION FOR UPSTREAM (A) BISCUIT

*Sample location for XRD shown on lower right quarter for clarity. Actual sample location from upper right quarter.

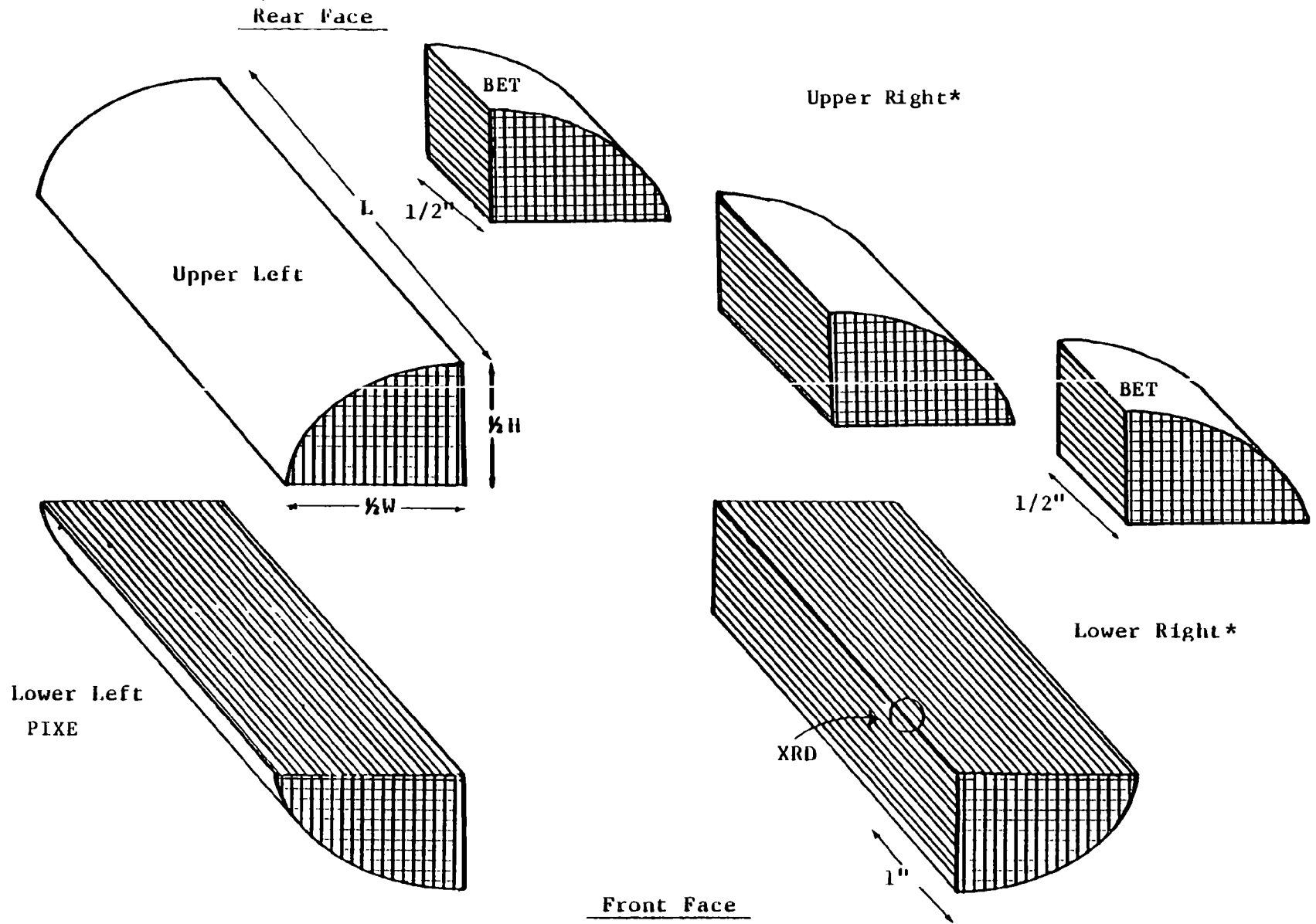


FIGURE 2. SAMPLE SECTIONS AND SAMPLE LOCATIONS FOR DOWNSTREAM (B) BISCUIT

*Sample location for XRD shown on lower right quarter for clarity. Actual sample location from upper right quarter.

also designated with respect to their locations in the biscuit. The location along the length of the quarter section was labeled 1, 2, or 3, respectively, for the upstream, middle, or downstream position. The exception to this rule was for the B biscuit; no middle sample was taken for the BET surface area analysis. In this case, "2" indicated the downstream location. The labeling designations are listed in Table 2. The term "biscuit" is used to refer to each individual piece of ceramic honeycomb material in a converter.

B. Whole Catalyst X-Ray

Two of the converters were examined by whole catalyst x-ray (A280/0005L and A246/0092). The other two whole converters in this work assignment (A254/0037 and A254/0191) were examined by whole catalyst x-ray in Work Assignment No. 20 of EPA Contract 68-03-3192. The radiographs taken in this work assignment are included in Appendix A. Both converters appear normal. Converter A246/0092 had several couplings welded to the outside of the case with thermocouple connectors. Upon careful examination, the positions of the holes drilled for the thermocouples can be observed in the radiographs.

C. Sample Weighing

The weights of the various samples were determined in several stages. All of the whole converters were weighed whole, and each biscuit was weighed after opening. All of the partial samples were weighed, but these weights are only a determination of the amount of sample received. In order to do additional calculations on these converters, the weights of the biscuits before the samples were taken must be known or estimated. All of the weights are presented in Table 3.

D. Visual Inspection

Each whole converter and biscuit was inspected for visual signs of overheating or damage. Catalyst A230/0734-A was severely melted. A large void had developed about two inches from the front face. This was the only visible example of melting in this work assignment. Several samples had developed cracks. They were: A221/0310-A, A220/0400-B, A230/0649-A&B, A230/0734-B, A246/0092-A&B, and A240/0270. Catalyst A246/0092 had been drilled in an effort to place thermocouples into the center of the biscuit. All of the catalysts showed typical signs of usage (dark front faces with rust on outer surfaces).

E. Specific Surface Area

The specific surface areas of the whole length of all biscuits were measured with a Micromeritics Flowsorb II dynamic surface area analyzer using the multipoint analysis technique. This analysis was conducted "in-house" during this Work Assignment. The advantages for "in-house" analysis include a stricter control of the analytical procedures, ease of repeating questionable samples, and assurance that the analysis is performed on a sample that represents the entire length of the biscuit. Losses in surface area are due to thermal degradation and/or plugging of the sub-microscopic pores with metals and other deposits. A loss in the active surface area results in the reduction of contact between exhaust gases and the catalyst material. A low surface area generally indicates converter overheating.

TABLE 2. LABELING PROCEDURE CODE

<u>Code</u>	<u>Description</u>
A	Upstream biscuit
B	Downstream biscuit
UL	Upper left portion of biscuit
UR	Upper right portion of biscuit
LI.	Lower left portion of biscuit
LR	Lower right portion of biscuit
1	Upstream piece of section
2	Middle piece of section or downstream when no middle piece taken
3	Downstream piece of section

TABLE 3. CONVERTER WEIGHTS

Converter Number	Whole Converter, lbs.	Biscuit Weights, g	
		Upstream (A)	Downstream (B)
A221/0198	--	264.4/277.8	112.4/108.3
A221/0310	--	257.3/229.0	116.3/110.4
A280/0005L	10.00	1121.6	463.1
A220/0400	--	216.3/237.7	155.6/149.0
A230/0649	--	188.4/197.5	145.5/144.0
A230/0734	--	189.0/192.2	138.5/155.5
A246/0092	11.37	865.7	731.0
A240/0007	--	106.9/104.9	144.6/144.5
A240/0270	--	99.9/103.5	135.4/152.0
A254/0037	9.65	797.5	838.6
A254/0191	11.58	794.0	790.00

Note: Converters A280/0005L, A246/0092, A254/0037, and A254/0191 were whole converters. All others represent lengthwise quarters. The first listed weight represents the lower left portion and the second weight represents the upper right portion.

Conversely, a normal surface area does not necessarily indicate a normal catalyst, because the deposits can increase the apparent surface area while covering the surface and preventing contact with the exhaust gases. In this work assignment, the surface area of 0.5 inch pieces from the front, middle, and rear of the upstream biscuit and the surface area from the front and rear pieces of the downstream biscuit were analyzed. These large wedges were placed in a large sample tube and analyzed whole. The sample tube consisted of a large tube with a ground glass joint in the middle, or the sample was entirely sealed in glass. Either method was equally effective, except the tube with the ground glass joint experienced a problem with breakage. In order to eliminate this problem, all subsequent samples were sealed in glass.

Upon completion of the analysis of the LL1 piece, the sample was ground to a coarse powder (approximately 100 mesh). This sample was also analyzed for surface area. The results for the specific surface areas are presented in Table 4. The plots for the BET equation versus the relative pressure for each converter are included in Appendix B.

F. X-Ray Diffraction

X-ray diffraction analysis of the samples was used to determine the crystal structure of the alumina. Gamma-alumina and several other very similar alumina structures are the original crystal structures used in the alumina washcoat. When a catalyst containing these types of alumina is overheated (temperatures greater than 1000°C), the crystal structure changes to the alpha-alumina form. This conversion in crystal structure can trap the active metals and change the active surface area of the catalyst. The Debye-Scherrer powder x-ray diffraction technique was used to determine the alumina crystal structure. This technique is well suited for the analysis of monolith catalysts because of the small quantities of sample required. In the case of monolith catalysts, the alumina is deposited as a thin wash-coat on the surface of the ceramic substrate. The alumina can be scraped off carefully and analyzed. The x-rays are diffracted by the various crystalline compounds within the sample. Each crystalline compound has a characteristic diffraction pattern. Amorphous compounds do not result in a diffraction pattern. These patterns are compared to known compounds in a Powder Data File for identification. Table 5 lists the alumina crystal structure of each sample and any other crystalline compounds observed in the samples.

G. Proton Induced X-Ray Emission

Proton induced x-ray emission (PIXE) was used to determine the concentrations of noble metals and the accumulation of poisons. This technique utilized protons to "knock" electrons from the inner orbital shells. The electron removal causes the element to fluoresce x-rays at characteristic wavelengths. These fluoresced x-rays are detected, and they represent the quantity of each element present in the sample.

The elements of concern were phosphorus (P), sulfur (S), calcium (Ca), manganese (Mn), zinc (Zn), lead (Pb), platinum (Pt), palladium (Pd), rhodium (Rh), and nickel (Ni). The elements P, S, Ca, Mn, Zn, and Pb are poisons or contaminants. They are derived from engine wear, dirt deposits, oil, fuel, and other sources. The noble metals are Pt, Pd, and Rh, and they perform the function of "cleaning up" the exhaust. Nickel was found in some converters, and is reportedly present to enhance

TABLE 4. CATALYST SPECIFIC SURFACE AREA

Biscuit No.	Specific Surface Area, m ² /g						Total Surface Area for Whole Biscuit,* m ²	
	Front Biscuit(A)				Rear Biscuit(B)		Front	Rear
	LL1	LL2	LL3	Powder	UR1	UR2		
A221/0310	2.3	2.7	3.5	3.8	4.9	5.1	2800	2300
A280/0005L	6.6	3.6	3.0	7.8	5.1	6.6	4900	2700
A220/0400	10.5	15.4	9.2	12.0	7.0	7.1	10600	4300
A230/0649	5.0	12.4	12.5	8.6	9.8	9.1	7700	5500
A246/0092	7.8	15.4	15.7	8.9	10.6	7.9	11200	6800
A240/0007	15.2	14.2	22.8	17.0	3.9	5.8	7400	2800
A240/0270	5.9	8.1	10.9	8.7	5.0	5.7	3400	3100
A254/0037	6.4	7.4	6.5	7.7	7.4	7.0	5400	6000
A254/0191	9.7	8.5	10.1	11.3	8.1	8.8	7500	6700

*Total biscuit surface area based on average of surface area and total weight of biscuit. For partial samples, the total weight of the biscuit was estimated based on the amount of sample received. The partial samples were A221/0310, A220/0400, A240/0007, and A240/0270.

TABLE 5. ALUMINA CRYSTAL STRUCTURE BY X-RAY DIFFRACTION

Biscuit Numbers	Alumina Crystal Structure and Other Crystalline Structures Found		
	Front Face (UR1)	Middle Outer Edge (UR2)	Rear Face (UR3)
A221/0198-A	intermediate alumina (gamma, delta, or theta) with trace of CeO ₂ or ZnS and AlPO ₄	intermediate alumina (gamma, delta, or theta) with CeO ₂ or ZnS	intermediate alumina (gamma, delta, or theta) with CeO ₂ or ZnS
A221/0198-B	intermediate alumina (gamma, delta, or theta)		
A221/0310-A	mostly alpha alumina with some theta, possible unidentified phosphate phases and CeO ₂ or ZnS	intermediate alumina (probably theta) with CeO ₂	intermediate alumina (probably theta) with CeO ₂
A221/0310-B	intermediate alumina (probably theta)		
A280/0005L-A	mostly theta alumina with CeO ₂	mostly theta alumina with trace of alpha with CeO ₂	intermediate alumina (gamma or delta) with CeO ₂
A280/0005L-B	intermediate alumina (gamma or delta)		
A220/0400-A	intermediate alumina (probably gamma) with NiO and CeO ₂ or ZnS, trace of AlPO ₄ and Ni, possible spinel cubic NiAl ₂ O ₄	intermediate alumina (probably gamma) with NiO and CeO ₂ , possible spinel cubic NiAl ₂ O ₄	intermediate alumina (probably gamma) with NiO and CeO ₂ , possible spinel cubic NiAl ₂ O ₄
A220/0400-B	intermediate alumina (probably theta)		
A230/0649-A	intermediate alumina (probably gamma or mixture of gamma and delta)	intermediate alumina (probably gamma or mixture of gamma and delta)	intermediate alumina (probably gamma or mixture of gamma and delta)
A230/0649-B	intermediate alumina (gamma) with CeO ₂		
A230/0734-A	mostly gamma alumina with possible AlPO ₄	mostly alpha alumina	mostly alpha alumina
A230/0734-B	mostly alpha alumina		
A246/0092-A	mostly gamma alumina with NiO	mostly gamma alumina with NiO	mostly gamma alumina with NiO
A246/0092-B	mostly theta alumina		
A240/0007-A	intermediate alumina (gamma, delta, or theta) with NiO and possible Ni	intermediate alumina (gamma, delta, or theta) with NiO and possible Ni	intermediate alumina (gamma, delta, or theta) with NiO and possible Ni
A240/0007-B	intermediate alumina (gamma, delta, or theta) with possible CeO ₂		
A240/0270-A	intermediate alumina with spinel cubic NiAl ₂ O ₄ , possible NiO and trace of AlPO ₄	intermediate alumina with spinel cubic NiAl ₂ O ₄ , possible NiO and CeO ₂ or ZnS	intermediate alumina with spinel cubic NiAl ₂ O ₄ , possible NiO and CeO ₂
A240/0270-B	intermediate alumina with CeO ₂		
A254/0037-A	mostly delta alumina with CeO ₂ or ZnS, possible NiO	mostly delta alumina with CeO ₂ , possible NiO and CeAlO ₃	mostly delta alumina with CeO ₂ , possible NiO and CeAlO ₃
A254/0037-B	mostly delta alumina with CeO ₂		
A254/0191-A	mostly delta alumina with CeO ₂ or ZnS	mostly delta alumina with CeO ₂ , possible NiO and CeAlO ₃	mostly delta alumina with CeO ₂ , possible NiO and CeAlO ₃
A254/0191-B	mostly delta alumina with CeO ₂ , possible CeAlO ₃		

the catalytic activity. Aluminum (Al), silicon (Si), and magnesium (Mg) are major constituents of the support material, and were not quantitatively determined. The minor constituents such as sodium (Na), potassium (K), titanium (Ti), iron (Fe), cerium (Ce), and barium (Ba) were also not quantified. The elements Na, K, and Ti are present in small amounts from the clays used to make the cordierite ceramic. Titanium is also probably present in the converters as a whitening agent for the ceramic substrate. Cerium was added to inhibit the conversion of gamma-alumina with a higher surface area to alpha alumina with a lower surface area at the elevated temperatures experienced within the converters, and also to increase the catalytic activity of the converter when present in concentrations of one percent or more. Iron was probably from the engine, as a wear product, the exhaust system due to rust, or as an impurity in the ceramic substrate. Barium was also found in some of the samples.

The samples were prepared by grinding the entire pieces to a coarse powder (approximately 50 mesh). Approximately 10 grams of the coarse powder were taken and ground in its entirety to a very fine powder (400 mesh). The analysis was conducted by Dr. Sene Bauman, Element Analysis Corporation. Matrix corrections and data analysis were performed at Elemental Analysis Corporation and reviewed by SwRI.

The weight percentages of each element are included in Table 6. Where the concentration of an element was at the detection limit of the analytical procedure, the word "trace" was used, and an asterisk (*) was used to identify those elements with concentrations below the detection limit. Table 6 also includes the other elements found in each sample which were not quantified.

H. X-Ray Fluorescence

In addition to PIXE, a sample from the rear biscuit was also analyzed by x-ray fluorescence. This technique uses x-rays as the incident radiation rather than protons to cause the characteristic x-rays to fluoresce for each element. The samples were prepared using the sample procedure described for PIXE. The samples were sent to Mr. Frank Black, EPA, Research Triangle Park, and analyzed by Mr. Robert Kellog, Northrup Services, Inc. Matrix connections and data analysis were performed at Northrup Services, Inc. and reviewed by SwRI. The data are summarized in Table 7, and the individual results are included in Appendix C.

L. Miscellaneous

In Work Assignment No. 20 of EPA Contract 68-03-3192, the normalized weight percent ratios were calculated for P, S, Ca, Mn, Pb, and Si from the SEM/EDX spectra. Zinc was not included in that work assignment. The data were resurrected in order to calculate the normalized weight percent ratios for zinc. Each element was normalized to the aluminum concentration in each sample. The data are summarized in Table 8.

IV. Quality Assurance and Correlation

The quality assurance plan for this work assignment is covered under sections 1 and 2D-11D of the Quality Assurance Plan for Contract 68-03-3353 "Emission Characterization and Control Studies for ECTD." This document discusses in detail project organization, responsibility, objectives, procedures, sample custody, control checks, preventive maintenance, and other aspects of the program to assure the

TABLE 6. ELEMENTAL ANALYSIS OF NOBLE METALS AND POISONS BY PIXE

Biscuit Number	Sample Location	Weight Percent of Element										Others
		P	S	Ca	Mn	Ni	Zn	Rh	Pd	Pt	Pb	
A221/0198-B	LL	*	0.07±0.02	0.06±0.01	0.01±0.0004	trace	0.02±0.0002	*	0.17±0.002	*	0.02±0.001	Na, Mg, Al, Si, Ti, Fe
A221/0310-A	LL1	1.7±0.5	*	0.13±0.01	0.07±0.003	0.04±0.001	0.46±0.001	trace	0.02±0.01	0.11±0.01	4.15±0.01	Mg, Al, Si, K, Ti, Fe, Ce
	LL2	0.44±0.04	0.06±0.03	0.06±0.01	0.02±0.002	0.02±0.0003	0.07±0.0003	0.01±0.003	*	0.13±0.004	0.44±0.002	Na, Mg, Al, Si, Ti, Fe, Ce
	LL3	0.11±0.05	0.08±0.02	0.06±0.01	0.01±0.002	0.01±0.0003	0.03±0.0003	0.01±0.003	*	0.10±0.003	0.19±0.002	Na, Mg, Al, Si, Ti, Fe, Ce
A221/0310-B	LL	*	0.06±0.02	0.04±0.01	0.01±0.0005	trace	0.02±0.0002	*	0.15±0.004	*	0.74±0.002	Na, Mg, Al, Si, Ti, Fe
A280/0005L-A	LL1	2.01±0.05	0.13±0.03	0.03±0.01	0.13±0.003	0.02±0.0004	0.63±0.001	0.01±0.004	*	0.08±0.01	0.31±0.003	Na, Mg, Al, Si, K, Ti, Fe, Ce
	LL2	0.41±0.06	0.06±0.03	0.08±0.01	0.02±0.001	0.01±0.0003	0.07±0.0004	0.01±0.002	*	0.08±0.003	0.04±0.001	Na, Mg, Al, Si, K, Ti, Fe, Ce
	LL3	0.19±0.05	0.17±0.02	0.07±0.02	0.02±0.002	trace	0.05±0.0003	0.01±0.0003	*	0.14±0.003	0.01±0.001	Na, Mg, Al, Si, K, Ti, Fe, Ba, Ce
A280/0005L-B	LL	trace	0.16±0.02	0.13±0.01	*	*	0.11±0.0002	*	0.39±0.002	0.01±0.003	0.20±0.001	Na, Mg, Al, Si, K, Ti, Fe
A220/0400-A	LL1	1.51±0.04	0.10±0.04	0.00±0.01	0.03±0.003	1.50±0.001	0.33±0.002	0.02±0.01	0.06±0.003	0.04±0.01	2.38±0.01	Na, Mg, Al, Si, K, Ti, Fe, Ba, Ce
	LL2	0.66±0.04	0.23±0.03	0.03±0.02	0.01±0.003	2.02±0.001	0.04±0.001	0.02±0.01	0.05±0.01	0.04±0.01	0.36±0.003	Na, Mg, Al, Si, K, Ti, Fe, Ba, Ce
	LL3	0.14±0.05	0.22±0.02	0.06±0.02	trace	1.61±0.001	0.04±0.001	0.02±0.01	0.05±0.01	0.04±0.004	0.11±0.002	Na, Mg, Al, Si, K, Ti, Fe, Ba, Ce
A220/0400-B	LL	0.14±0.03	0.15±0.02	0.10±0.01	0.01±0.0004	0.01±0.0002	0.01±0.0002	*	0.01±0.001	0.17±0.002	0.18±0.001	Na, Mg, Al, Si, Ti, Fe
A230/0649-A	LL1	1.61±0.04	0.18±0.04	0.24±0.02	0.02±0.002	0.05±0.0004	0.52±0.001	trace	0.05±0.001	0.11±0.01	0.61±0.003	Na, Mg, Al, Si, K, Ti, Fe, Ce
	LL2	0.47±0.05	0.07±0.03	0.07±0.02	trace	0.02±0.0003	0.03±0.0003	0.01±0.003	0.05±0.003	0.11±0.003	0.03±0.002	Na, Mg, Al, Si, K, Ti, Fe, Ce
	LL3	0.13±0.05	0.12±0.03	0.05±0.02	*	0.03±0.0003	0.02±0.0003	0.02±0.003	0.05±0.004	0.11±0.002	0.03±0.002	Na, Mg, Al, Si, K, Ti, Fe, Ce
A230/0649-B	LL	trace	0.17±0.03	0.08±0.02	*	0.01±0.0003	0.02±0.0004	0.02±0.002	0.06±0.003	0.16±0.003	0.04±0.002	Na, Mg, Al, Si, Ti, Fe, Ce
A230/0734-B	LL	0.14±0.04	0.17±0.02	0.10±0.02	*	0.01±0.0004	0.03±0.0004	0.03±0.001	0.09±0.004	0.20±0.003	0.01±0.002	Na, Mg, Al, Si, Ti, Fe, Ce
A246/0092-A	LL1	1.45±0.04	0.46±0.03	0.06±0.01	0.03±0.003	1.96±0.001	0.12±0.001	0.02±0.004	0.04±0.004	0.08±0.01	0.73±0.01	Na, Mg, Al, Si, K, Ti, Fe, Ba, Ce
	LL2	0.36±0.04	0.58±0.02	0.04±0.01	trace	2.80±0.001	0.02±0.001	0.03±0.001	0.05±0.002	0.11±0.004	0.14±0.001	Na, Mg, Al, Si, K, Ti, Fe, Ba, Ce
	LL3	0.12±0.04	0.66±0.02	0.05±0.01	*	3.13±0.002	0.02±0.001	0.03±0.01	0.06±0.003	0.13±0.005	0.06±0.003	Na, Mg, Al, Si, K, Ti, Fe, Ba, Ce
A246/0092-B	LL	trace	0.74±0.02	0.06±0.01	0.01±0.001	0.02±0.0003	0.01±0.0003	*	0.04±0.002	0.29±0.002	0.04±0.001	Na, Mg, Al, Si, Ti, Fe, Ba
A240/0007-A	LL1	2.33±0.05	0.57±0.03	0.05±0.02	0.05±0.003	2.11±0.001	0.28±0.001	0.03±0.01	*	0.11±0.01	0.38±0.004	Na, Mg, Al, Si, K, Ti, Fe, Ba, Ce
	LL2	0.87±0.05	0.49±0.03	0.04±0.01	0.02±0.002	1.75±0.001	0.06±0.001	0.02±0.01	*	0.08±0.004	0.09±0.002	Na, Mg, Al, Si, K, Ti, Fe, Ba, Ce
	LL3	0.17±0.05	0.26±0.03	0.04±0.01	0.01±0.001	0.70±0.0004	0.01±0.0004	0.01±0.002	*	0.04±0.002	0.01±0.001	Na, Mg, Al, Si, K, Ti, Fe, Ba, Ce
A240/0007-B	LL	0.25±0.04	0.56±0.02	0.07±0.01	0.01±0.002	0.20±0.0003	0.09±0.0004	*	0.07±0.0007	0.12±0.004	0.08±0.002	Na, Mg, Al, Si, Ti, Fe, Ce
A240/0270-A	LL1	2.02±0.05	0.20±0.03	0.13±0.02	0.08±0.003	2.81±0.001	0.52±0.001	0.02±0.005	*	0.07±0.02	0.84±0.01	Na, Mg, Al, Si, K, Ti, Fe, Ce
	LL2	1.25±0.04	0.17±0.03	0.08±0.02	0.05±0.004	4.92±0.002	0.16±0.002	0.03±0.004	*	0.13±0.01	0.32±0.01	Na, Mg, Al, Si, K, Ti, Fe, Ce
	LL3	0.46±0.05	0.09±0.03	0.07±0.02	0.02±0.002	2.02±0.001	0.05±0.001	0.01±0.004	*	0.05±0.01	0.10±0.003	Na, Mg, Al, Si, K, Ti, Fe, Ce
A240/0270-B	LL	0.16±0.04	0.14±0.02	0.05±0.01	0.01±0.001	0.07±0.002	0.03±0.0003	*	0.04±0.002	0.05±0.002	0.05±0.001	Na, Mg, Al, Si, Ti, Fe, Ce
A254/0037-A	LL1	1.75±0.04	0.35±0.03	0.15±0.01	0.12±0.004	0.01±0.0004	0.21±0.001	0.05±0.004	*	0.24±0.01	0.41±0.003	Na, Mg, Al, Si, K, Ti, Fe, Ba, Ce
	LL2	0.34±0.04	0.86±0.03	0.08±0.02	0.01±0.005	0.01±0.0004	0.02±0.0004	0.03±0.005	*	0.24±0.004	0.06±0.002	Na, Mg, Al, Si, K, Ti, Fe, Ba, Ce
	LL3	0.16±0.05	0.83±0.03	0.08±0.02	0.01±0.004	0.01±0.0004	0.02±0.0004	0.03±0.004	*	0.22±0.004	0.03±0.002	Na, Mg, Al, Si, K, Ti, Fe, Ba, Ce
A254/0037-B	LL	trace	1.49±0.03	0.10±0.02	*	*	0.03±0.0001	0.07±0.01	*	0.42±0.004	0.04±0.002	Na, Mg, Al, Si, K, Fe, Ba, Ce
A254/0191-A	LL1	1.45±0.04	1.06±0.04	0.09±0.02	0.04±0.01	0.02±0.001	0.21±0.001	0.03±0.01	*	0.25±0.01	0.87±0.01	Na, Mg, Al, Si, K, Ti, Fe, Ba, Ce
	LL2	0.34±0.05	0.89±0.03	0.07±0.02	*	trace	0.03±0.005	0.03±0.01	*	0.22±0.004	0.18±0.003	Na, Mg, Al, Si, K, Ti, Fe, Ba, Ce
	LL3	0.12±0.05	1.01±0.03	0.07±0.02	*	trace	0.01±0.0004	0.02±0.004	*	0.20±0.003	0.06±0.002	Na, Mg, Al, Si, K, Ti, Fe, Ba, Ce
A254/0191-B	LL	*	1.40±0.03	0.09±0.02	*	*	0.04±0.0007	0.05±0.007	*	0.53±0.01	0.09±0.003	Na, Mg, Al, Si, K, Fe, Ba, Ce

* - below the detection limit
 trace - at the detection limit

TABLE 7. ELEMENTAL ANALYSIS OF CATALYST POISONS BY X-RAY FLUORESCENCE

<u>Biscuit Number</u>	<u>P</u>	<u>S</u>	<u>Ca</u>	<u>Mn</u>	<u>Ni</u>	<u>Zn</u>	<u>Pb</u>	<u>Others</u>
A221/0198-B-LL	0.11±0.01	0.15±0.01	0.24±0.01	trace	trace	0.02±0.001	0.04±0.002	Mg,Al,Si,K,Ti,Fe,Ce,Pt
A221/0310-B-LL	0.07±0.004	0.16±0.01	0.08±0.004	0.01±0.001	trace	0.03±0.002	1.24±0.06	Mg,Al,Si,K,Ti,Fe,Ce,Pt
A280/0005L-B-LL	0.08±0.005	0.13±0.01	0.09±0.005	0.02±0.001	trace	0.06±0.003	0.13±0.01	Na,Mg,Al,Si,K,Ti,Fe,Ba,Ce,Pt
A220/0400-B-LL	0.06±0.004	0.09±0.01	0.08±0.004	trace	0.01±0.0004	0.04±0.002	0.11±0.01	Na,Mg,Al,Si,K,Ti,Fe,Ba,Ce,Pt
A230/0649-B-LL	0.04±0.003	0.13±0.01	0.08±0.004	trace	0.01±0.001	0.01±0.001	0.02±0.001	Mg,Al,Si,K,Ti,Fe,Ba,Ce,Pt
A230/0734-B-LL	0.05±0.003	0.10±0.01	0.09±0.004	trace	0.01±0.0005	0.02±0.001	0.01±0.001	Mg,Al,Si,K,Ti,Fe,Ba,Ce,Pt
A246/0092-B-LL	0.02±0.002	0.56±0.03	0.05±0.003	0.01±0.001	0.01±0.001	0.01±0.001	0.02±0.001	Mg,Al,Si,K,Ti,Fe,Ba,Ce,Pt
A240/0007-B-LL	0.10±0.01	0.36±0.02	0.07±0.004	0.01±0.001	0.10±0.001	0.05±0.003	0.04±0.002	Mg,Al,Si,K,Ti,Fe,Ba,Ce,Pt
A240/0270-B-LL	0.22±0.01	0.30±0.02	0.10±0.005	0.02±0.002	0.13±0.01	0.07±0.004	0.14±0.01	Mg,Al,Si,K,Ti,Fe,Ba,Ce,Pt
A254/0037-B-LL	0.03±0.002	1.01±0.05	0.07±0.004	0.01±0.001	*	0.01±0.001	0.01±0.001	Mg,Al,Si,K,Ti,Fe,Ce,Pt
A254/0191-B-LL	0.03±0.002	0.91±0.05	0.05±0.003	trace	*	0.01±0.001	0.02±0.001	Mg,Al,Si,K,Ti,Fe,Ce,Pt

trace - at detection limit

* - below detection limit

**TABLE 8. SURFACE WEIGHT PERCENT OF ELEMENTS
NORMALIZED TO ALUMINUM**

Biscuit Number	Normalized Weight Percent						
	P	S	Ca	Mn	Pb	Si	Zn
A180/0094	17.40	0.21	3.61	1.24	82.64	0.25	26.13
A193/0908	3.09	2.80	0.54	0.36	1.55	2.84	3.75
A218/0045	15.06	2.04	4.08	0.91	42.56	2.26	26.03
A218/0045X	15.65	10.17	2.48	0.75	34.38	11.44	32.53
A218/0045X*	0.20	0.01	0.04	ND	0.09	0.02	0.07
A218/0068	49.54	2.89	11.04	1.23	155.73	3.42	97.31
A220/0392	3.34	2.09	0.77	0.08	5.17	2.23	3.80
A220/0392*	0.12	0.02	0.01	ND	0.03	0.02	0.02
A220/0810	11.45	0.68	2.95	0.10	8.15	0.80	18.44
A221/0152	10.90	24.96	2.58	5.20	19.51	24.36	20.65
A221/0204	12.64	1.55	2.41	0.24	14.88	1.94	37.71
A221/0447	2.03	2.94	0.28	0.12	13.07	3.14	2.82
A221/0447*	0.03	0.04	0.003	ND	0.02	0.06	0.002
A230/0177X	0.56	0.37	0.09	0.05	0.27	0.42	0.45
A230/0177X*	0.05	0.03	0.01	ND	0.02	0.05	0.03
A230/0636X	1.68	0.23	0.23	0.08	3.09	0.27	1.60
A240/0016L	2.40	0.61	0.35	ND	8.58	0.72	3.62
A240/0016L*	0.45	0.10	0.04	ND	0.87	0.12	0.14
A240/0102	3.47	1.20	1.01	0.08	3.42	1.33	3.93
A240/0141L	6.12	37.62	0.85	4.03	6.20	30.63	7.17
A240/0153	1.71	0.10	0.13	0.27	1.15	0.11	1.02
A240/0334L	0.74	0.41	0.03	0.03	1.46	0.45	0.31
A249/0169-1	1.48	0.58	0.08	0.05	1.08	0.54	0.18
A249/0169-1*	0.05	0.01	0.01	ND	0.04	0.02	0.02
A249/0169-2	1.76	4.04	0.10	0.12	1.83	3.56	0.39
A249/0169-3	1.29	0.41	0.87	ND	14.60	0.56	0.73
A280/0001L	9.04	2.19	2.27	1.68	3.60	2.49	13.21
A155/0941-1	2.64	0.60	0.67	0.51	0.70	0.64	2.15
A155/0941-2	0.72	0.52	0.21	0.07	2.26	0.52	1.32
A207/0101	0.35	0.07	0.01	0.07	0.03	0.08	0.05

*Rear Face of A biscuit for comparison within each engine family
ND - none detected

accuracy and precision of the results presented in this report. A listing of precision, accuracy, and completeness is presented in Table 9. All measurements are representative of the catalyst properties and conditions being measured.

The Micromeritics Flowsorb II dynamic surface area analyzer was set up to analyze the catalyst samples "in-house." Two NBS Standard Reference Materials and seven standards from Duke Scientific Corporation were used to establish the instrument operating range and linearity, as well as confidence in the analytical procedure. In this work assignment, the surface areas were determined with a multipoint technique. A curve was established for the various gas concentrations to determine the calibration knob setting for the instrument (Figure 3). The standards were analyzed using this technique, and the results are given in Table 10. A plot of the BET equation versus the relative pressure for the standards is presented in Appendix D. In general, the standards repeated within the published confidence limits for the entire range of standards ($0.62 \text{ m}^2/\text{g}$ to $265 \text{ m}^2/\text{g}$).

In an effort to correlate the data from this work assignment with previous work assignments, an alternative procedure for preparing the samples for surface area was used. The coarse powder (approximately 50 mesh) from ten samples was analyzed for surface area and compared to the results for the bulk strips which were cut from the center core of the biscuit and analyzed as a single sample. The results for the two sampling techniques are presented in Table 11, and the plots of the BET equation versus the relative pressure are included in Appendix E. The surface areas for the ground samples were lower in all cases except for A220/0810-A, A221/0447-A, and A155/0941-1-A. All three of these samples were from the A biscuits. The A220/0810-A was the only sample from the group which contained alpha alumina. The other two catalysts were from Chrysler vehicles. Ground catalyst samples from the upstream biscuit apparently result in higher surface areas than the unground samples. These results were also observed for front face samples listed in Table 4. No conclusions can be drawn without additional work to confirm the sources of this phenomenon.

In an effort to demonstrate the precision and accuracy for the XRF procedure, a sample analyzed in Work Assignment No. 20 from EPA Contract 68-03-3192 was selected at random and repeated during this work assignment. The results are listed in Table 12 and Figure 4. In general, the current results agreed very well with the previously published results. The largest error was for Ni, but the concentration was so low that the error does not indicate a significant problem. When Ni is excluded, the average percent difference is 0.3 ± 3.8 . Phosphorus and lead values were higher, while sulfur and platinum were lower. The precision and accuracy for XRF depend on the concentration of the elements, the elements present, the homogeneity of the sample, and the size of the particles in the pellet.

V. Summary

In summary, a total of 11 catalysts were examined by whole converter x-ray, x-ray fluorescence, x-ray diffraction, PIXE, and BET surface area analysis. Of these 11 catalysts, 4 were whole converters and 7 were partial catalyst samples. This letter report is a compilation of all of the data available at the time of submittal, and is intended to serve as the final report of the results for the program.

TABLE 9. PRECISION, ACCURACY, AND COMPLETENESS OBJECTIVES

<u>Analytical Procedures</u>	<u>Precision Coeff. of Variation, %</u>	<u>Accuracy</u>	<u>Completeness %</u>
Whole catalyst X-ray	NA ^a	0.02 ^b 2-2T ^c	> 95
X-ray fluorescence	1-3	±15%	> 95
X-ray diffraction	5	±5%	> 95
BET surface area	7	±3%	> 95
PIXE	±5	±5%	95

^aNA = not applicable

^bgeometric unsharpness

^csensitivity

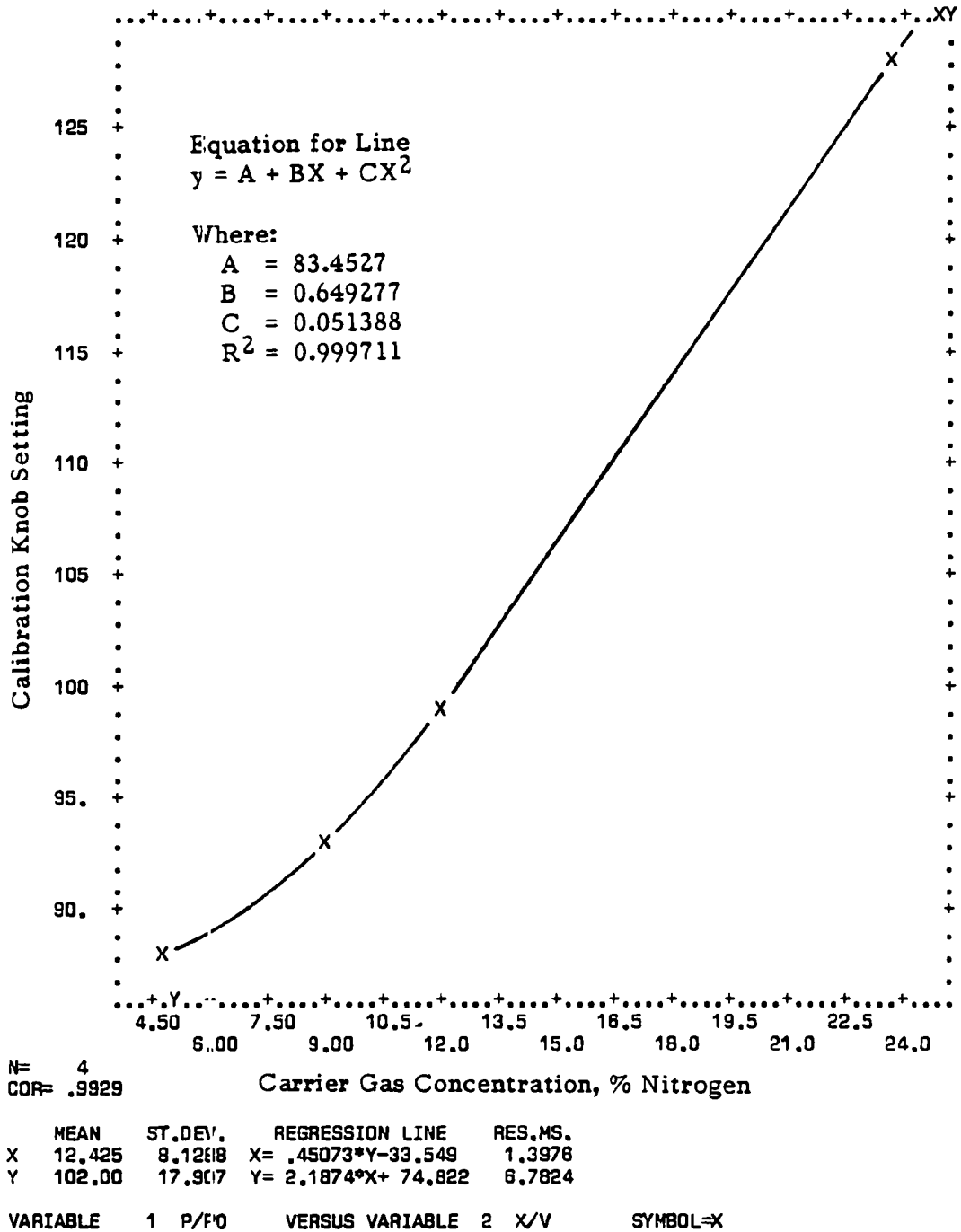


FIGURE 3. CALIBRATION KNOB SETTING FOR BET INSTRUMENT

TABLE 10. QUALITY ASSURANCE OF SURFACE AREA STANDARDS

<u>Standard Composition</u>	<u>Standard Surface Area, m²/g</u>	<u>Measured Surface Area, m²/g</u>	<u>Percent Difference</u>
Zinc oxide	0.62±0.04	0.61	-1.6
Alpha alumina	0.78 NBS	0.73	-6.4
Alumina	1.39±0.12	1.38	-0.7
Alumina	3.04±0.25	3.21	5.6
Titanium dioxide	7.05±0.7	6.97	-1.1
Alumina	14.0±0.6	14.00	0.0
Graphitized Carbon Black	71.3 NBS	73.13	2.6
Alumina	81.4±6.2	82.37	1.2
Alumina	265±11	220.5	-16.8
		Average	-1.9±6.5

TABLE 11. SPECIFIC SURFACE AREA OF SELECTED POWDER SAMPLES

<u>Converter</u>	<u>Specific Surface Area, m²/g</u>		<u>Total Surface Area, m²</u>		<u>Percent Difference^b</u>
	<u>Core</u>	<u>Powder</u>	<u>Core</u>	<u>Powder</u>	
A221/0447-A	4.8	5.8	5300	6400	20.8
A221/0447-B	8.0	6.0	3800	2800	-25.0
A220/0810-A	4.7	9.4	4200	8500	100.0
A220/0810-B	9.4	7.4	5900	4600	-21.3
A230/0177X-A	21.4	14.9	17,100	11,900	-30.4
A230/0117X-B	14.3	12.0	9400	7900	-16.1
A155/0941-1A	3.6	6.0	4500 ^a	7600 ^a	66.7
A155/0941-2-A	3.1	2.3	1500 ^a	1100 ^a	-25.8
A240/0141L-B	9.7	8.8	4900	4400	-9.3
A240/0334L-A	19.9	12.7	8000	5100	-36.2

^atotal surface area based on biscuit weights of converter A155/0926

^bbased on specific surface areas

TABLE 12. QUALITY ASSURANCE FOR XRF (SAMPLE A220/0810-B)

Element	Work Assignment		Percent Difference
	20 ^a	8 ^b	
P	0.48±0.02	0.50±0.03	4.2
S	1.15±0.06	1.09±0.05	-5.2
Ca	0.20±0.01	0.20±0.01	0.0
Mn	0.01±0.001	0.01±0.001	0.0
Ni	0.02±0.001	0.01±0.001	-50.0 ^c
Zn	0.25±0.01	0.25±0.01	0.0
Pt	0.37±0.02	0.36±0.02	-2.7
Pb	0.17±0.01	0.18±0.01	5.9
Others	Na,Mg,Al,Si, K,Ti,Fe,Ba,Ce	Na,Mg,Al,Si, K,Ti,Fe,Ce	

^aEPA Contract 68-03-3192, Work Assignment No. 20

^bEPA Contract 68-03-3353, Work Assignment No. 8

^cLarge percent difference due to low value. Probably not significant

RUN DESCRIPTION: AUCAT1 - AUTO CATALYST SWRI
 DATE OF XRAY ANALYSIS: 04/30/87
 SAMPLE TYPE: BRIQUETTE
 SITE ID: N/A
 MISCELLANEOUS INFO: RE-RUN OF OLD SAMPLE AS QA CONTROL
 SAMPLE SEQUENCE NO.: 13
 SAMPLE ID: A22070810-B

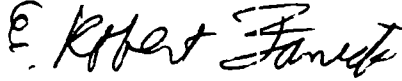
ELEMENT	DETN LIM	MASS %	±STDMA
NA	.210384E-01	.163845	+-.321902E-01
MG	.196613E-02	2.76064	+-.118866
AL	.257528E-01	31.4279	+-.157227
SI	.841549E-02	9.64556	+-.403362
P	.258094E-03	.498937	+-.257558E-01
S	.168881E-02	1.08975	+-.547663E-01
CL X	.984317E-03	-.113197E-02	+-.103988E-02
F	.225832E-03	.144844	+-.726653E-02
CA	.191874E-03	.195903	+-.993622E-02
TI	.15757E-03	.188644	+-.953012E-02
V	.548898E-03	.432425E-02	+-.64918E-03
CR	.970063E-03	.180009E-01	+-.204632E-02
MN	.450773E-03	.612693E-02	+-.744951E-03
FE	.430305E-03	.404594	+-.204071E-01
CO X	.306313E-03	-.969629E-04	+-.287532E-03
NI	.253437E-03	.884821E-02	+-.563457E-03
CU	.270925E-03	.167652E-02	+-.286644E-03
ZN	.290046E-03	.24947	+-.125051E-01
SE X	.305792E-03	-.372902E-02	+-.317056E-03
BR X	.215055E-02	-.367318E-02	+-.215898E-02
SR X	.493812E-02	-.12941E-02	+-.00494
MO X	.693048E-02	-.100575E-02	+-.493194E-02
CD D	.199053E-03	.318519E-03	+-.312976E-03
SN D	.117962E-02	.238133E-02	+-.12065E-02
SB X	.561786E-03	.71913E-05	+-.529030E-04
HA D	.492747E-03	.112195E-02	+-.503573E-03
CE	.194678E-02	.106951E-01	+-.215341E-02
PT	.763173E-03	.361267	+-.181052E-01
HG X	.792004E-03	-.473169E-02	+-.753067E-03
PB	.824246E-03	.177079	+-.897717E-02

TOTAL DETECTED BY XRF = 46.9609

FIGURE 4. ELEMENTAL CONCENTRATIONS OF METALS AND POISONS FOR BULK SAMPLE BY X-RAY FLUORESCENCE

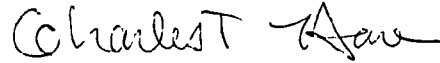
We hope that the results from these catalyst evaluations will help to answer some of the EPA questions about relationships concerning the catalyst condition. Please contact us if there are additional questions, or if we can be of further assistance.

Prepared by:



E. Robert Fanick
Research Scientist
Department of Emissions Research

Reviewed by:

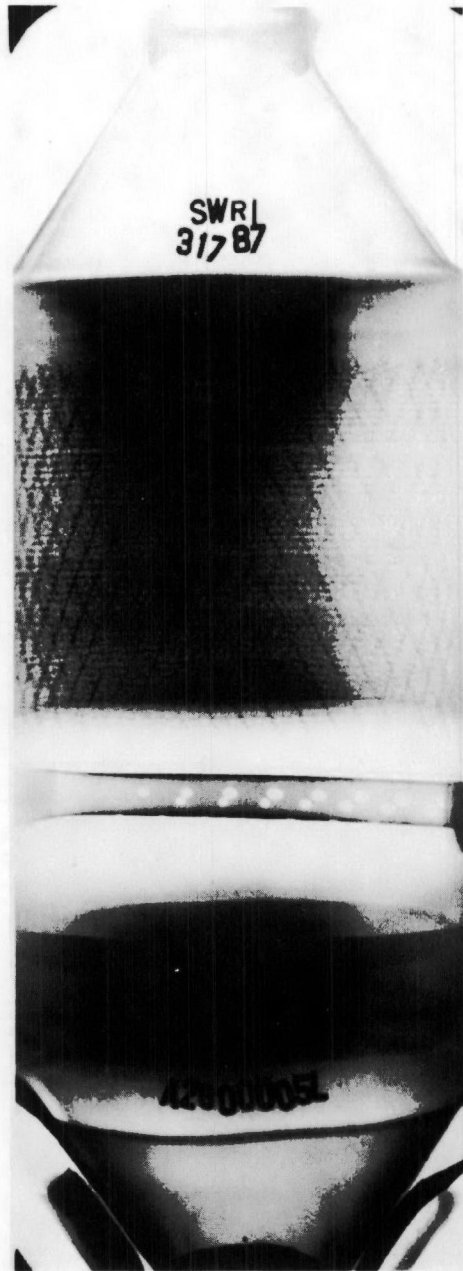


Charles T. Hare
Director
Department of Emissions Research

APPENDIX A

WHOLE CATALYST X-RAY RADIOGRAPHS

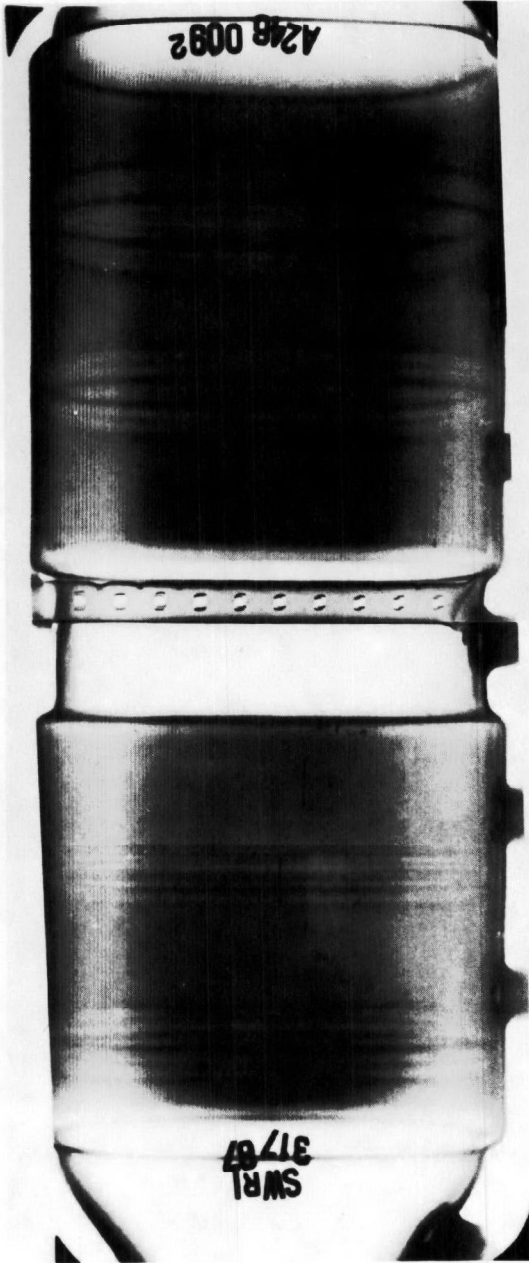
INLET



OUTLET

Figure A-1. X-Ray Radiograph of A280/0005L

INLET



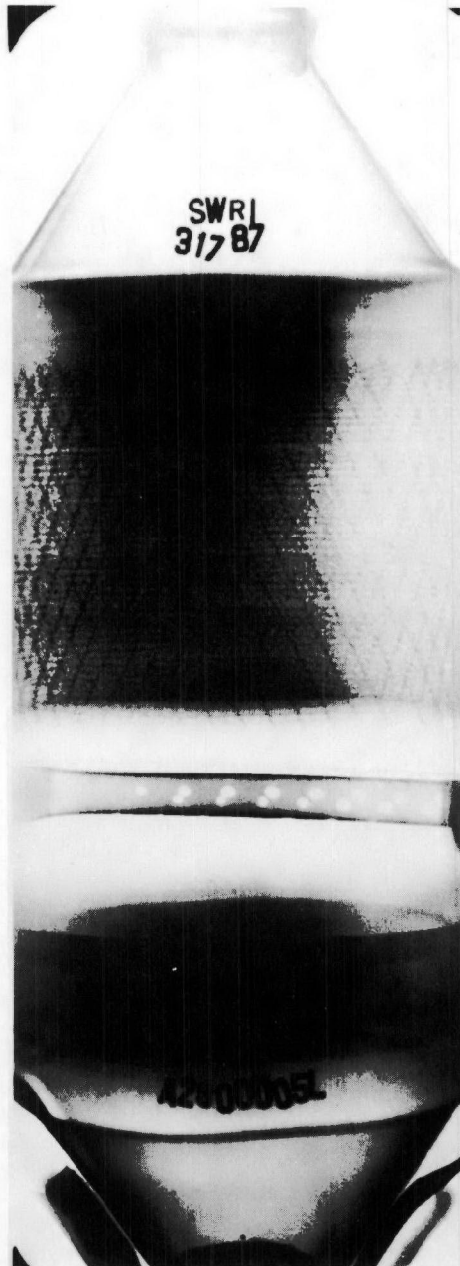
OUTLET

Figure A-2. X-Ray Radiograph of A246/0092

APPENDIX A

WHOLE CATALYST X-RAY RADIOGRAPHS

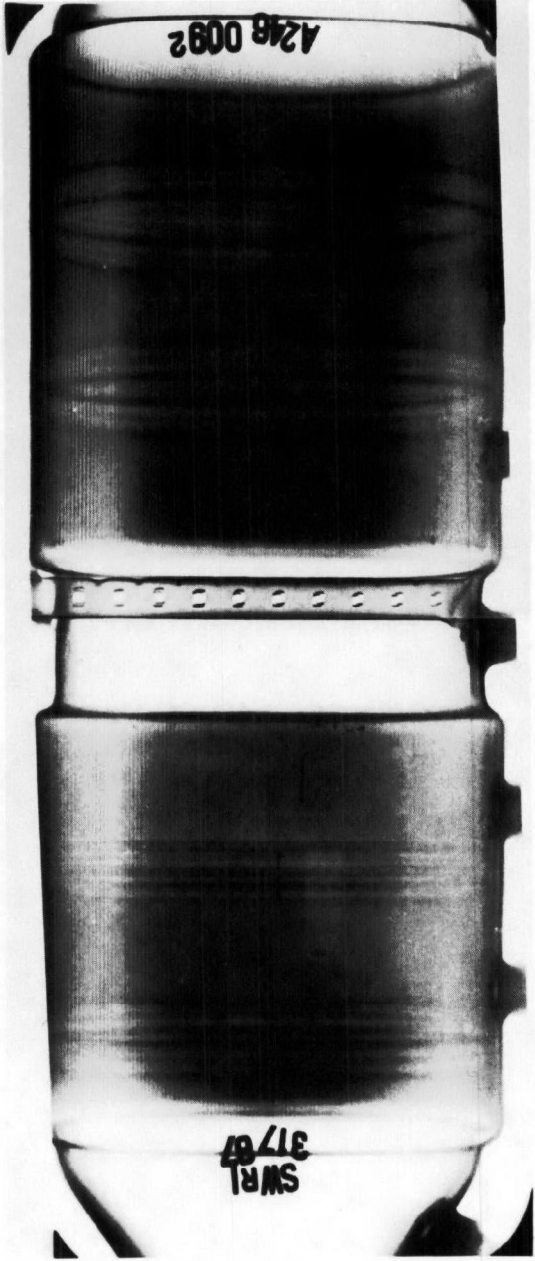
INLET



OUTLET

Figure A-1. X-Ray Radiograph of A280/0005L

INLET

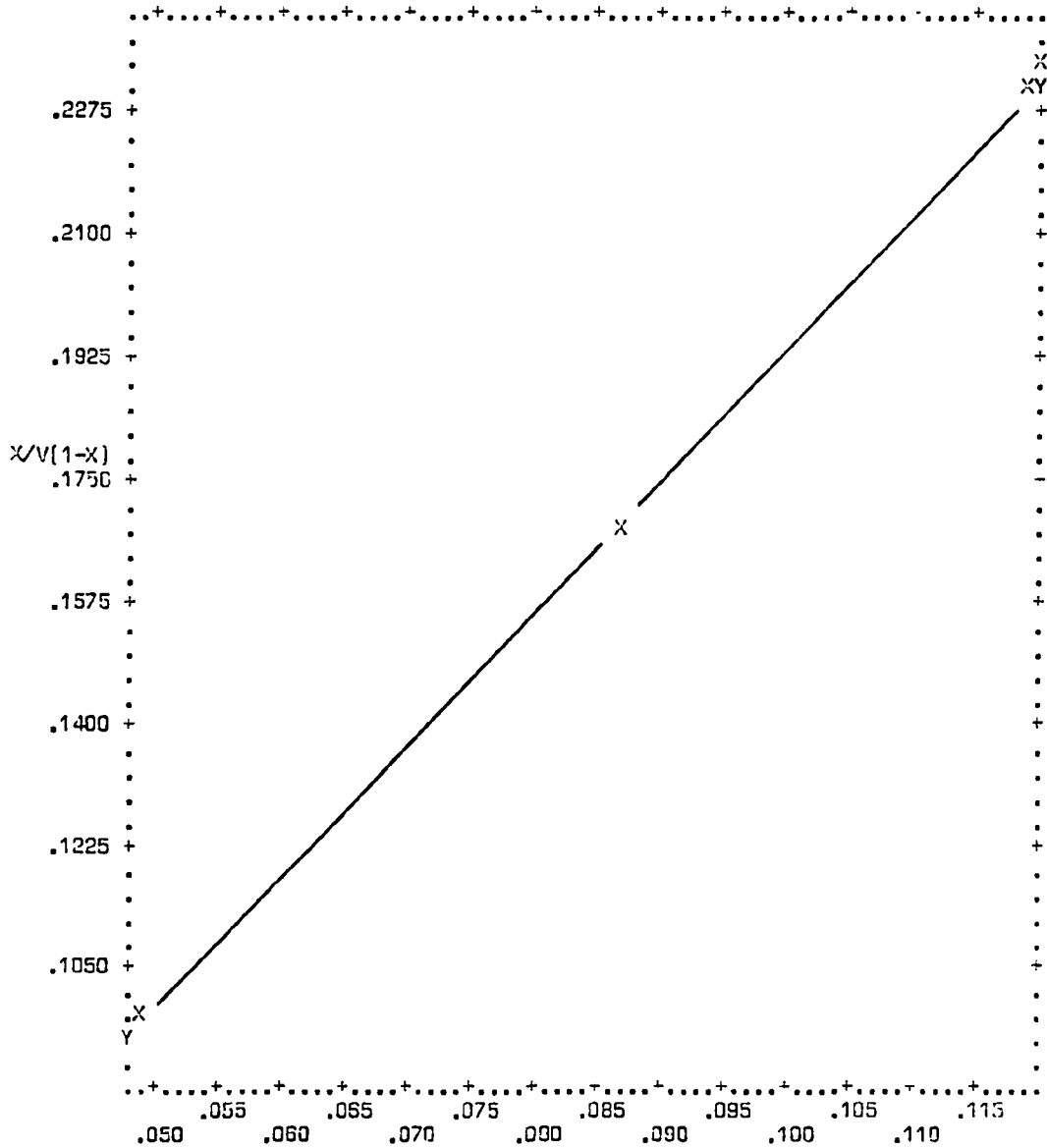


OUTLET

Figure A-2. X-Ray Radiograph of A246/0092

APPENDIX B

BET EQUATION VERSUS RELATIVE PRESSURE



N= 3
COR= .9996

	MEAN	ST.DEV.	REGRESSION LINE	RES.HS.
X	.08482	.03484	X= .52270*Y-.00166	172E-3
Y	.16545	.06663	Y= 1.9118*X+.00330	531E-3

VARIABLE 1 P/P0 VERSUS VARIABLE 2 X/V SYMBOL=X

Figure B-1. Plot of BET equation versus relative pressure for Converter A221/0310-A-LL1

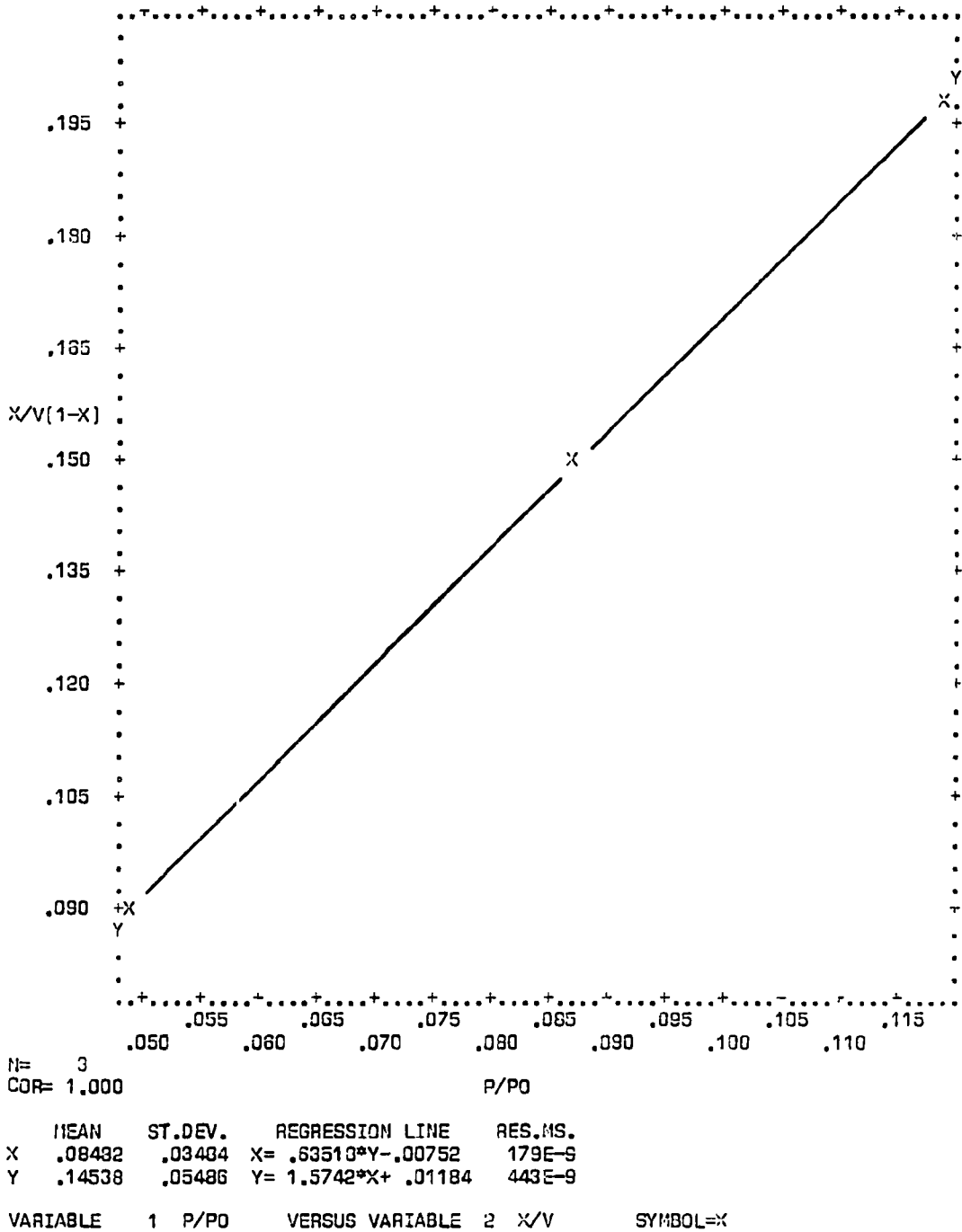
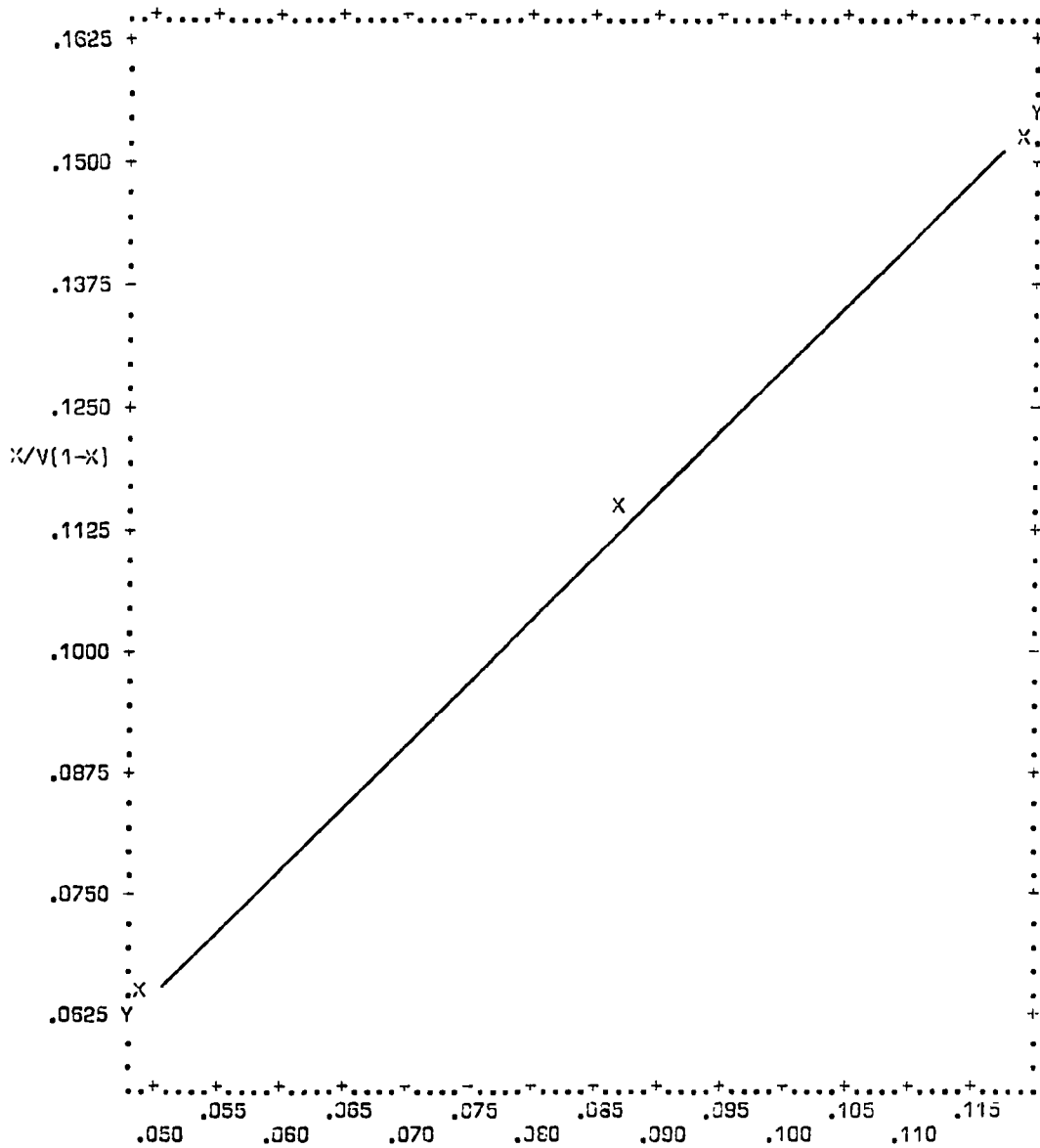


Figure B-2. Plot of BET equation versus relative pressure for Converter A221/0310-A-LL2

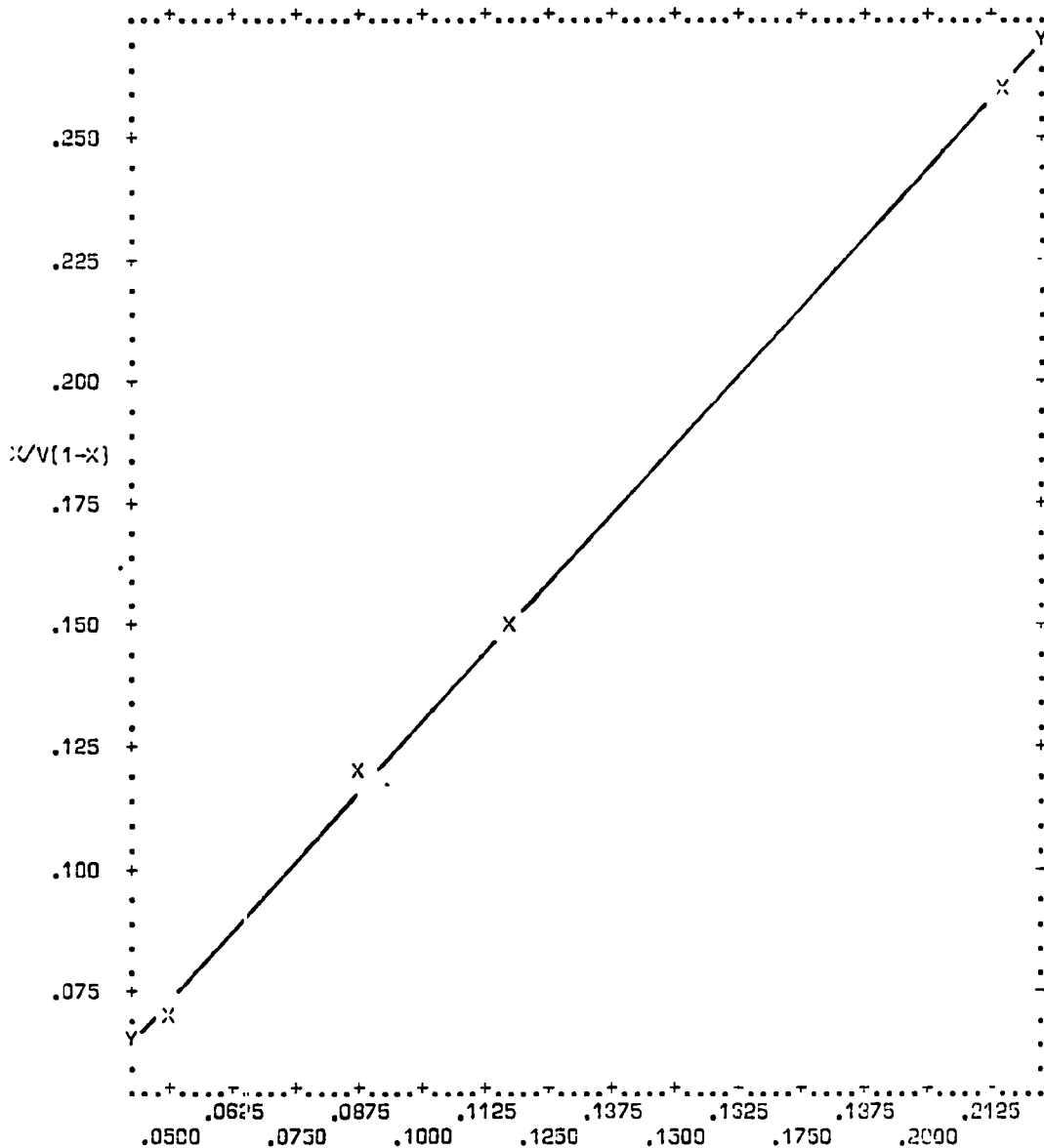


N= 3
COR= .9993 P/P0

	MEAN	ST.DEV.	REGRESSION LINE	RES. MS.
X	.08482	.03484	X= .79438*Y-.00251	332E-8
Y	.10994	.04383	Y= 1.2571*X+.00331	526E-8

VARIABLE 1 P/P0 VERSUS VARIABLE 2 X/V SYMBOL=X

Figure B-3. Plot of BET equation versus relative pressure for Converter A221/0310-A-LL3



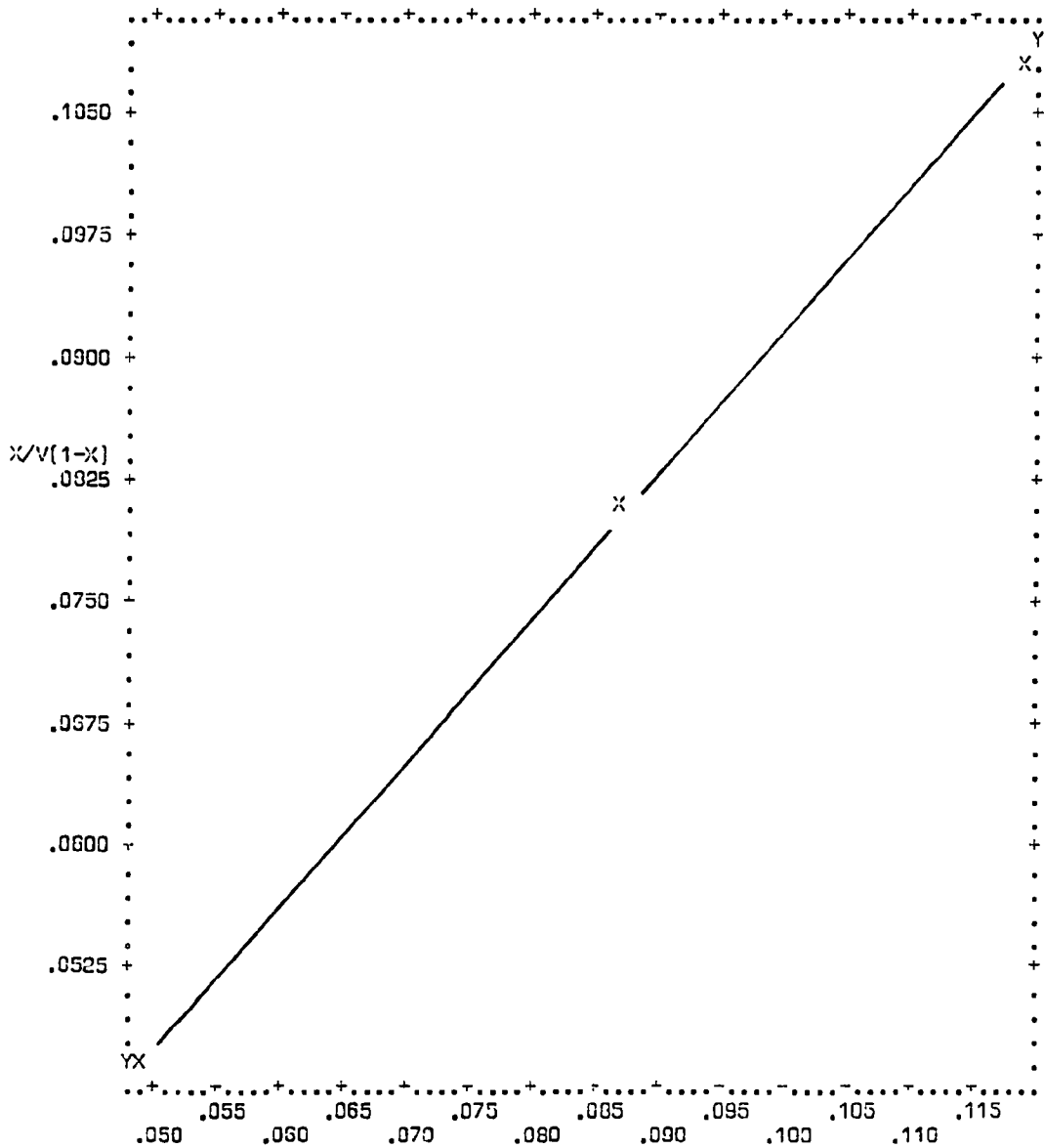
N= 4
COR= .9990

P/P0

	MEAN	ST.DEV.	REGRESSION LINE	RES.IIS.
X	.11752	.07130	X= .87828*Y-.01542	146E-7
Y	.15136	.08114	Y= 1.1364*X+.01781	189E-7

VARIABLE 1 P/P0 VERSUS VARIABLE 2 X/V SYMBOL=X

Figure B-4. Plot of BET equation versus relative pressure for Converter A221/0310-A-LL1 (Powder)



n= 3
COR= .9990

P/P0

	MEAN	ST.DEV.	REGRESSION LINE	RES.SIS.
X	.03482	.03484	X= 1.1320*Y-.00436	103E-8
Y	.07073	.03077	Y= .80298*X+.00389	640E-9

VARIABLE 1 P/P0 VERSUS VARIABLE 2 X/V SYMBOL=X

Figure B-5. Plot of BET equation versus relative pressure for Converter A221/0310-B-UR1

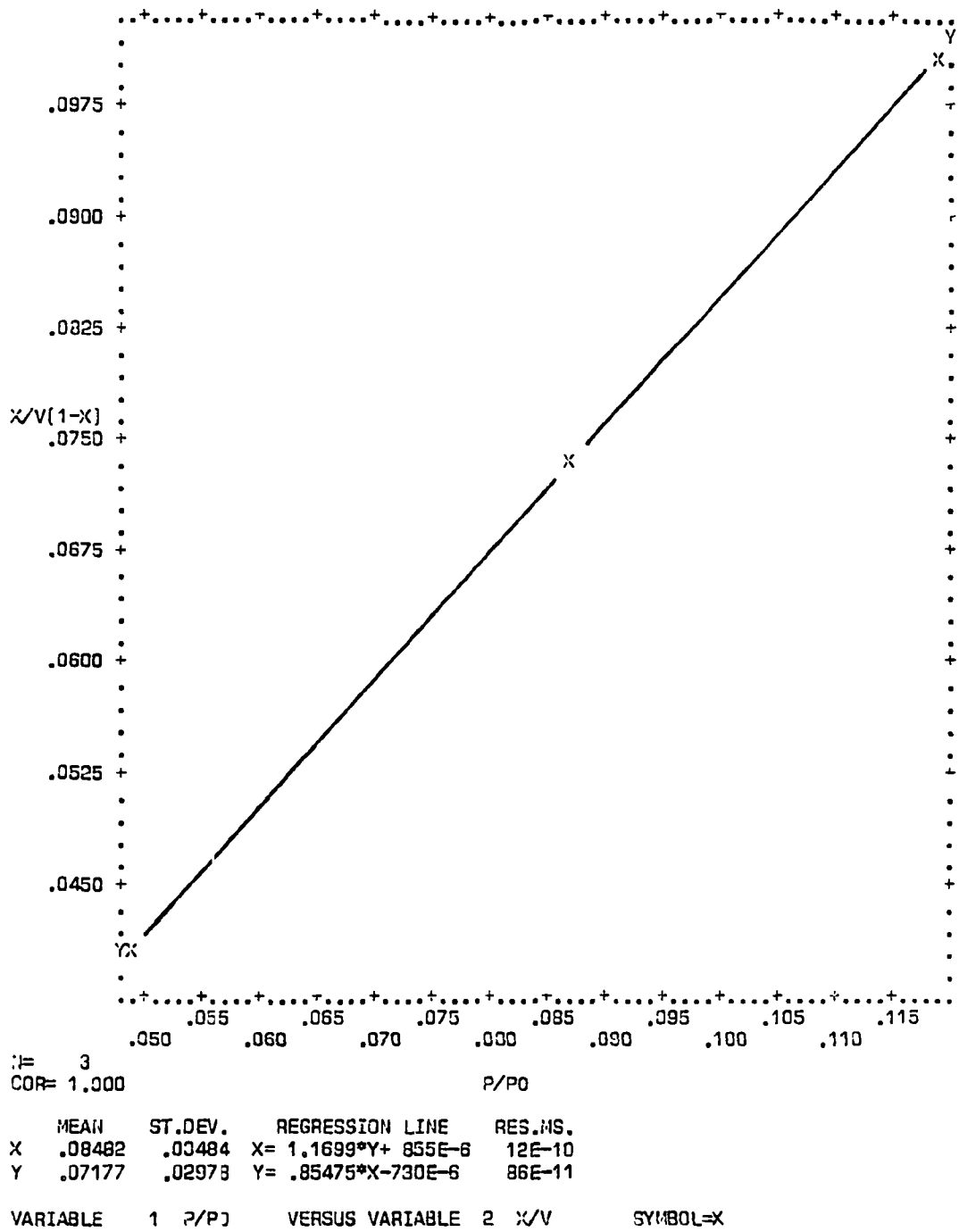


Figure B-6. Plot of BET equation versus relative pressure for Converter A221/0310-B-UR2

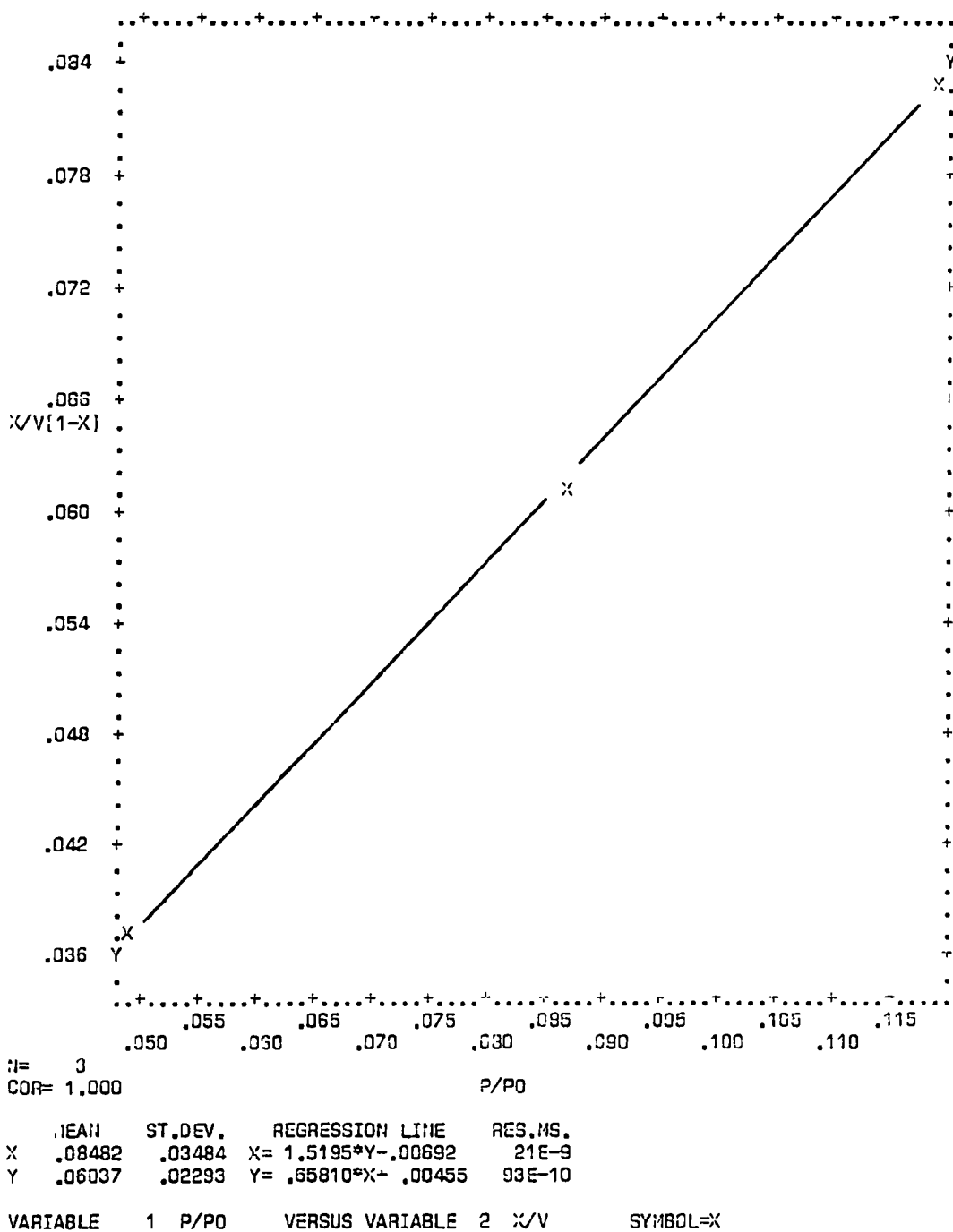


Figure B-7. Plot of BET equation versus relative pressure for Converter A280/0005L-A-LL1

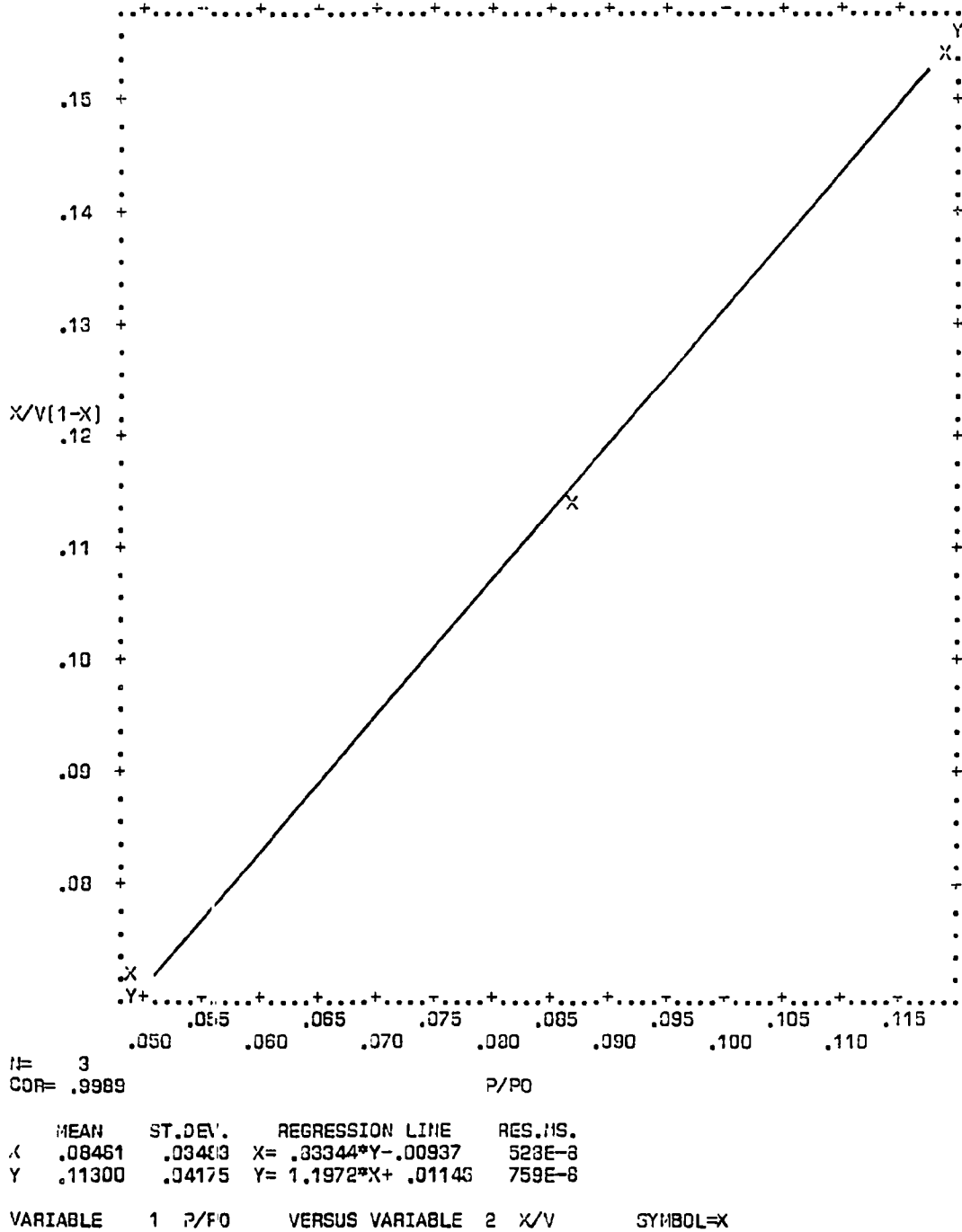
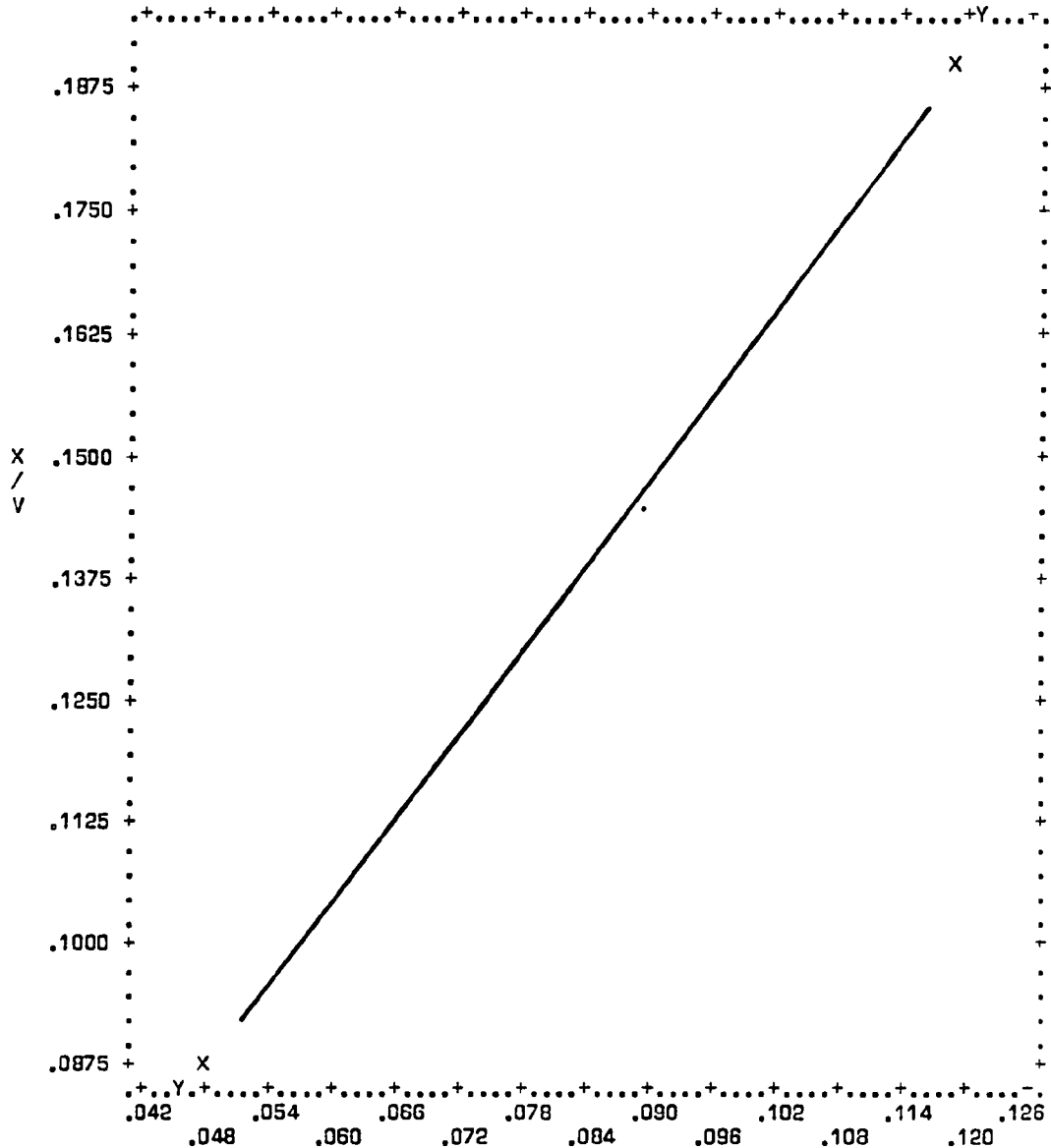


Figure B-8. Plot of BET equation versus relative pressure for Converter A280/0005L-A-LL2



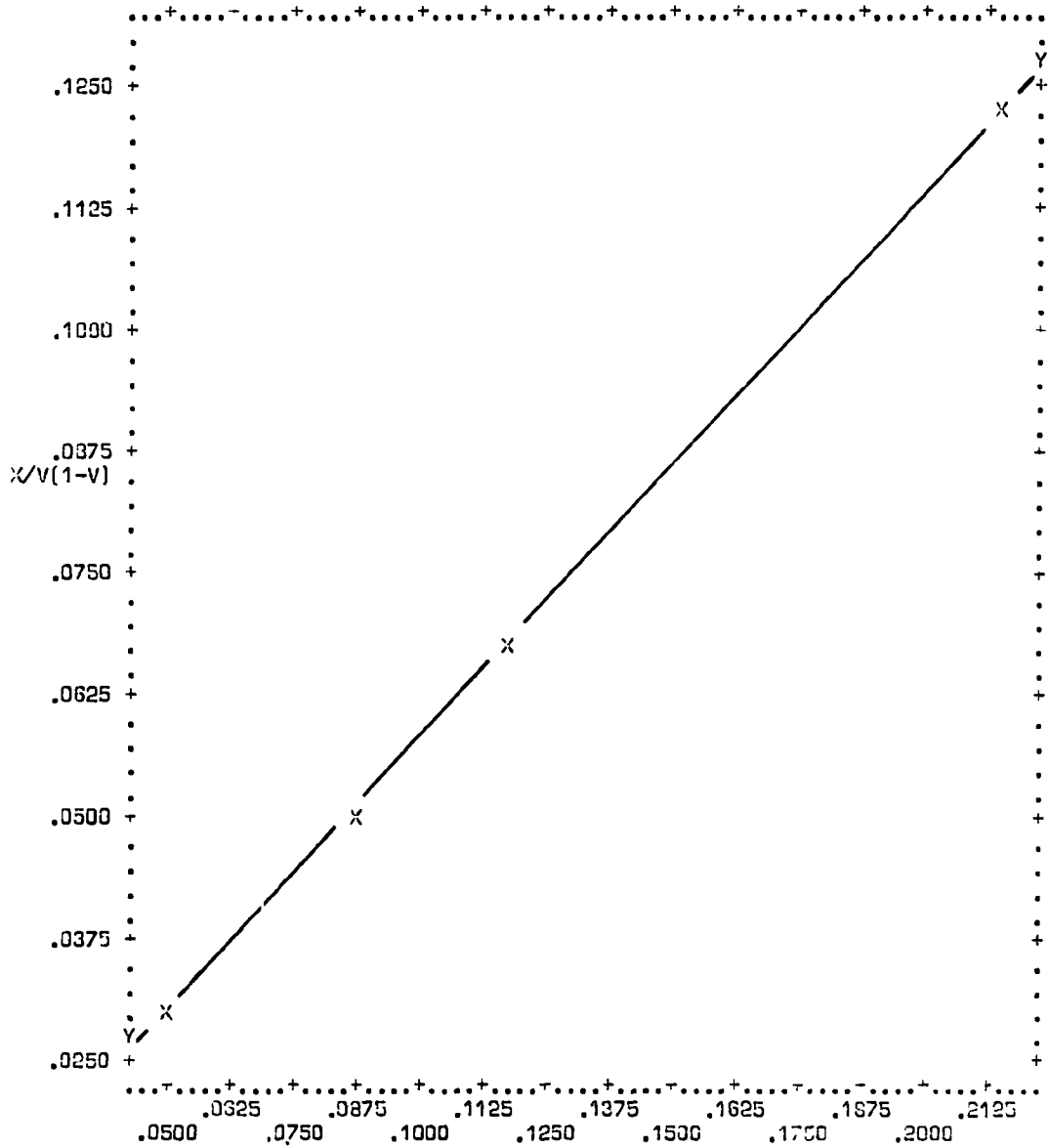
N= 2
COR= 1.000

P/P0

	MEAN	ST.DEV.	REGRESSION LINE	RES.MS.
X	.08351	.04962	X = .58716*Y - .01224	0.0000
Y	.13933	.07222	Y = 1.4553*X + .01781	0.0000

VARIABLE 1 P/P0 VERSUS VARIABLE 2 X/V SY11B0L=X

Figure B-9. Plot of BET equation versus relative pressure for Converter A280/0005L-A-LL3



N= 4
COR= .9998

P/P0

	MEAN	ST.DEV.	REGRESSION LINE	RES. IS.
X	.11752	.07132	X= 1.8041*Y-.00539	346E-3
Y	.03813	.03952	Y= .55403*X+ .00302	106E-8

VARIABLE 1 P/P0 VERSUS VARIABLE 2 X/V SYMBOL=X

Figure B-10. Plot of BET equation versus relative pressure for Converter A280/0005L-A-LL1 (Powder)

IDLE

1PAGE 4 CONVERTER SURFACE AREA ANALYSIS A280/0005L-B UR-1

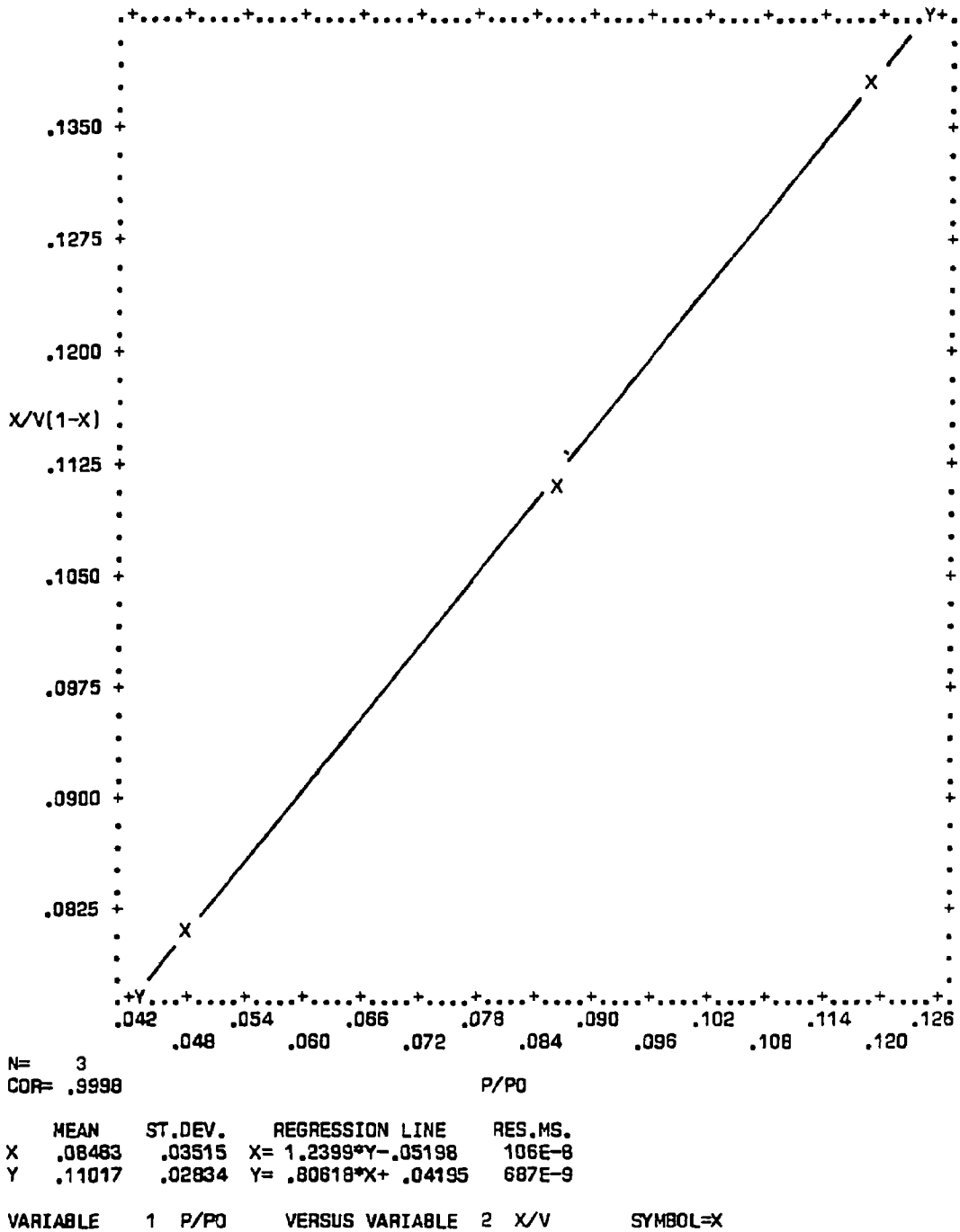
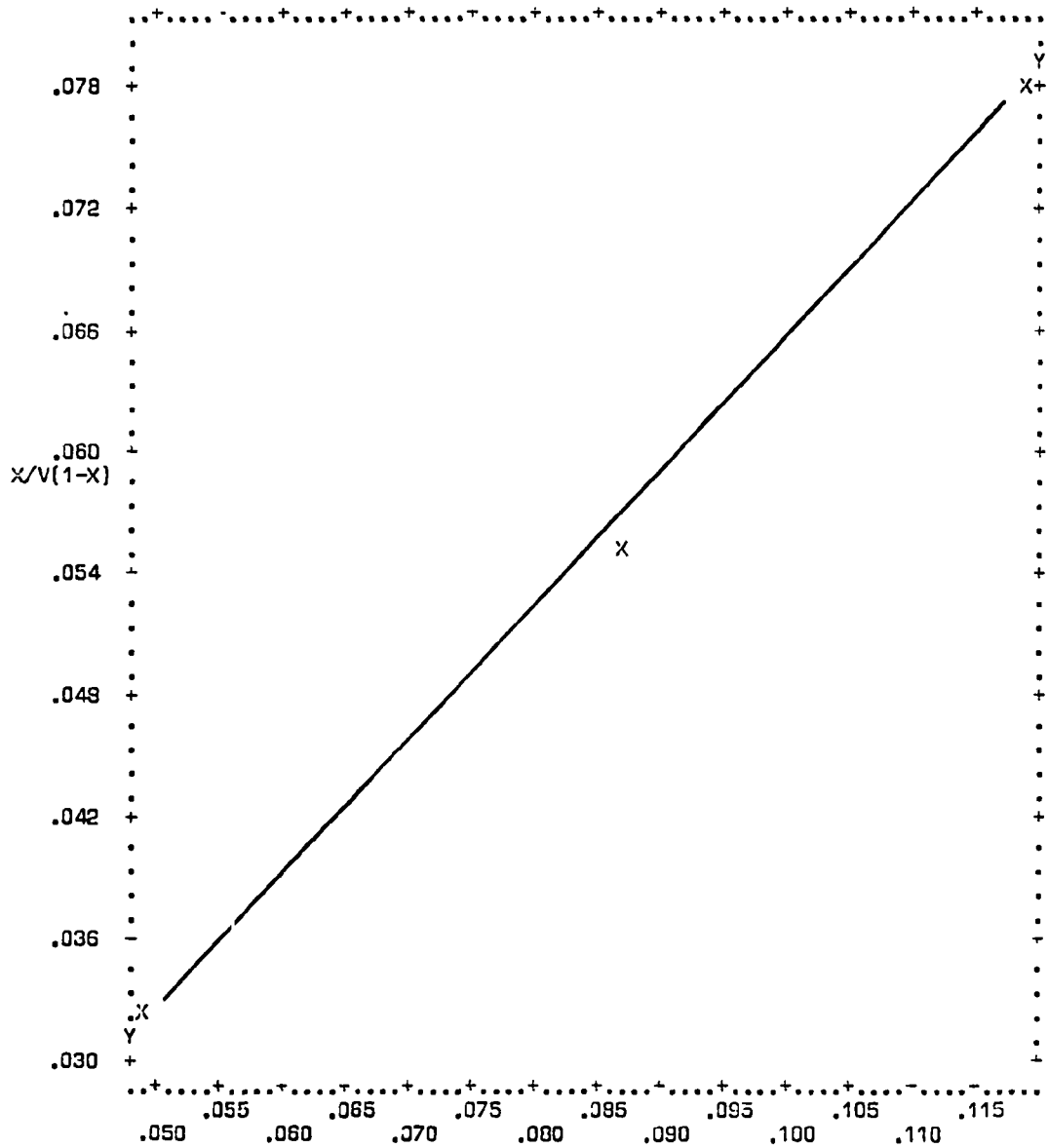


Figure B-11. Plot of BET equation versus relative pressure for Converter A280/0005L-B-UR1



N= 3
COR= .9987

	MEAN	ST.DEV.	REGRESSION LINE	RES.IIS.
X	.08482	.03484	X= 1.5223*Y+ 111E-6	655E-8
Y	.05564	.02283	Y= .65513*X+ 773E-7	282E-8

VARIABLE 1 P/P0 VERSUS VARIABLE 2 X/V SYMBOL=X

Figure B-12. Plot of BET equation versus relative pressure for Converter A280/0005L-B-UR2

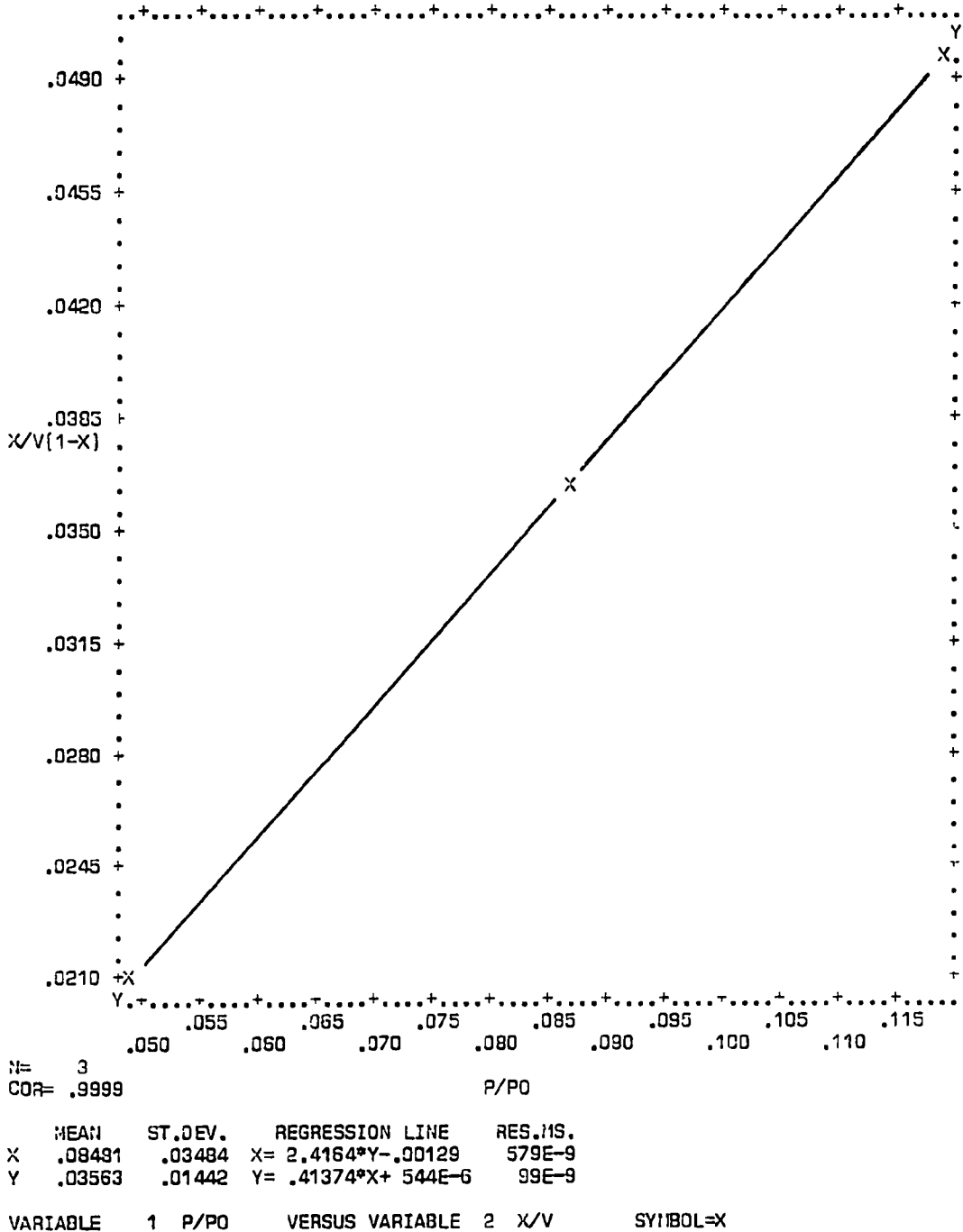


Figure B-13. Plot of BET equation versus relative pressure for Converter A220/0400-A-LL1

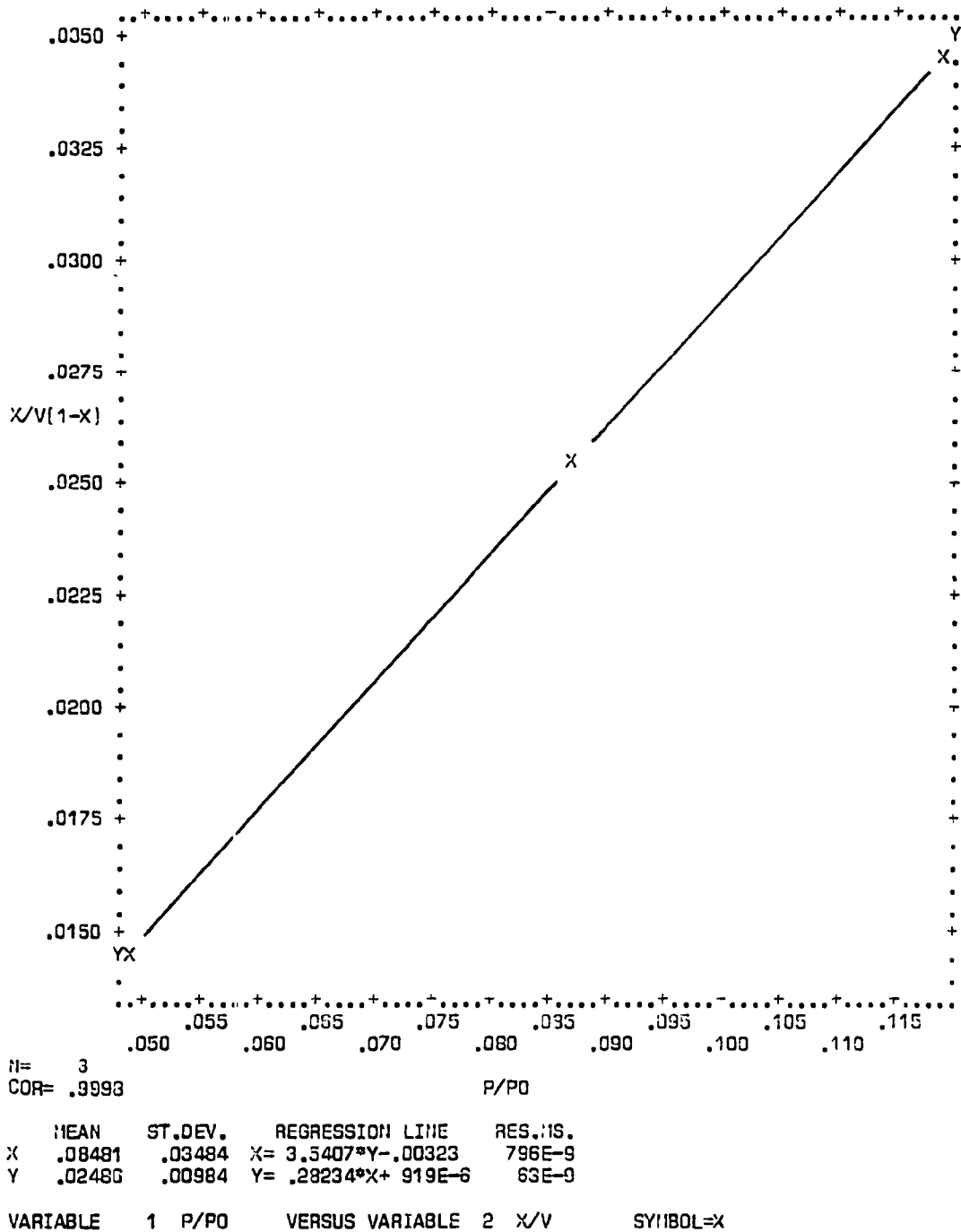
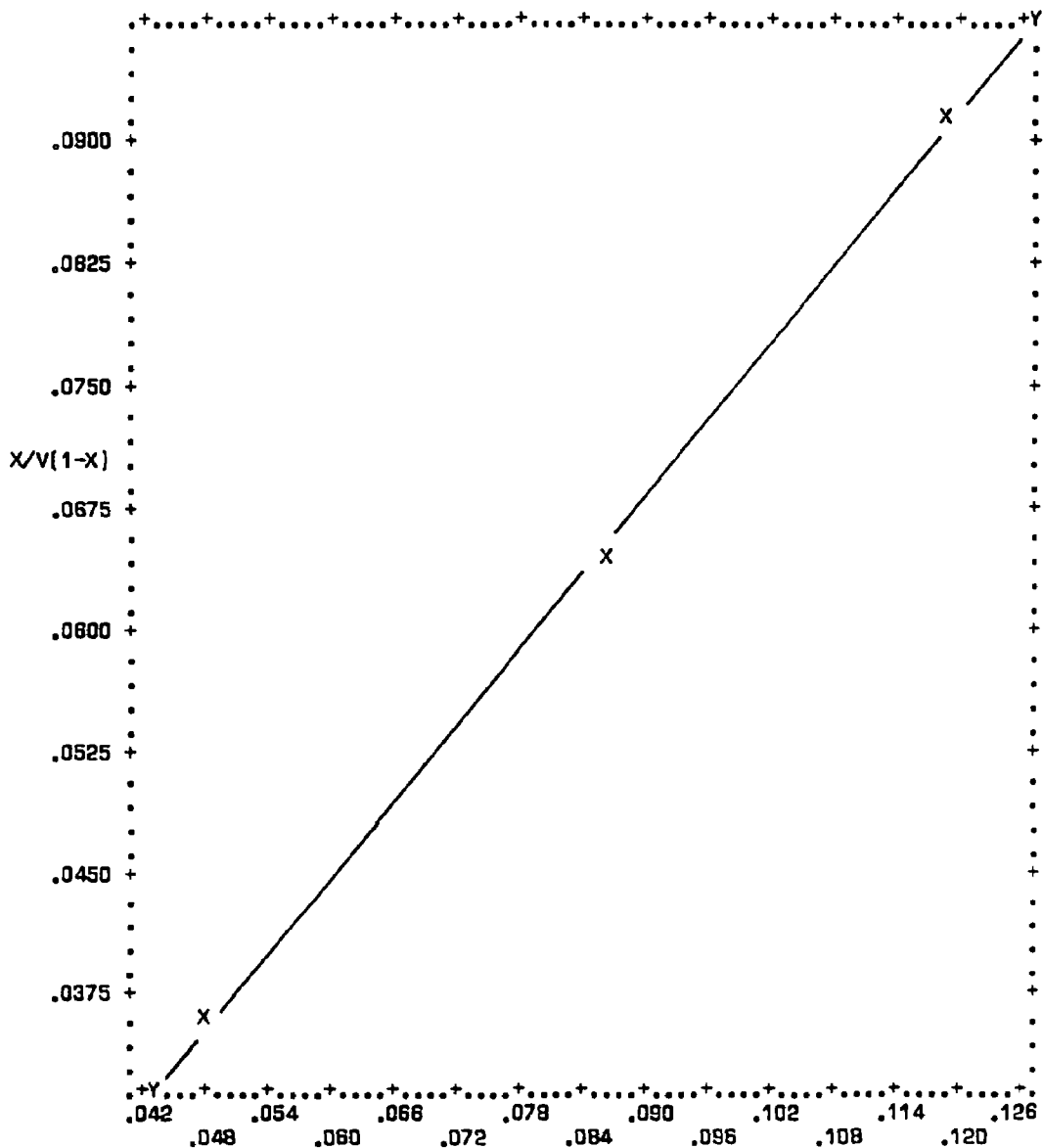


Figure B-14. Plot of BET equation versus relative pressure for Converter A220/0400-A-LL2

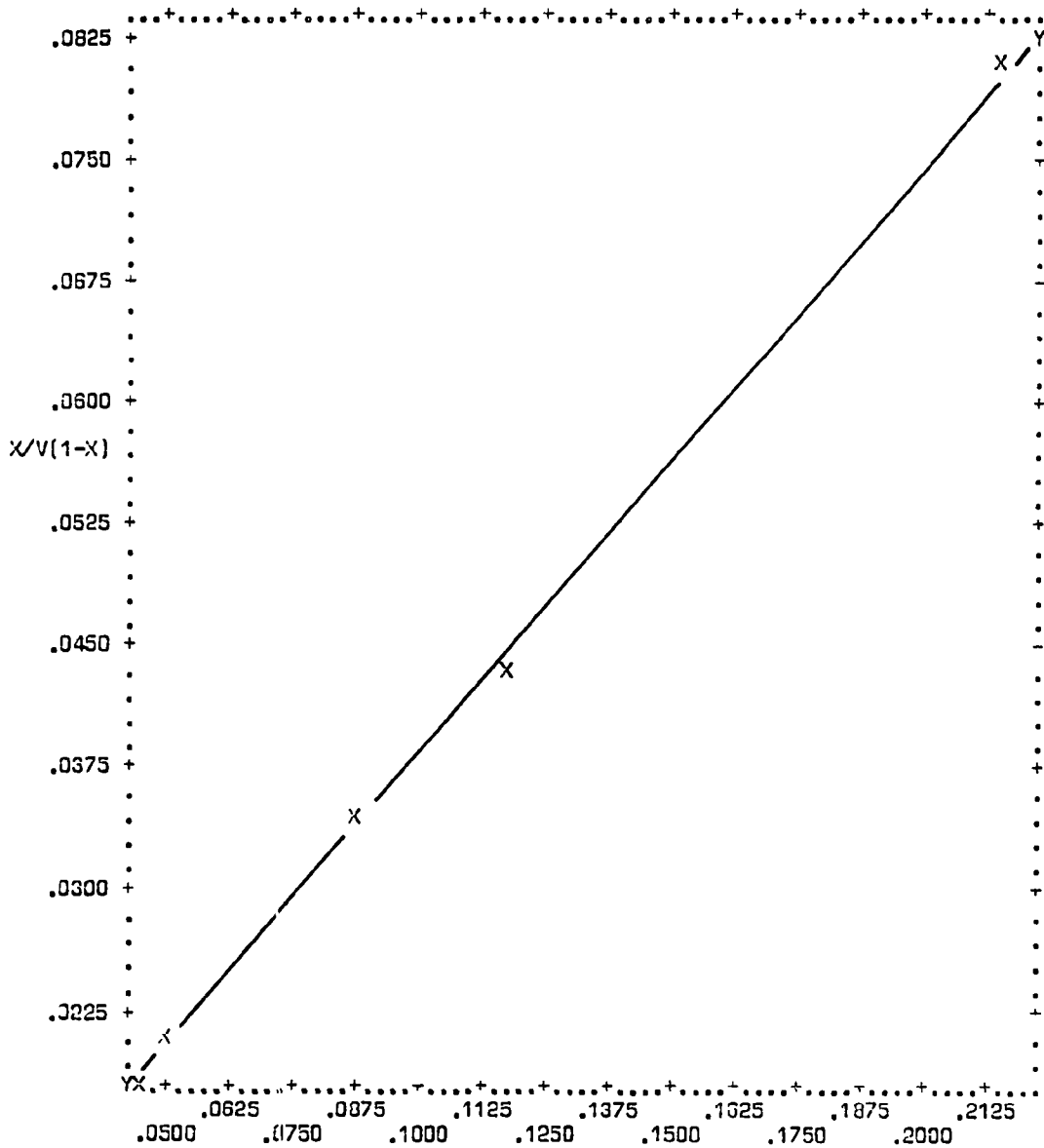


N= 3
COR= .9993

	MEAN	ST.DEV.	REGRESSION LINE	RES.MS.
X	.08462	.03514	X= 1.2771*Y+ .00346	334E-8
Y	.06355	.02750	Y= .78198*X-.00262	205E-8

VARIABLE 1 P/P0 VERSUS VARIABLE 2 X/V SYMBOL=X

Figure B-15. Plot of BET equation versus relative pressure for Converter A220/0400-A-LL3

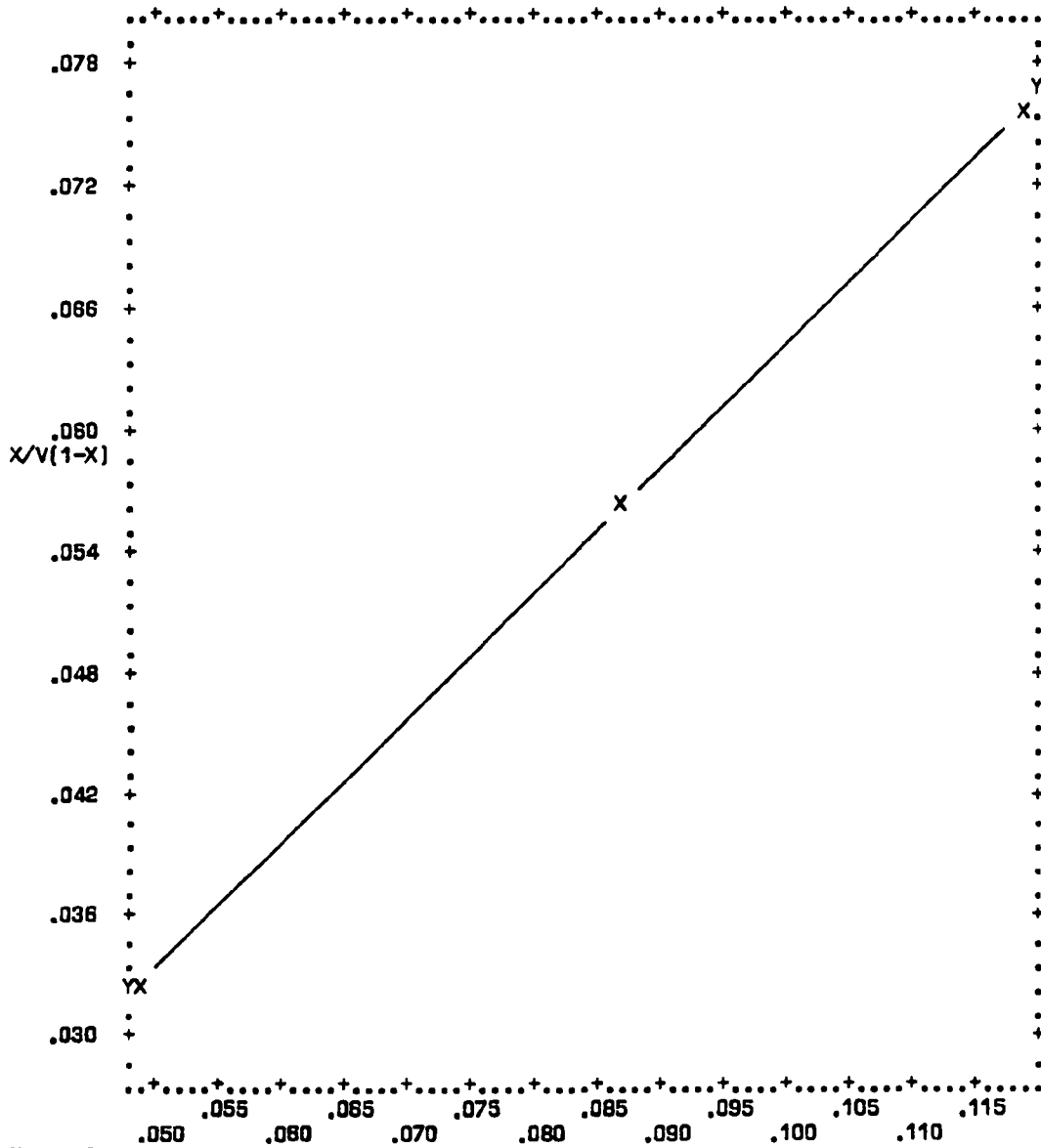


$n = 4$
 $CON = .9990$

	MEAN	ST.DEV.	REGRESSION LINE	RES.MS.
X	.11752	.07133	$y = 2.7752 * X - .00608$	148E-7
Y	.04454	.02568	$y = .35964 * X + .00227$	192E-8

VARIABLE 1 P/P0 VERSUS VARIABLE 2 X/V SYMBOL=X

Figure B-16. Plot of BET equation versus relative pressure for Converter A220/0400-A-LL1 (Powder)



N= 3
COR= .9997

	MEAN	ST.DEV.	REGRESSION LINE	RES.MS.
X	.08482	.03484	X= 1.6170*Y-.00408	188E-8
Y	.05497	.02154	Y= .61800*X+ .00255	641E-9

VARIABLE 1 P/P0 VERSUS VARIABLE 2 X/V SYMBOL=X

Figure B-17. Plot of BET equation versus relative pressure for Converter A220/0400-B-UR1

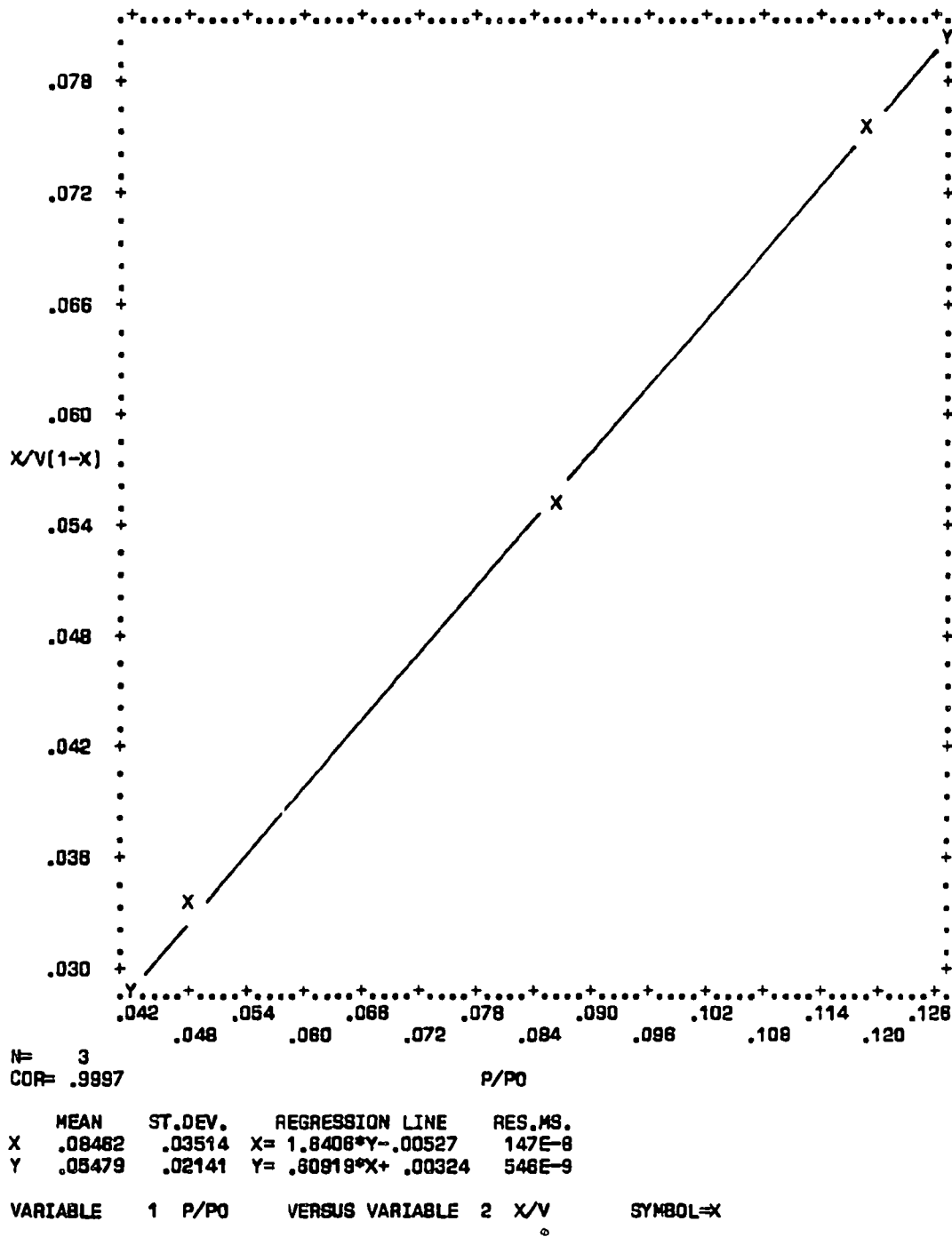
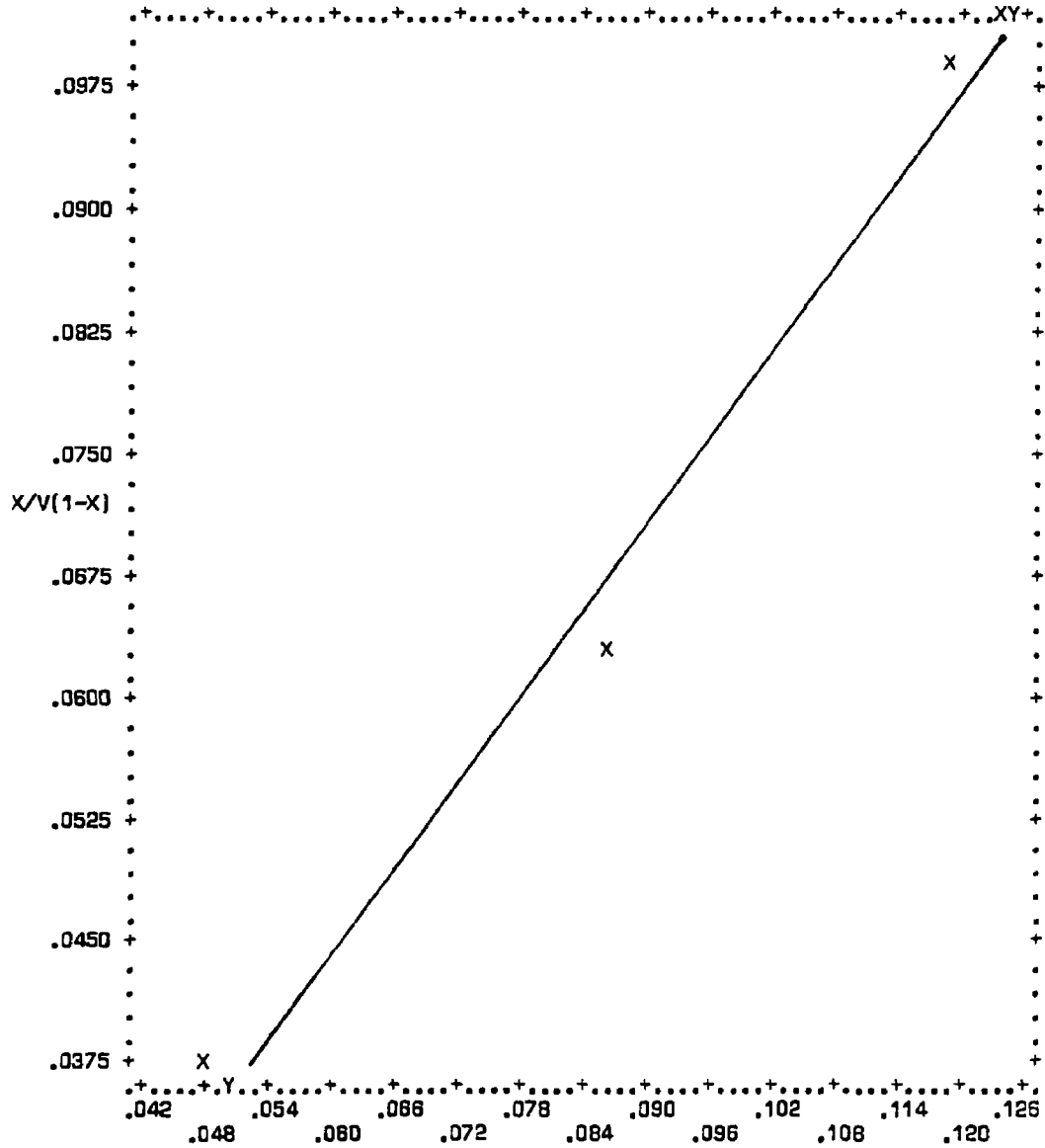


Figure B-18. Plot of BET equation versus relative pressure for Converter A220/0400-B-UR2

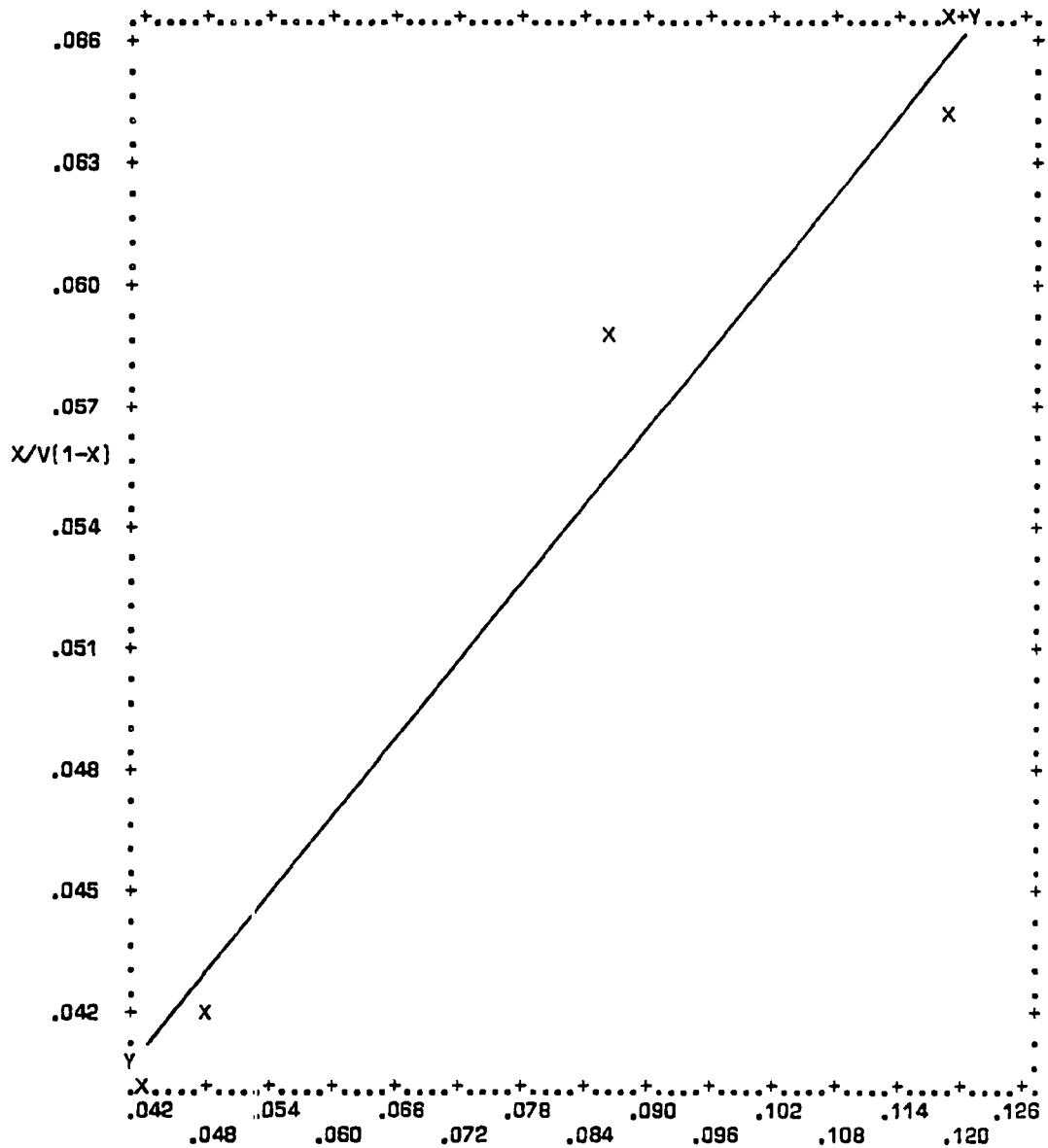


N= 3
COR= .9907 P/P0

	MEAN	ST.DEV.	REGRESSION LINE	RES.MS.
X	.08462	.03514	X= 1.1154*Y+ .01040	457E-7
Y	.06654	.03121	Y= .87993*X-.00792	360E-7

VARIABLE 1 P/P0 VERSUS VARIABLE 2 X/V SYMBOL=X

Figure B-19. Plot of BET equation versus relative pressure for Converter A230/0649-A-LL1

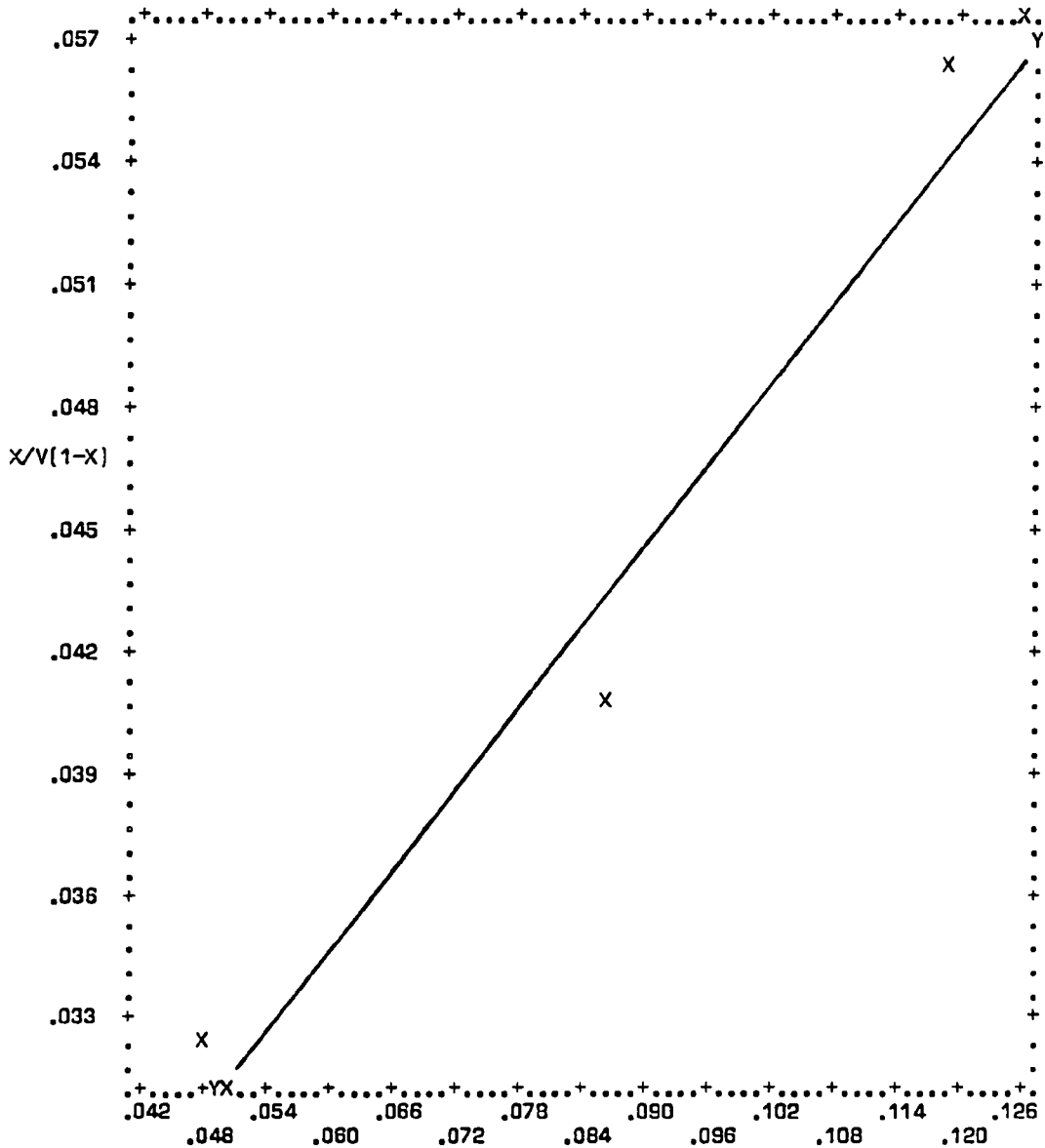


N= 3
COR= .9709

	MEAN	ST.DEV.	REGRESSION LINE	RES.MS.
X	.08461	.03514	X= 2.9115*Y-.07527	142E-6
Y	.05491	.01172	Y= .32375*X+.02752	158E-7

VARIABLE 1 P/P0 VERSUS VARIABLE 2 X/V SYMBOL=X

Figure B-20. Plot of BET equation versus relative pressure for Converter A230/0649-A-LL2



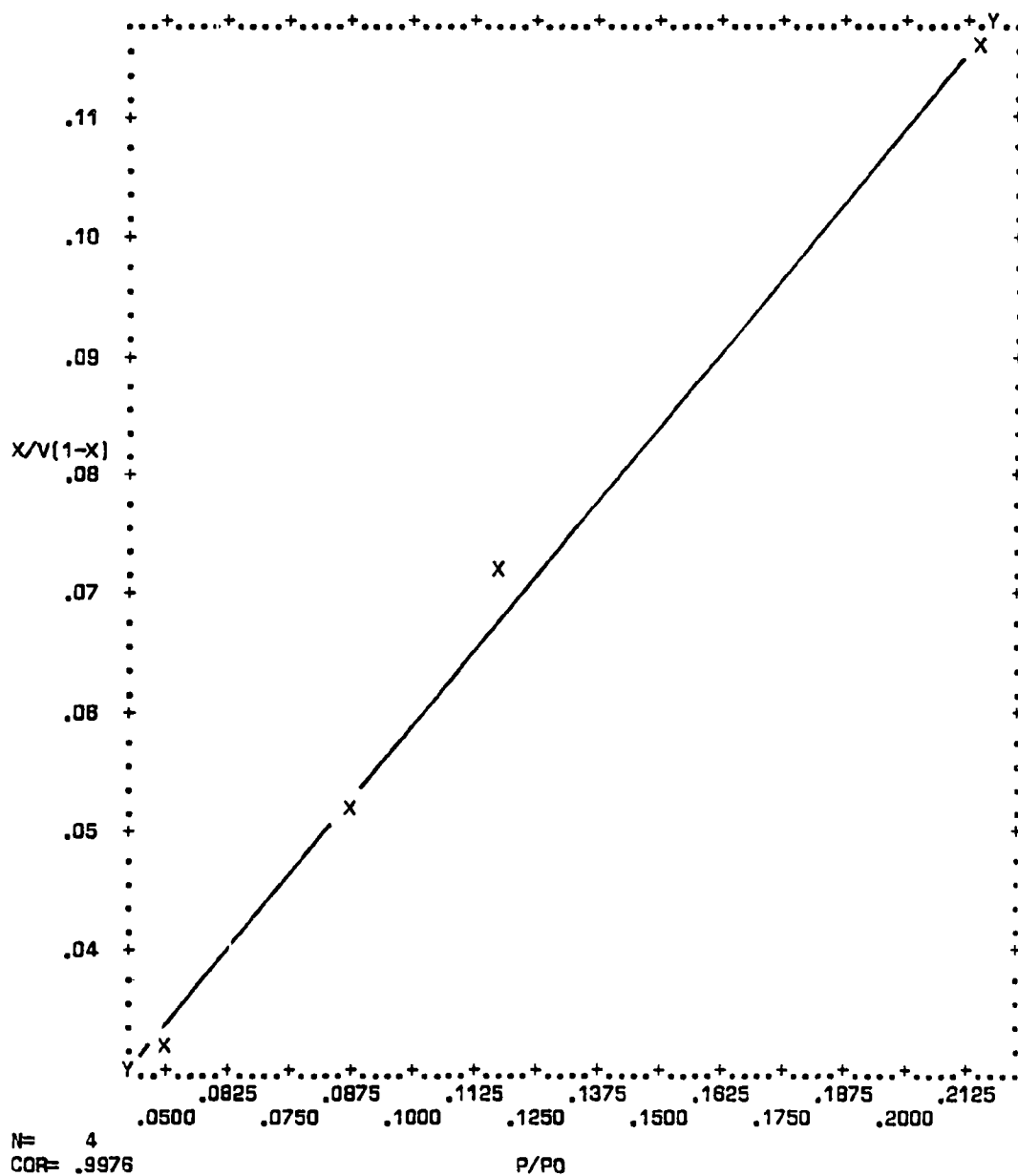
N= 3
COR= .9718

P/P0

	MEAN	ST.DEV.	REGRESSION LINE	RES. MS.
X	.08482	.03514	X= 2.8408*Y-.03767	137E-6
Y	.04305	.01202	Y= .33247*X+ .01491	160E-7

VARIABLE 1 P/P0 VERSUS VARIABLE 2 X/V SYMBOL=X

Figure B-21. Plot of BET equation versus relative pressure for Converter A230/0649-A-LL3

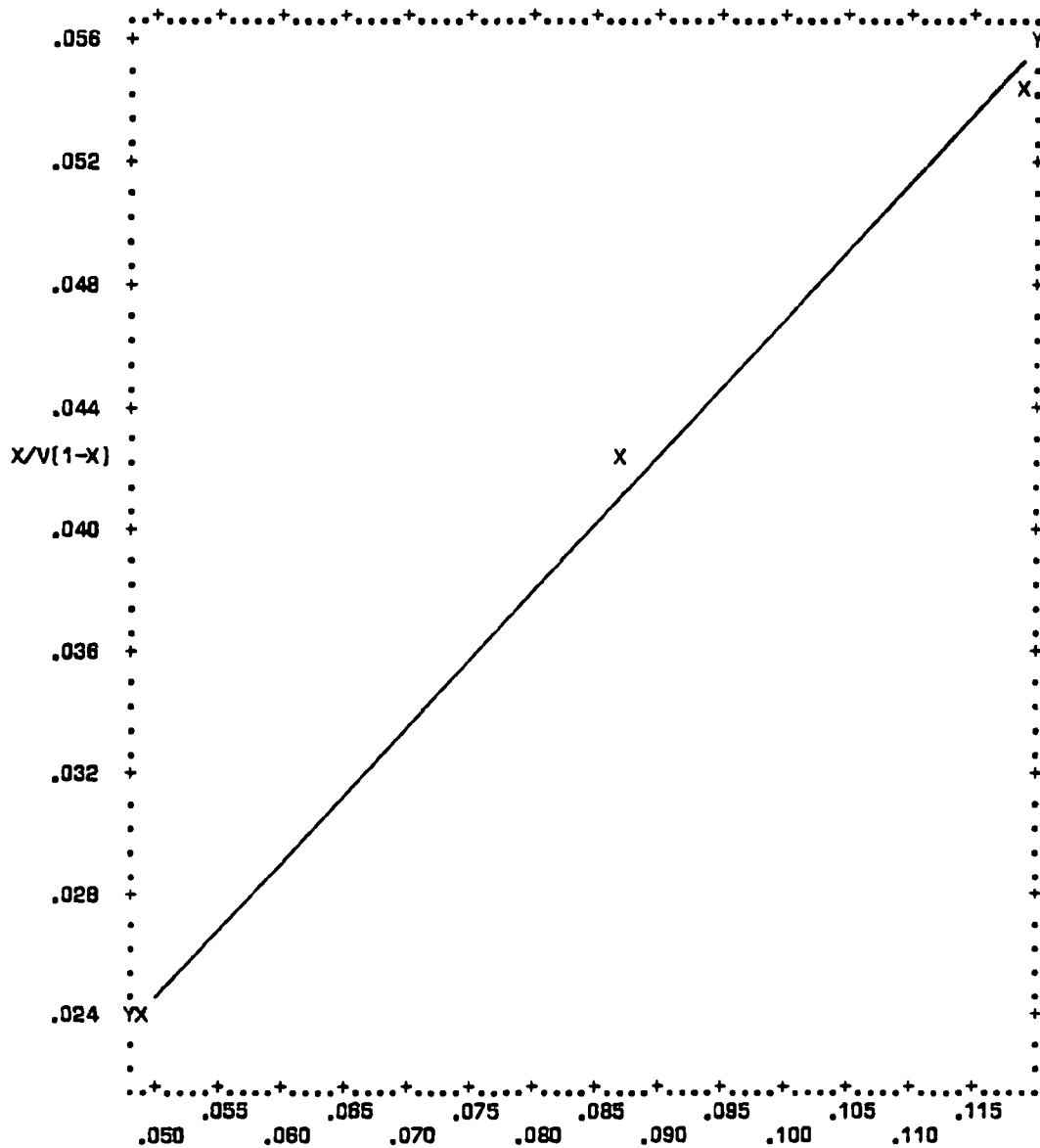


N= 4
COR= .9976 P/P0

	MEAN	ST.DEV.	REGRESSION LINE	RES.MS.
X	.11752	.07132	X= 1.9953*Y-.01739	381E-7
Y	.06761	.03563	Y= .49881*X+ .00899	901E-8

VARIABLE 1 P/P) VERSUS VARIABLE 2 X/V SYMBOL=X

Figure B-22. Plot of BET equation versus relative pressure for Converter A230/0649-A-LL1 (Powder)

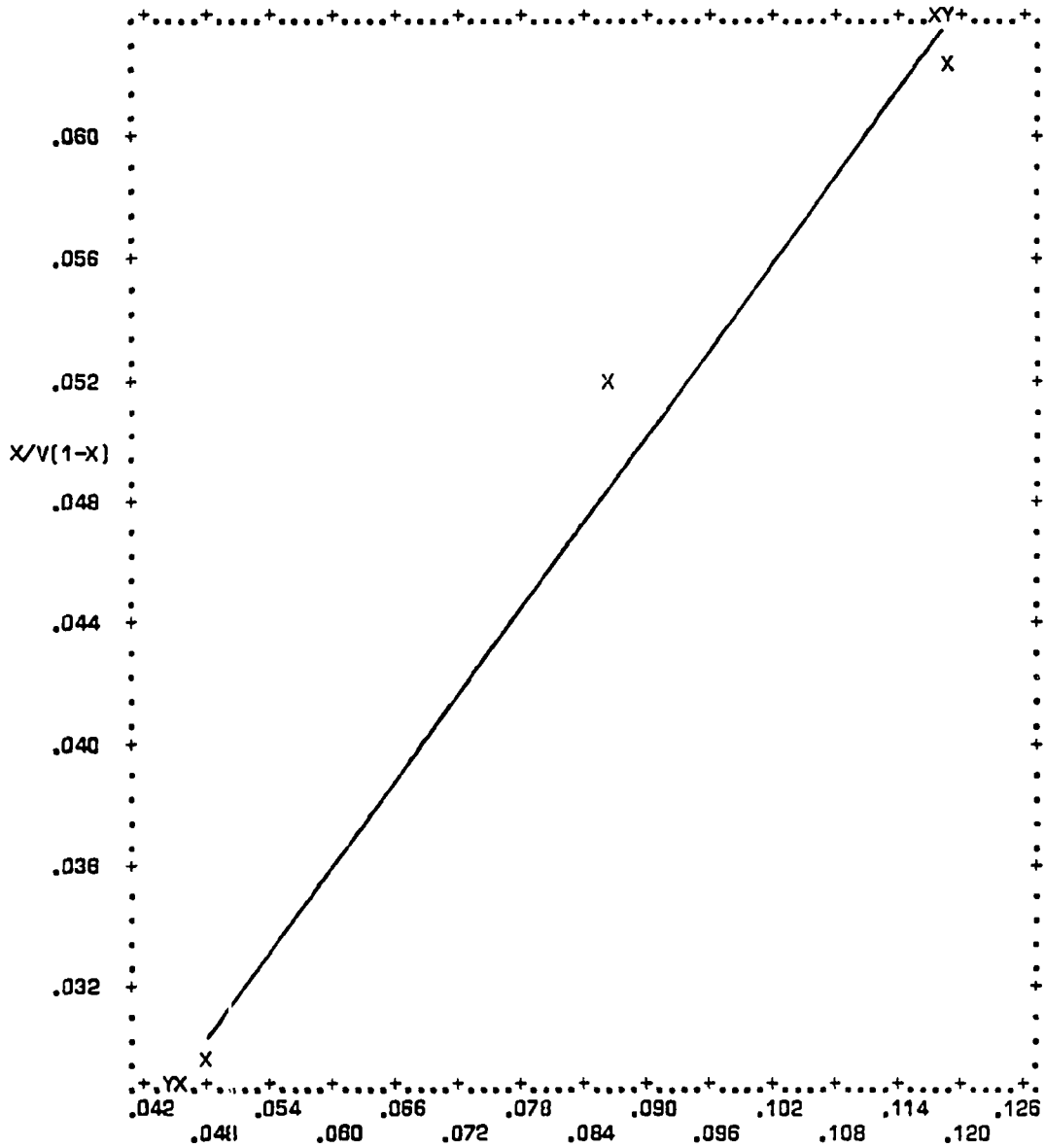


N= 3
 COR= .9984

	MEAN	ST.DEV.	REGRESSION LINE	RES.MS.
X	.08482	.03484	X= 2.2495*Y-.00563	774E-8
Y	.04021	.01548	Y= .44314*X+ .00262	152E-8

VARIABLE 1 P/P0 VERSUS VARIABLE 2 X/V SYMBOL=X

Figure B-23. Plot of BET equation versus relative pressure for Converter A230/0649-B-UR1



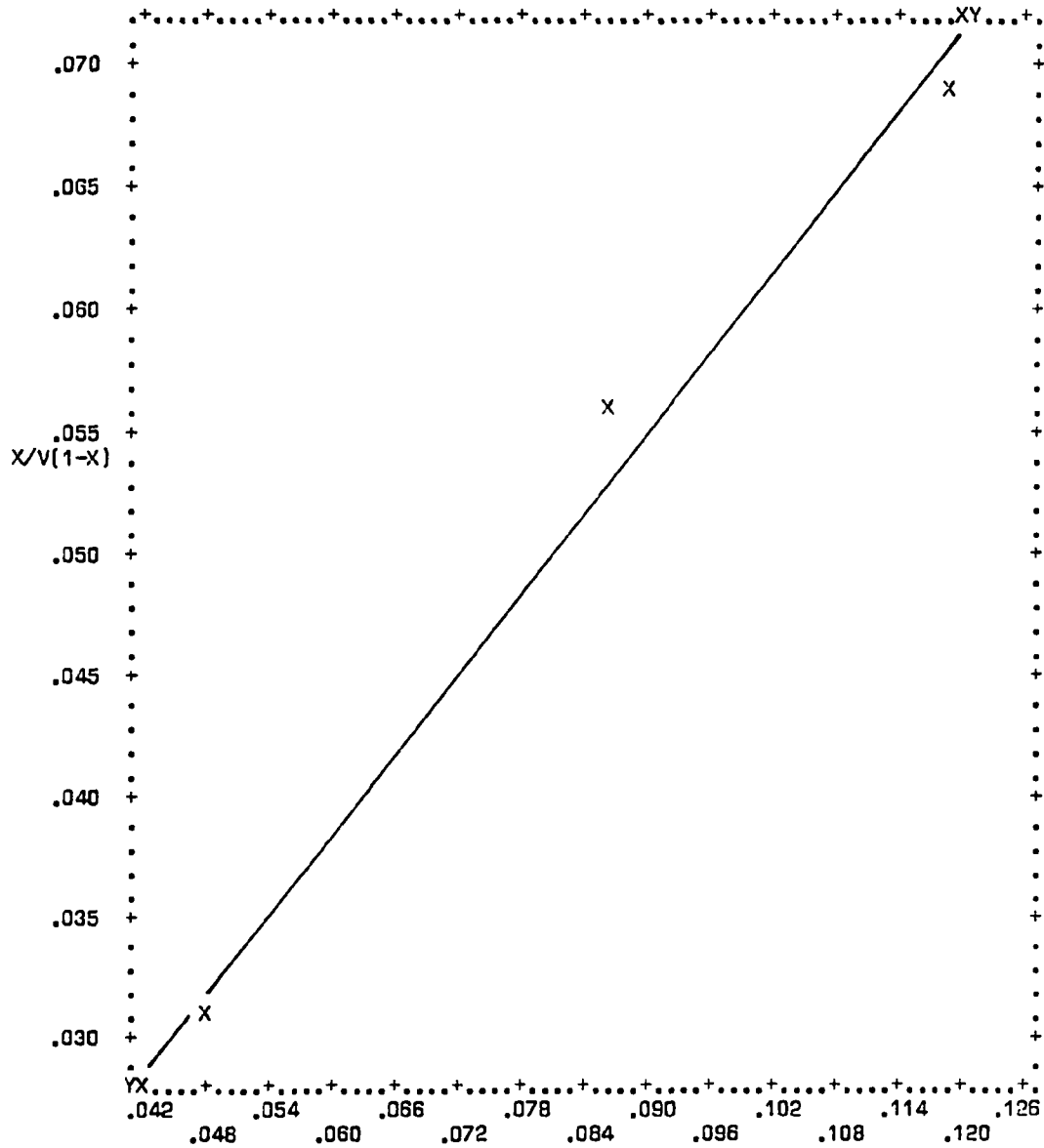
N= 3
COR= .9849

P/P0

	MEAN	ST.DEV.	REGRESSION LINE	RES.MS.
X	.08462	.03514	$X = 2.0612*Y - .01410$	740E-7
Y	.04789	.01679	$Y = .47062*X + .00807$	169E-7

VARIABLE 1 P/F0 VERSUS VARIABLE 2 X/V SYMBOL=X

Figure B-24. Plot of BET equation versus relative pressure for Converter A230/0649-B-UR2

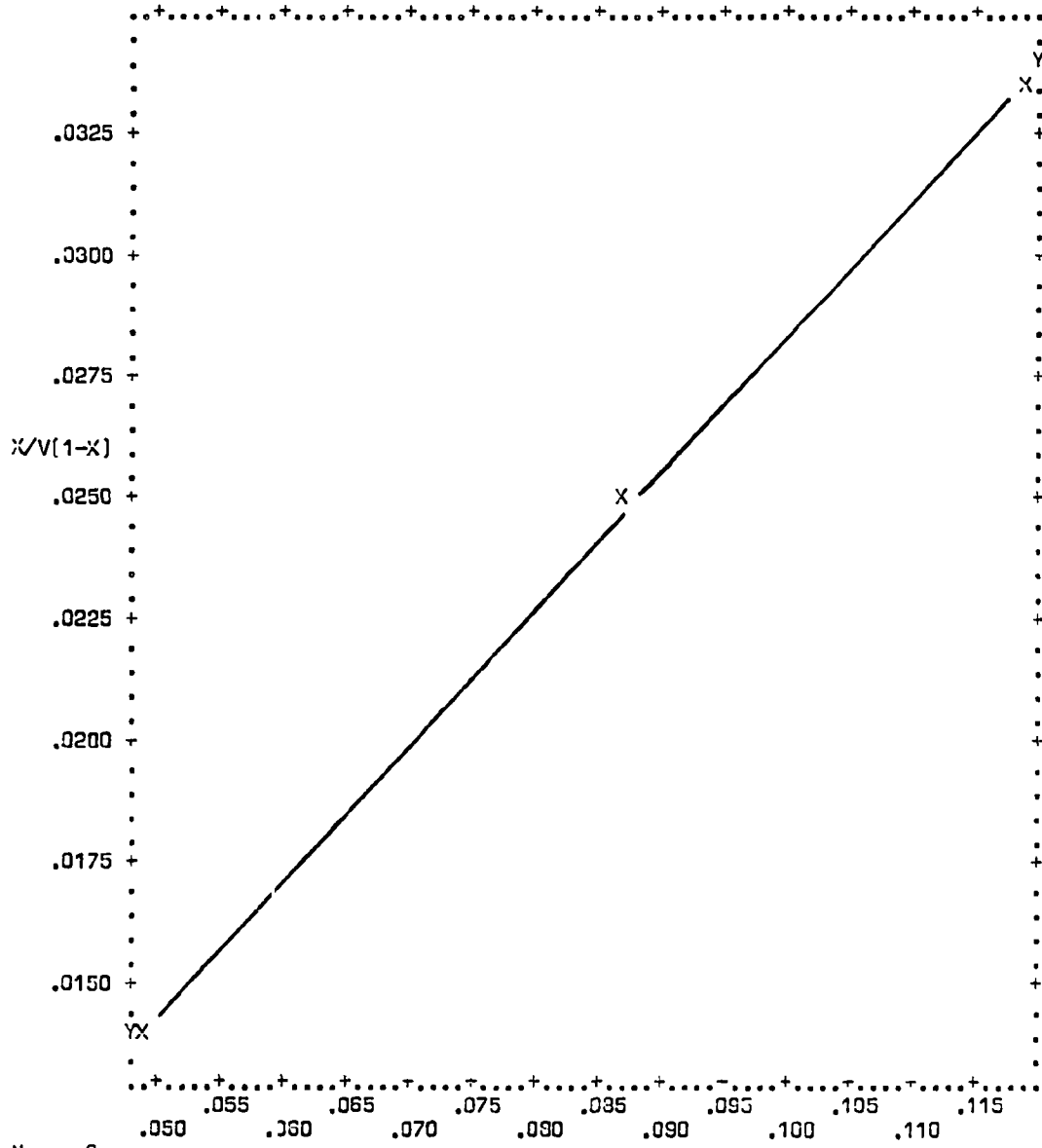


N= 3
 COR= .9903

	MEAN	ST.DEV.	REGRESSION LINE	RES.MS.
X	.08462	.03514	X= 1.7726*Y-.00763	476E-7
Y	.05204	.01963	Y= .55327*X+ .00522	149E-7

VARIABLE 1 P/P0 VERSUS VARIABLE 2 X/V SYMBOL=X

Figure B-25. Plot of BET equation versus relative pressure for Converter A246/0092-A-LL1



N= 3
COR= .9996

	MEAN	ST.DEV.	REGRESSION LINE	RES.MS.
X	.08482	.03484	X= 3.5302*Y-597E-6	204E-8
Y	.02420	.00987	Y= .28303*X+ 109E-6	163E-9

VARIABLE 1 P/P0 VERSUS VARIABLE 2 X/V SYMBOL=X

Figure B-26. Plot of BET equation versus relative pressure for Converter A246/0092-A-LL2

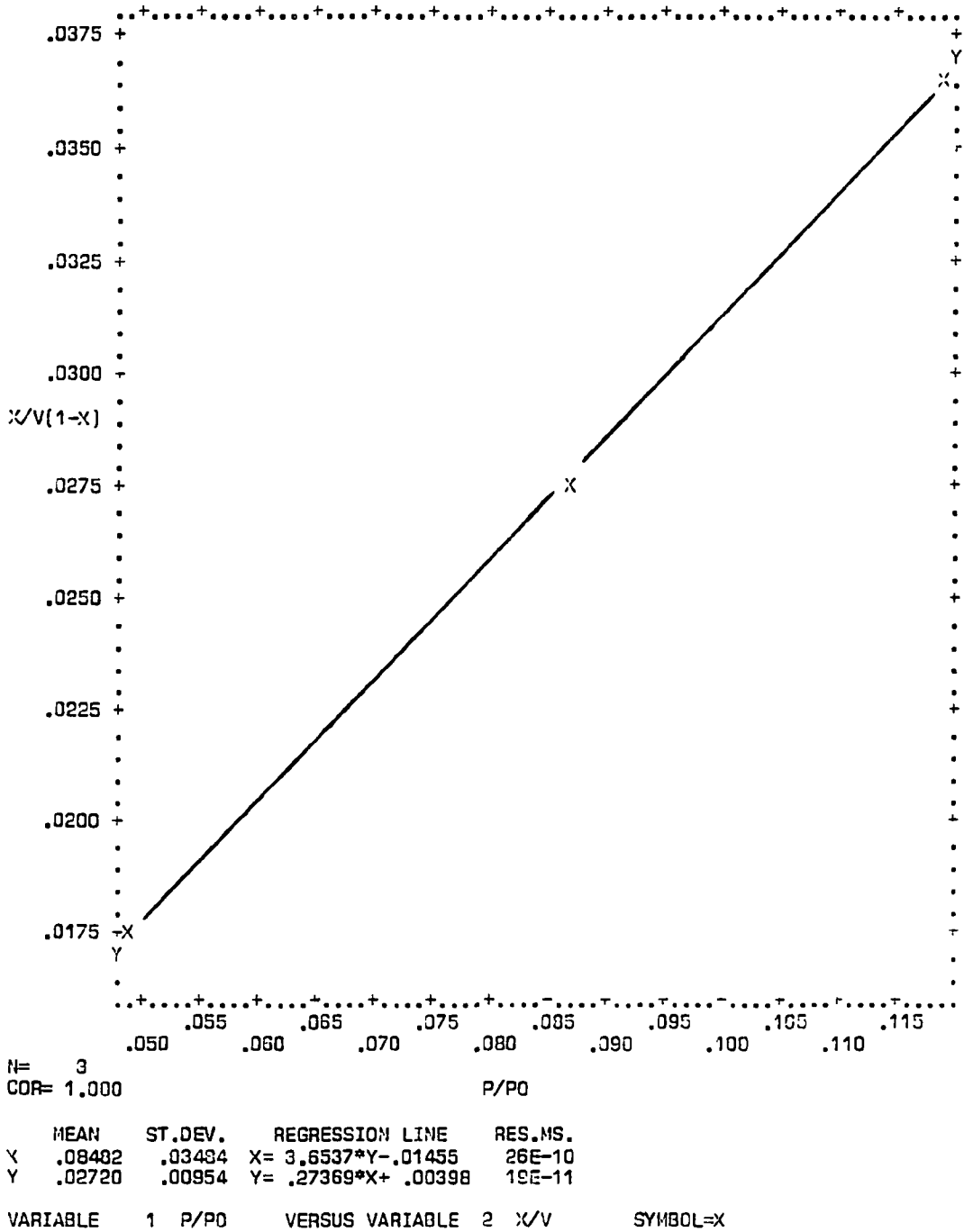


Figure B-27. Plot of BET equation versus relative pressure for Converter A246/0092-A-LL3

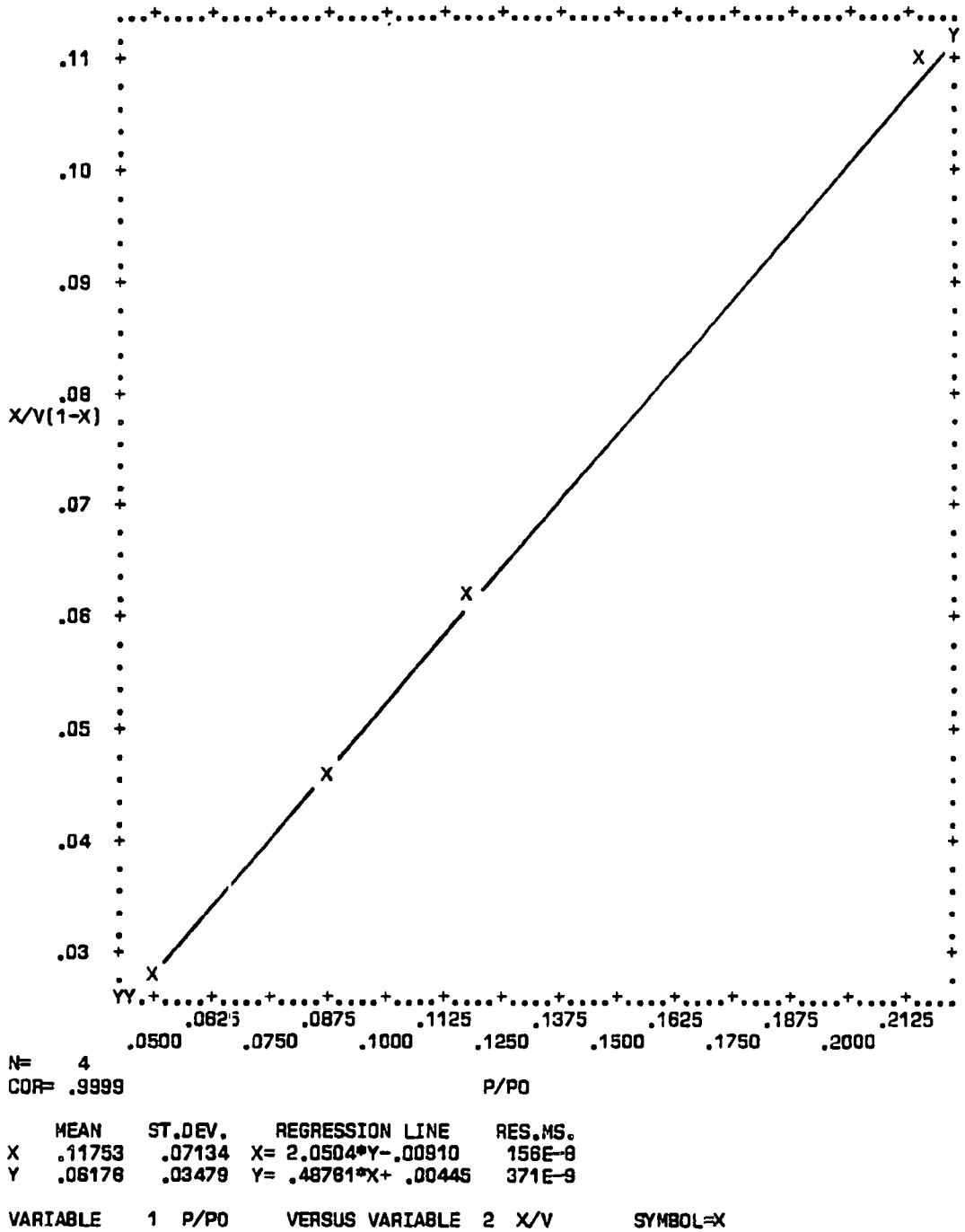
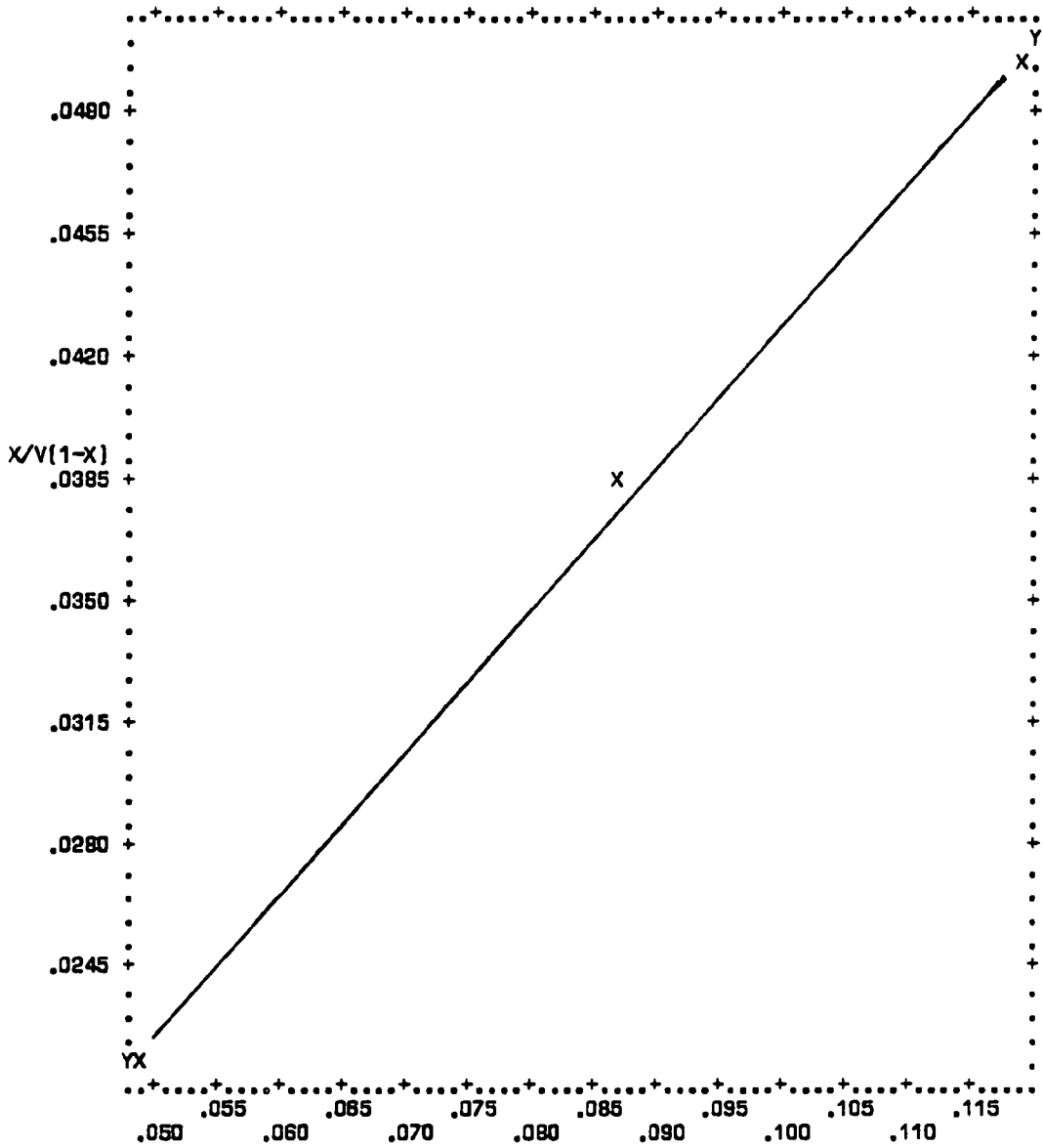


Figure B-28. Plot of BET equation versus relative pressure for Converter A246/0092-A-LL1 (Powder)

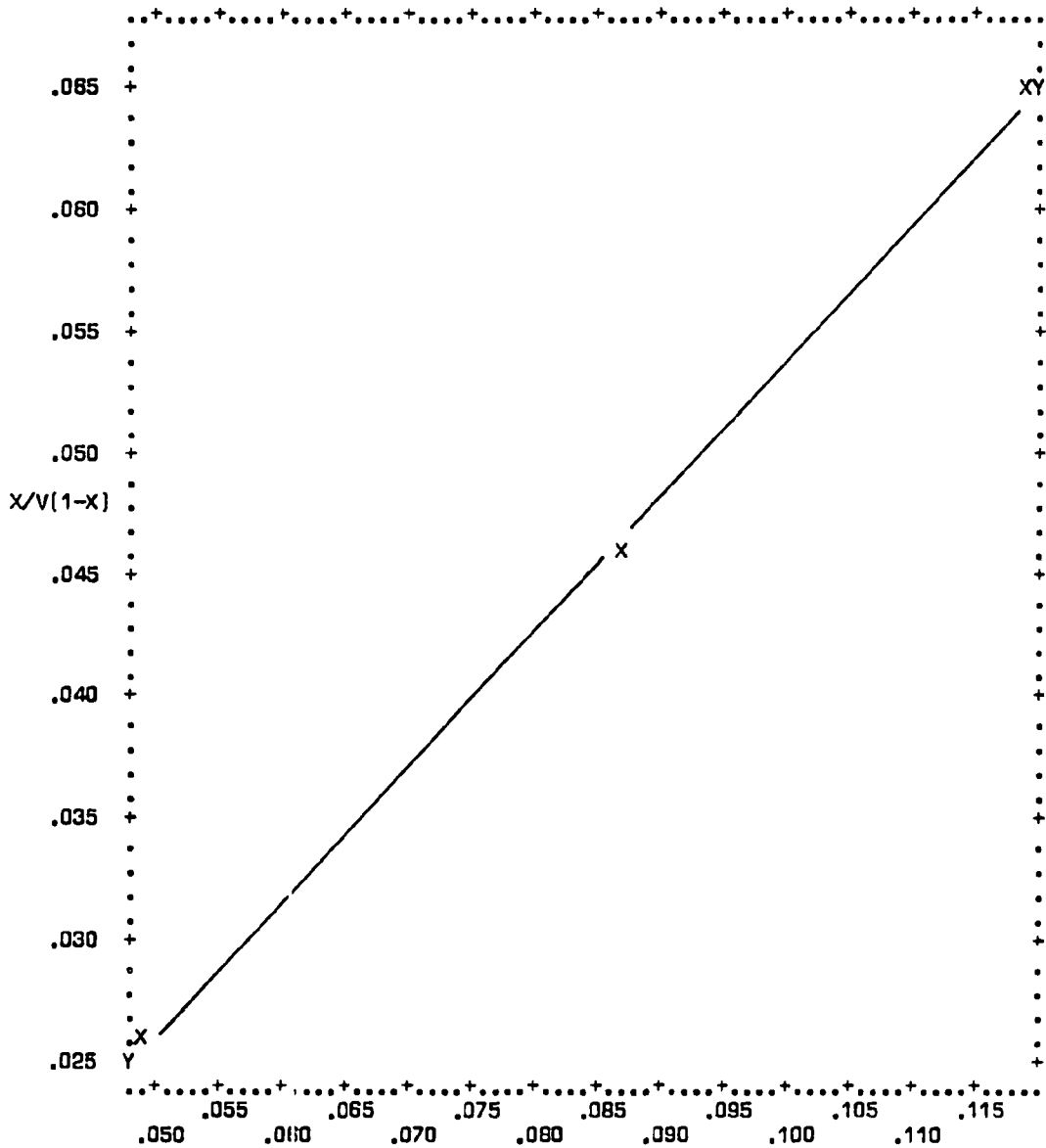


N= 3
 COR= .9984

	MEAN	ST.DEV.	REGRESSION LINE	RES.MS.
X	.08482	.03484	$X = 2.4346*Y - .00474$	782E-8
Y	.03879	.01429	$Y = .40942*X + .00206$	131E-8

VARIABLE 1 P/P0 VERSUS VARIABLE 2 X/V SYMBOL=X

Figure B-29. Plot of BET equation versus relative pressure for Converter A246/0092-B-UR1



N= 3
COR= .9992

P/P0

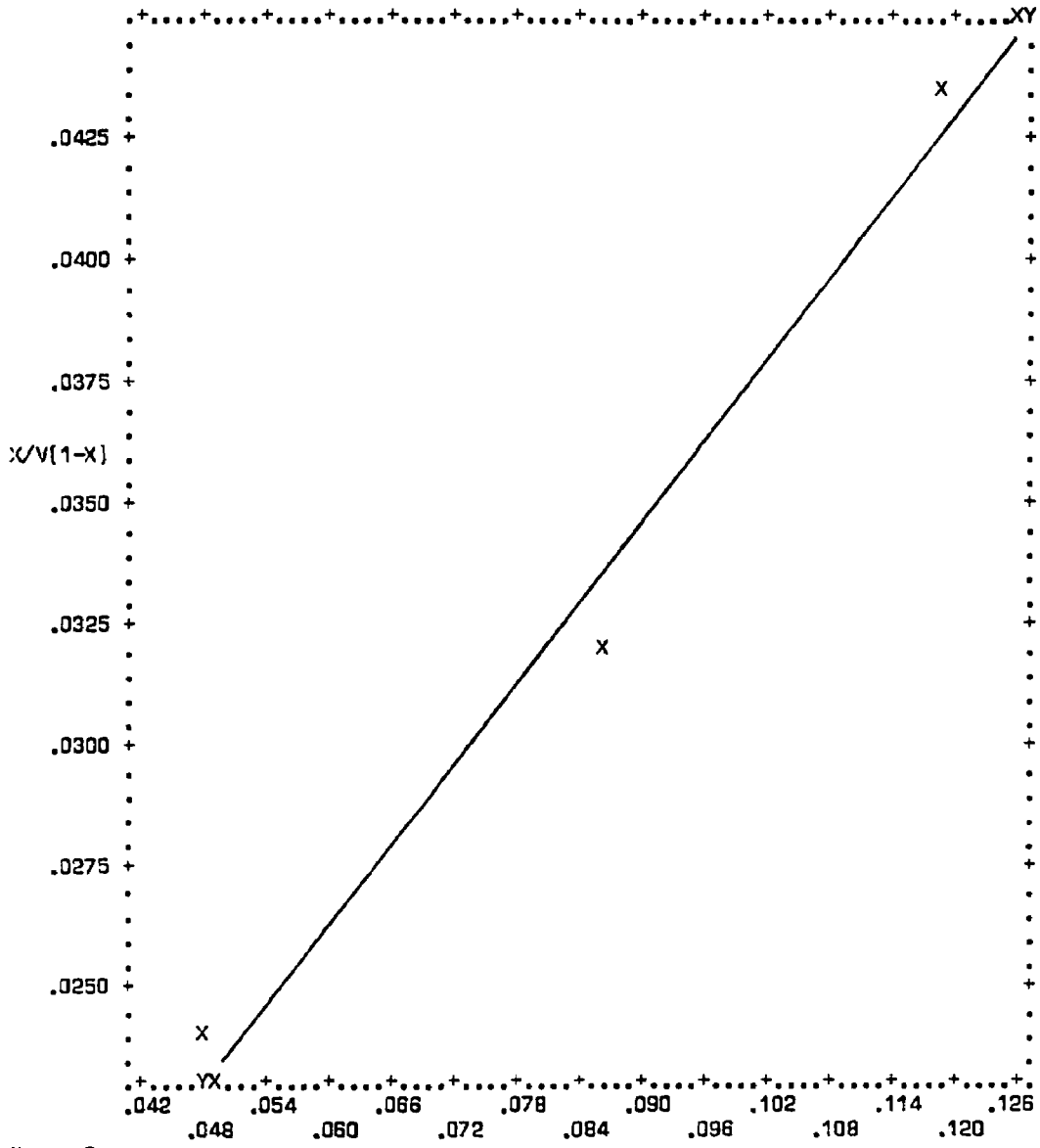
	MEAN	ST.DEV.	REGRESSION LINE	RES.MS.
X	.08482	.03484	X= 1.7999*Y+ .00244	383E-8
Y	.04577	.01934	Y= .55471*X-.00128	118E-8

VARIABLE 1 P/P0 VERSUS VARIABLE 2 X/V SYMBOL=X

Figure B-30. Plot of BET equation versus relative pressure for Converter A246/0092-B-UR2

IDLE

1PAGE 4 CONVERTER SURFACE AREA ANALYSIS A240/0007-A LL-1



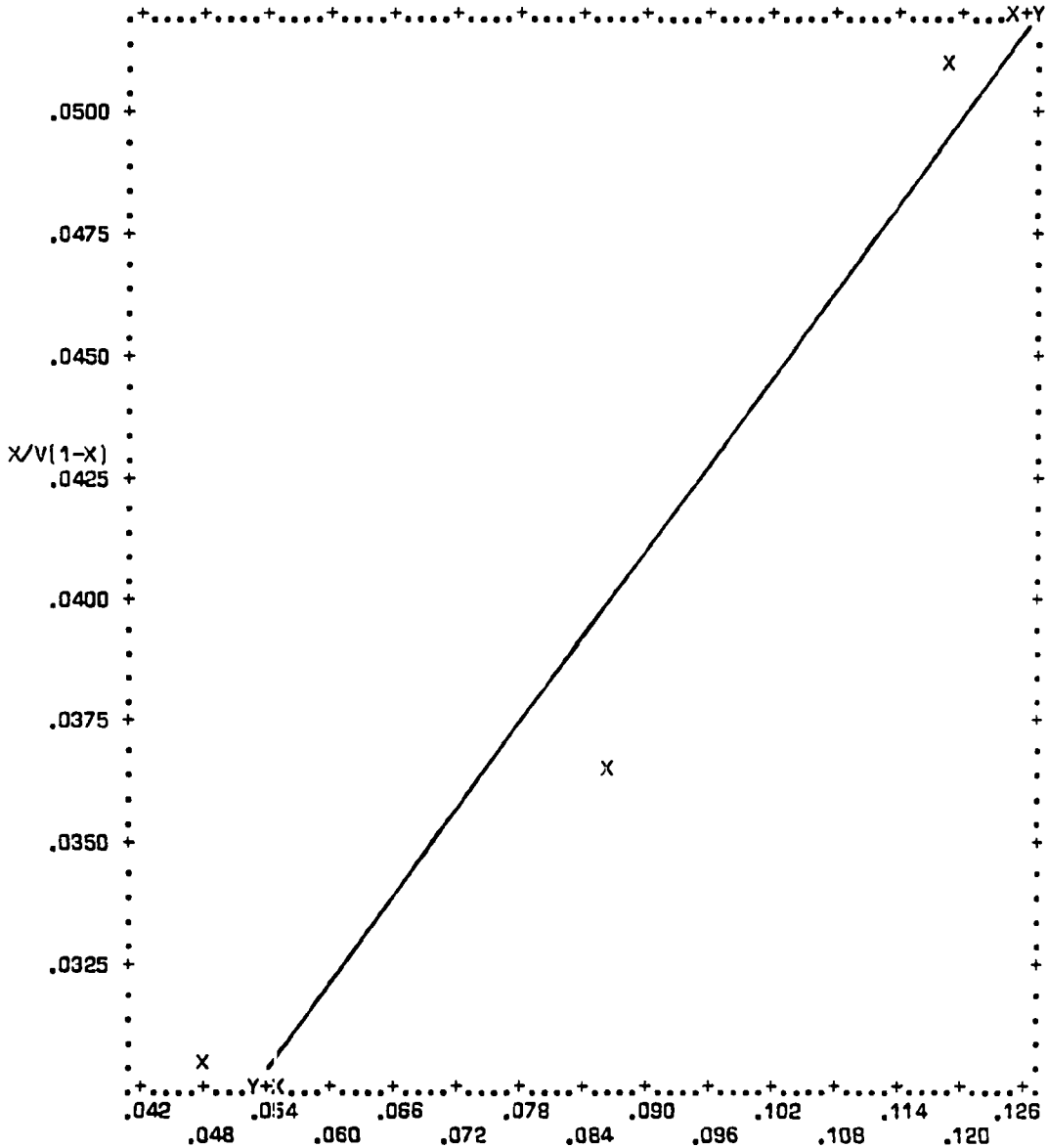
N= 3
COR= .9859

P/P0

	MEAN	ST.DEV.	REGRESSION LINE	RES.MS.
X	.08483	.03515	X= 3.5148*Y-.03189	694E-7
Y	.03315	.00988	Y= .27652*X+ .00975	548E-8

VARIABLE 1 P/P0 VERSUS VARIABLE 2 X/V SYMBOL=X

Figure B-31. Plot of BET equation versus relative pressure for Converter A240/0007-A-LL1



N= 3
COR= .9597

P/P0

	MEAN	ST.DEV.	REGRESSION LINE	RES.MS.
X	.08462	.03514	$X = 3.1485*Y - .03915$	195E-6
Y	.03931	.01071	$Y = .29254*X + .01455$	181E-7

VARIABLE 1 P/P0 VERSUS VARIABLE 2 X/V SYMBOL=X

Figure B-32. Plot of BET equation versus relative pressure for Converter A240/0007-A-LL2

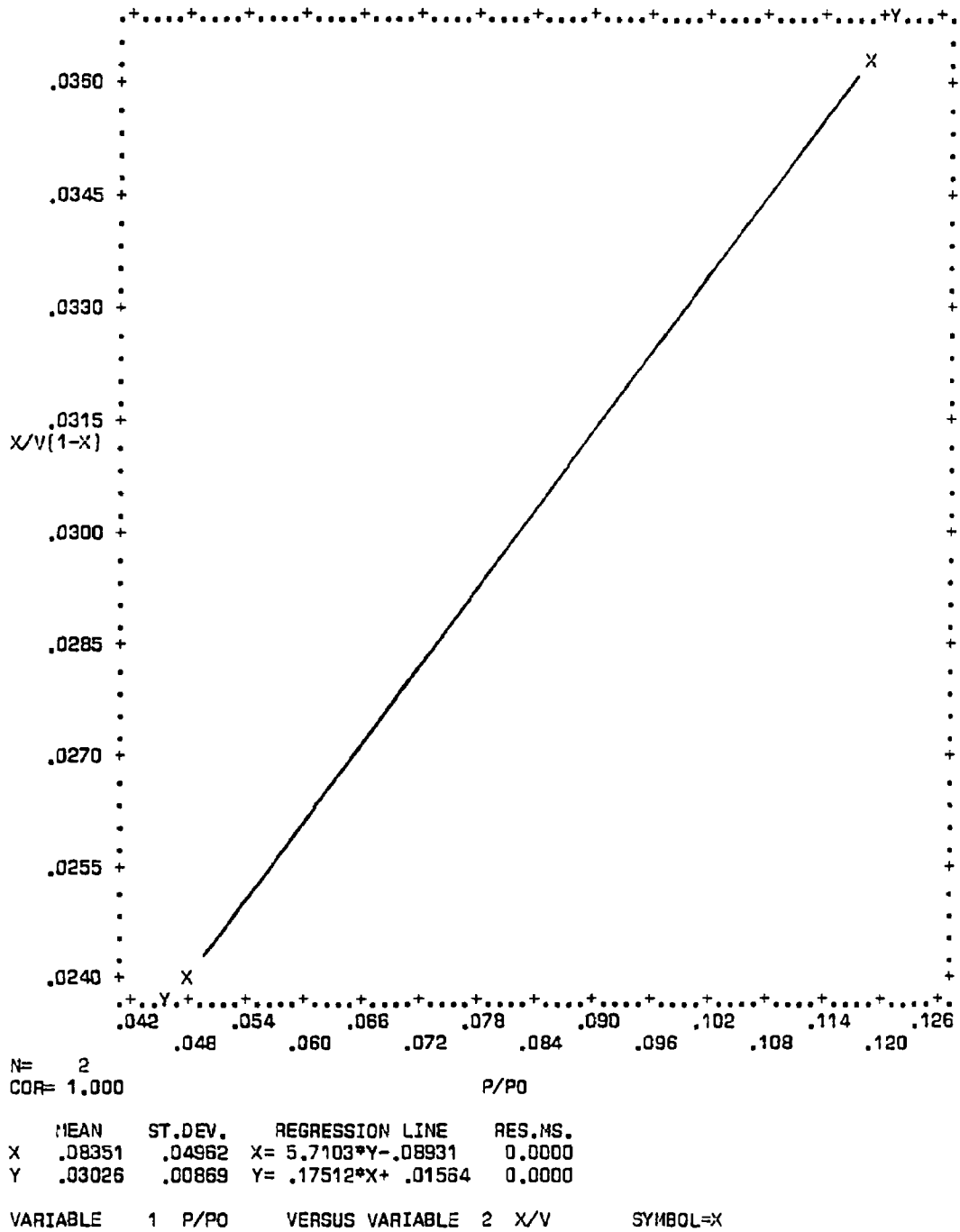
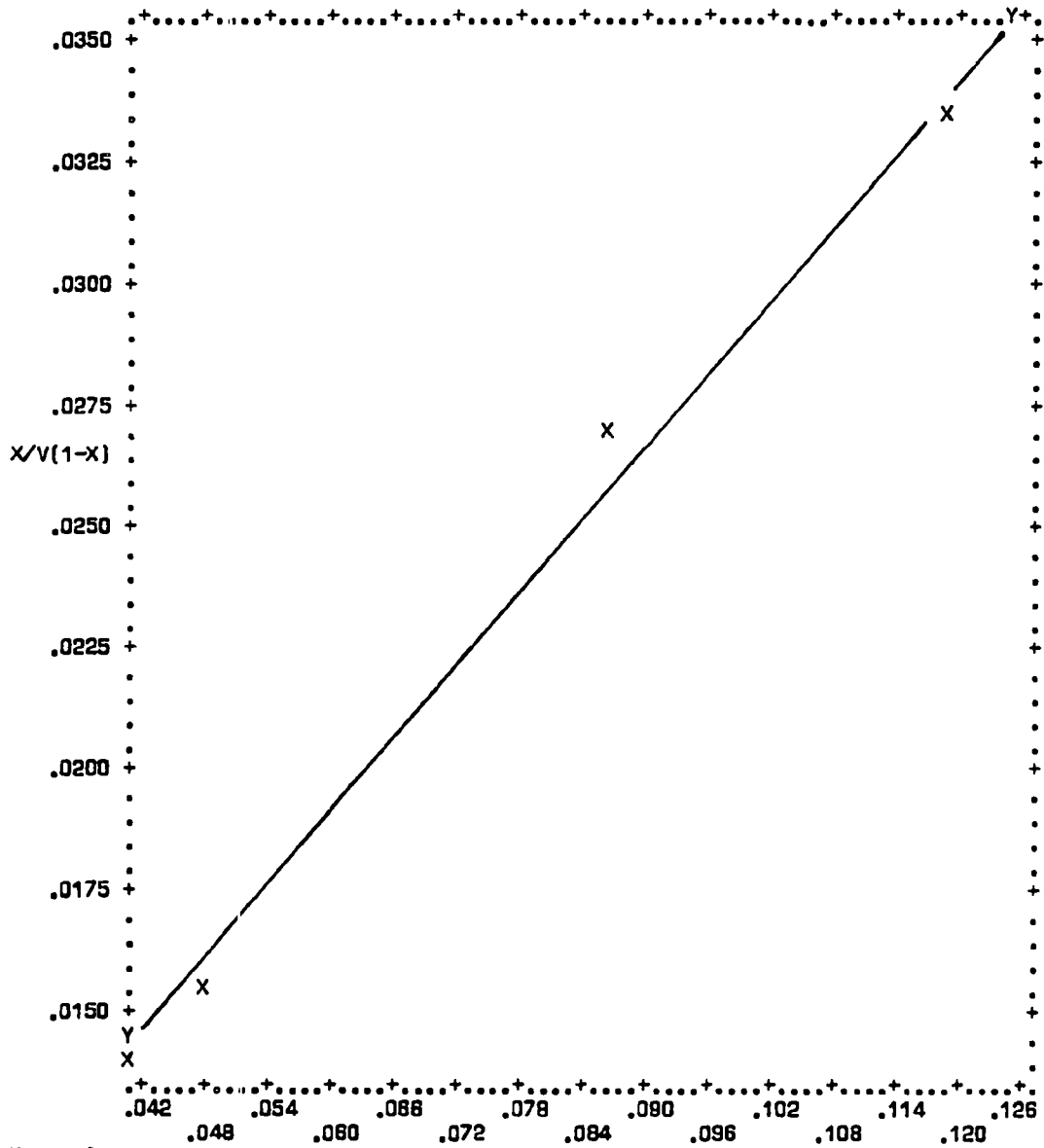


Figure B-33. Plot of BET equation versus relative pressure for Converter A240/0007-A-LL3



N= 3
 COR= .9936

	MEAN	ST.DEV.	REGRESSION LINE	RES.MS.
X	.08482	.03514	X= 3.9137*Y-.01458	315E-7
Y	.02535	.00892	Y= .25225*X+.00400	203E-8

VARIABLE 1 P/P0 VERSUS VARIABLE 2 X/V SYMBOL=X

Figure B-34. Plot of BET equation versus relative pressure for Converter A240/0007-A-LL1 (Powder)

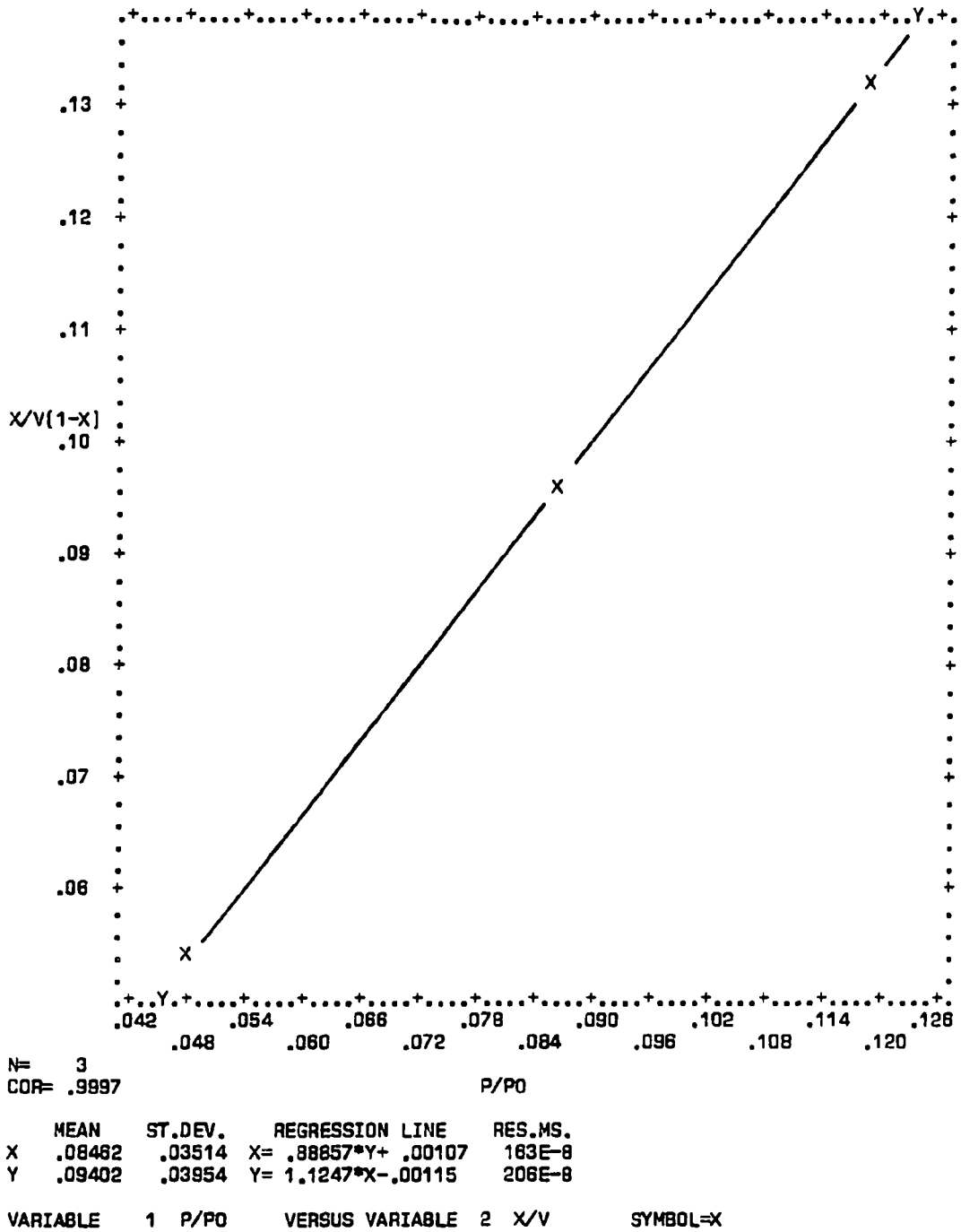
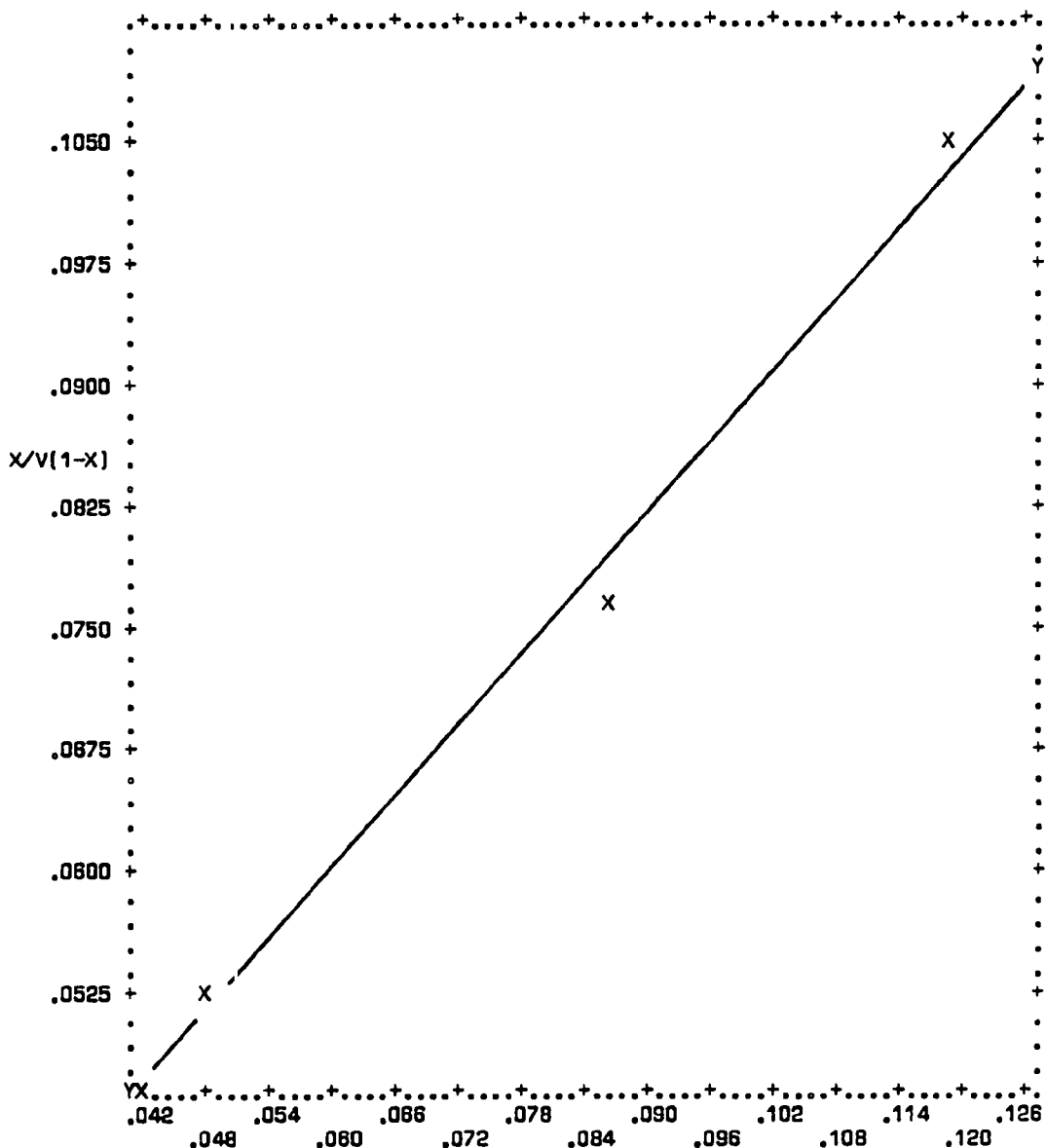


Figure B-35. Plot of BET equation versus relative pressure for Converter A240/0007-B-UR1

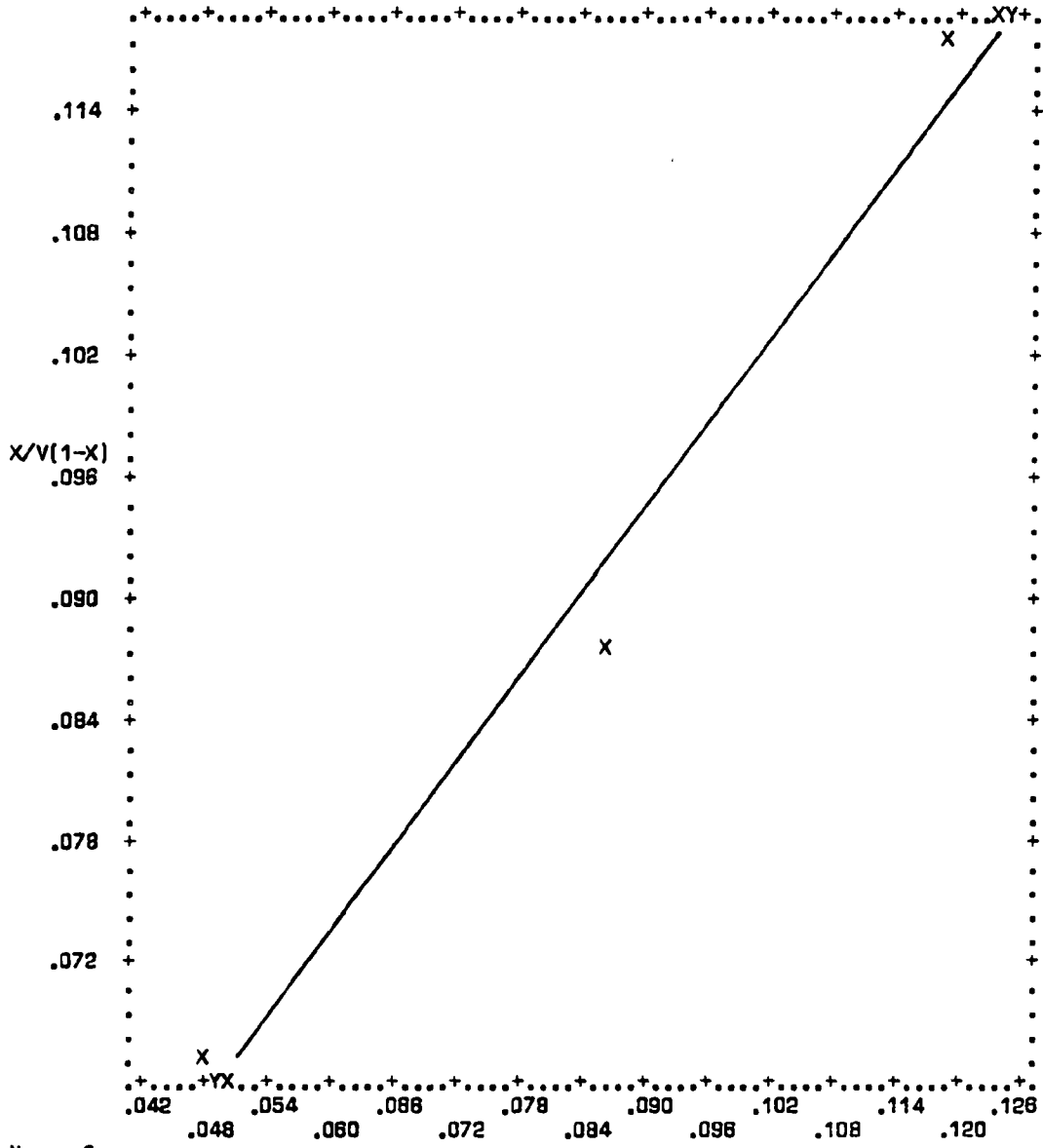


$\bar{r} = 3$
 COR = .9951

	MEAN	ST.DEV.	REGRESSION LINE	RES.MS.
X	.08462	.03514	$X = 1.3492*Y - .02098$	240E-7
Y	.07827	.02592	$Y = .73398*X + .01616$	131E-7

VARIABLE 1 P/P0 VERSUS VARIABLE 2 X/V SYMBOL=X

Figure B-36. Plot of BET equation versus relative pressure for Converter A240/0007-B-UR2

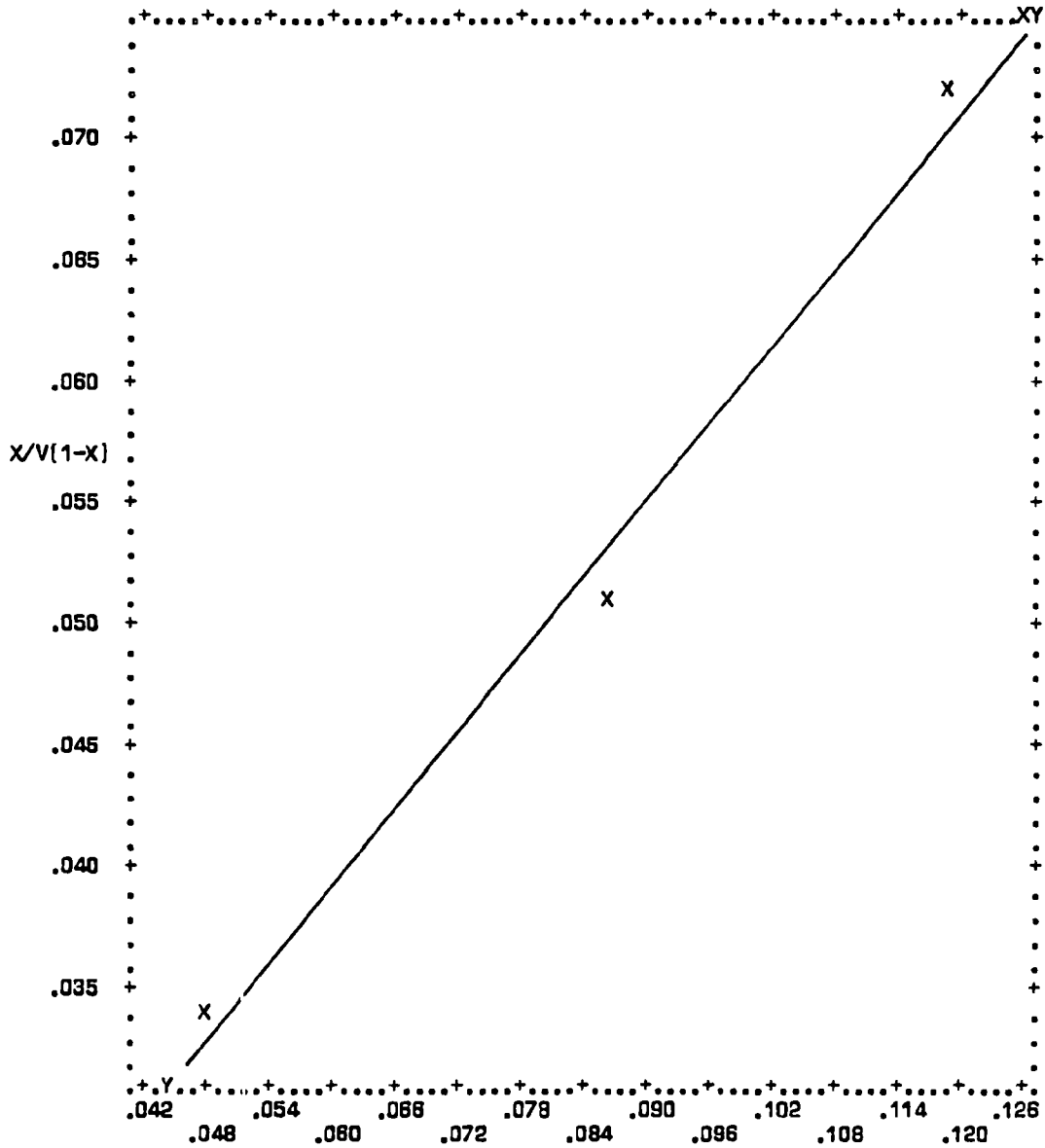


$N = 3$
 $COR = .9873$

	MEAN	ST.DEV.	REGRESSION LINE	RES.MS.
X	.08483	.03515	$X = 1.3838 * Y - .04078$	623E-7
Y	.09083	.02508	$Y = .70442 * X + .03101$	317E-7

VARIABLE 1 P/P0 VERSUS VARIABLE 2 X/V SYMBOL=X

Figure B-37. Plot of BET equation versus relative pressure for Converter A240/0270-A-LL1



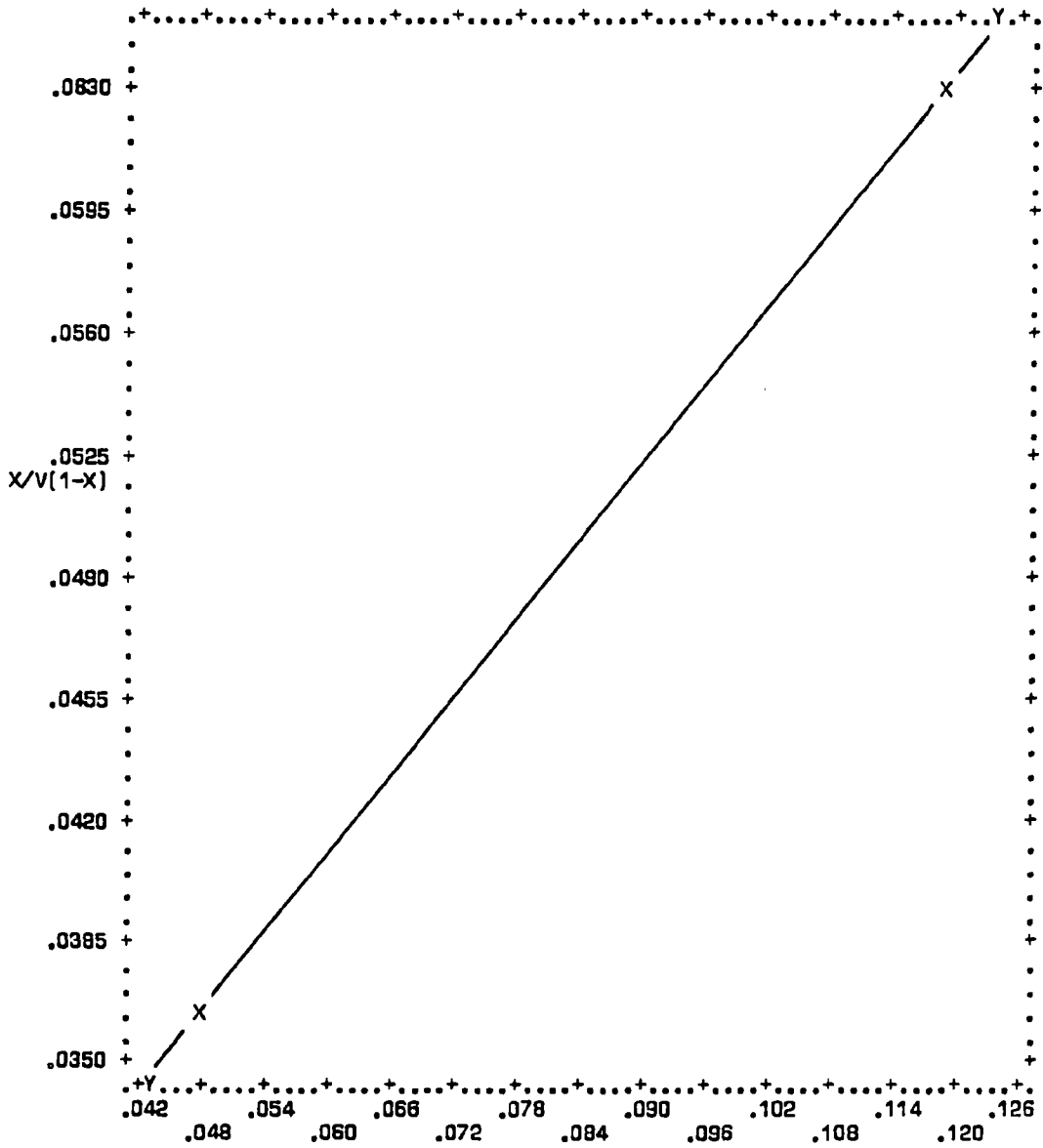
N= 3
COR= .9939

P/P0

	MEAN	ST.DEV.	REGRESSION LINE	RES.MS.
X	.08462	.03514	X= 1.8608*Y-.01317	303E-7
Y	.05255	.01877	Y= .53081*X+ .00783	883E-8

VARIABLE 1 P/P0 VERSUS VARIABLE 2 X/V SYMBOL=X

Figure B-38. Plot of BET equation versus relative pressure for Converter A240/0270-A-LL2



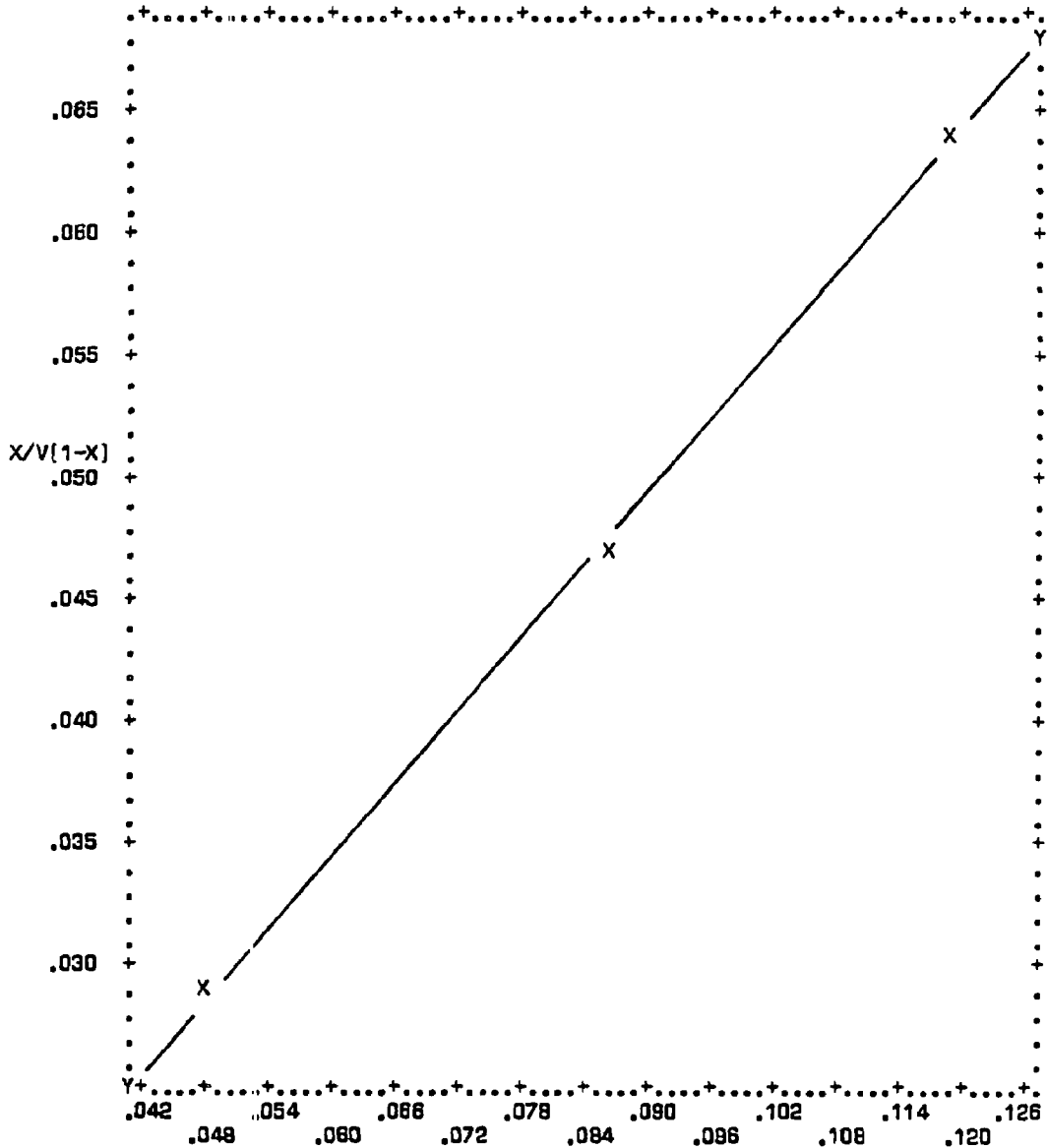
N= 2
COR= 1.000

P/P0

	MEAN	ST.DEV.	REGRESSION LINE	RES.MS.
X	.08351	.04962	X= 2.8177*Y-.04702	0.0000
Y	.04888	.01898	Y= .38202*X+.01796	0.0000

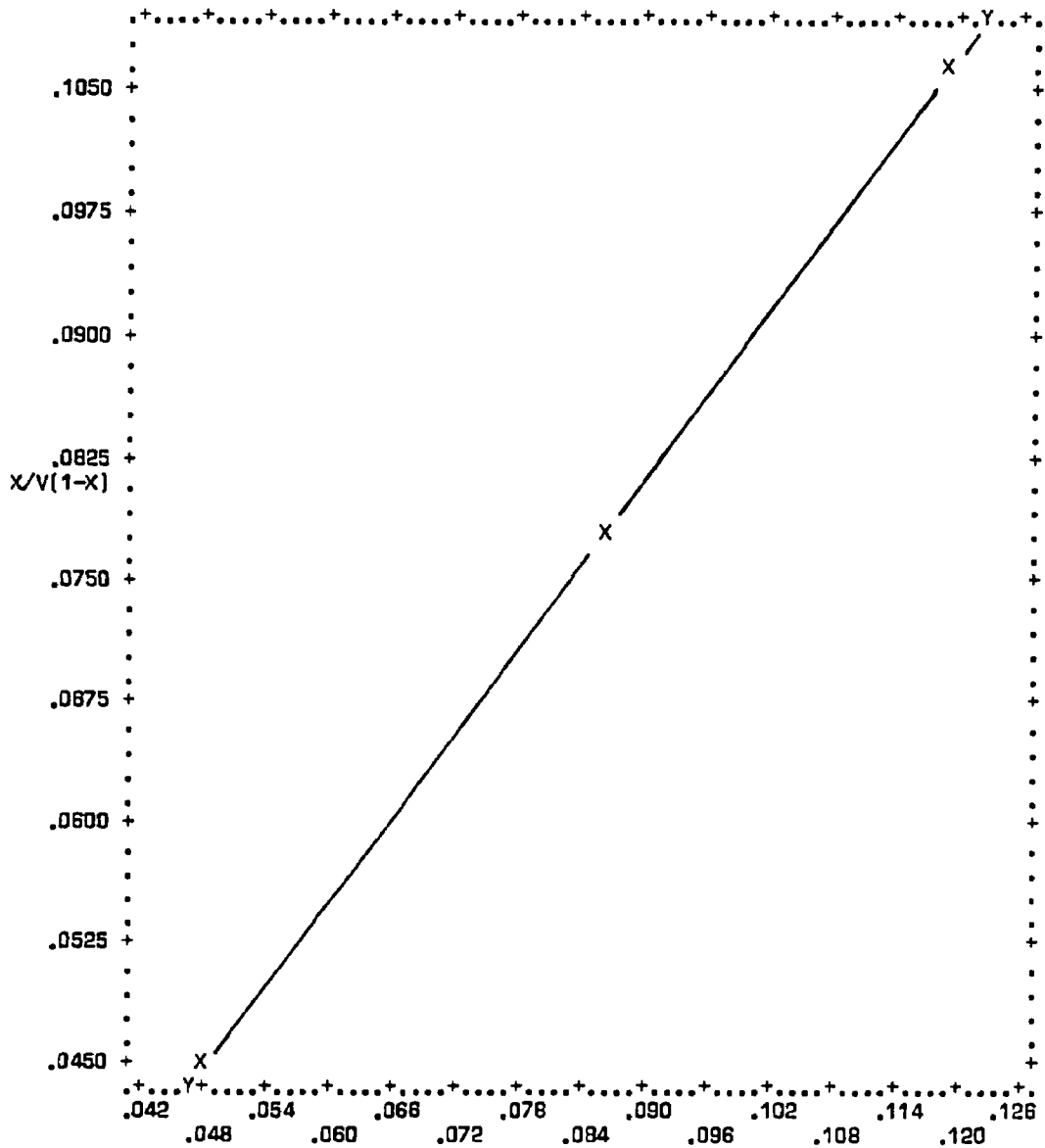
VARIABLE 1 P/P0 VERSUS VARIABLE 2 X/V SYMBOL=X

Figure B-39. Plot of BET equation versus relative pressure for Converter A240/0270-A-LL3



N=	3			
COR=	.9999			P/P0
	MEAN	ST.DEV.	REGRESSION LINE	RES.MS.
X	.08461	.03514	X= 2.0098*Y-.00915	563E-9
Y	.04665	.01748	Y= .49745*X+.00456	139E-9
VARIABLE	1	P/P0	VERSUS VARIABLE	2 X/V
				SYMBOL=X

Figure B-40. Plot of BET equation versus relative pressure for Converter A240/0270-A-LL1 (Powder)



N= 3
COR= .9998

P/P0

	MEAN	ST.DEV.	REGRESSION LINE	RES.MS.
X	.08462	.03514	X= 1.1453*Y-.00267	102E-8
Y	.07622	.03068	Y= .87278*X+.00237	775E-9

VARIABLE 1 P/P0 VERSUS VARIABLE 2 X/V SYMBOL=X

Figure B-41. Plot of BET equation versus relative pressure for Converter A240/0270-B-UR1

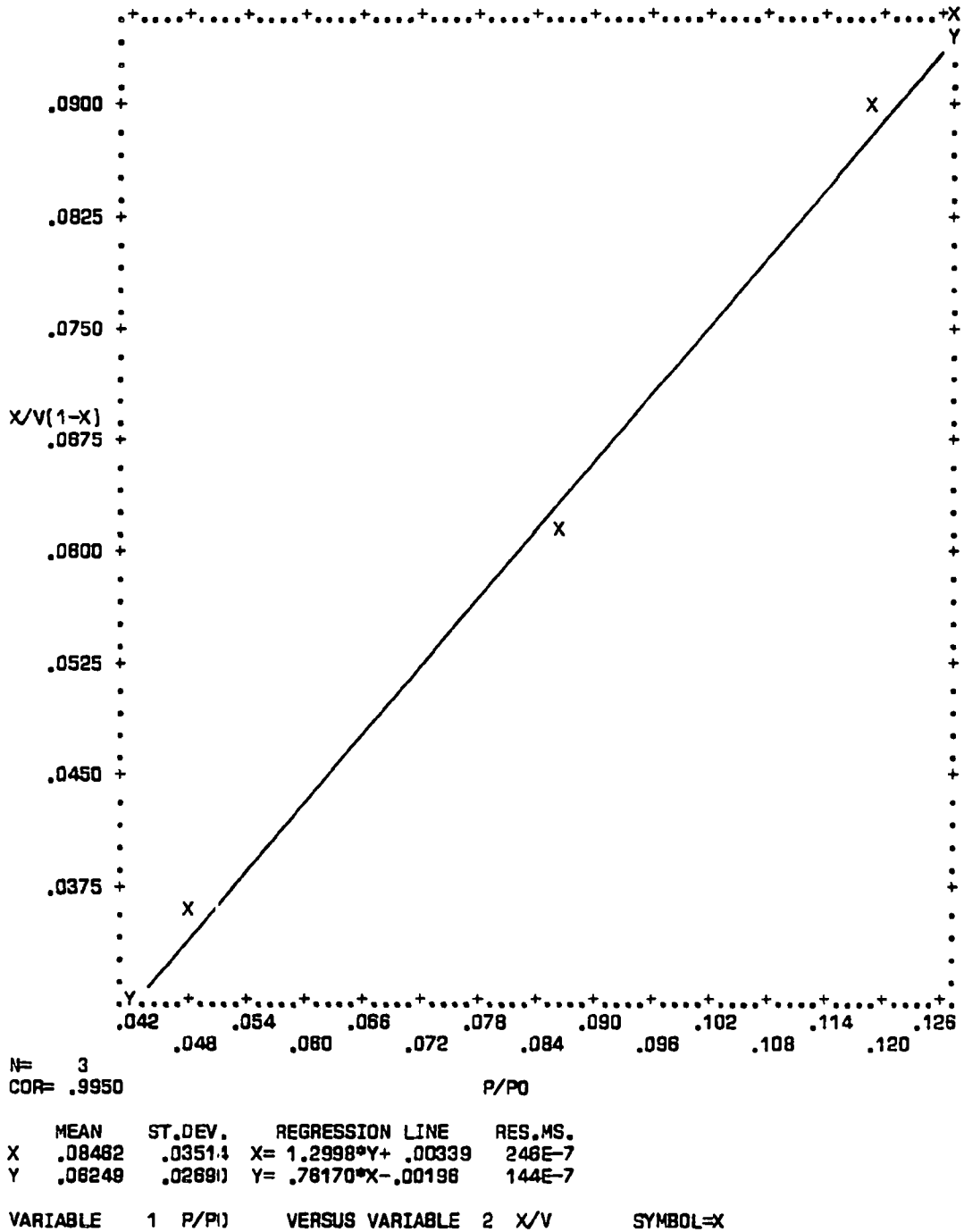


Figure B-42. Plot of BET equation versus relative pressure for Converter A240/0270-B-UR2

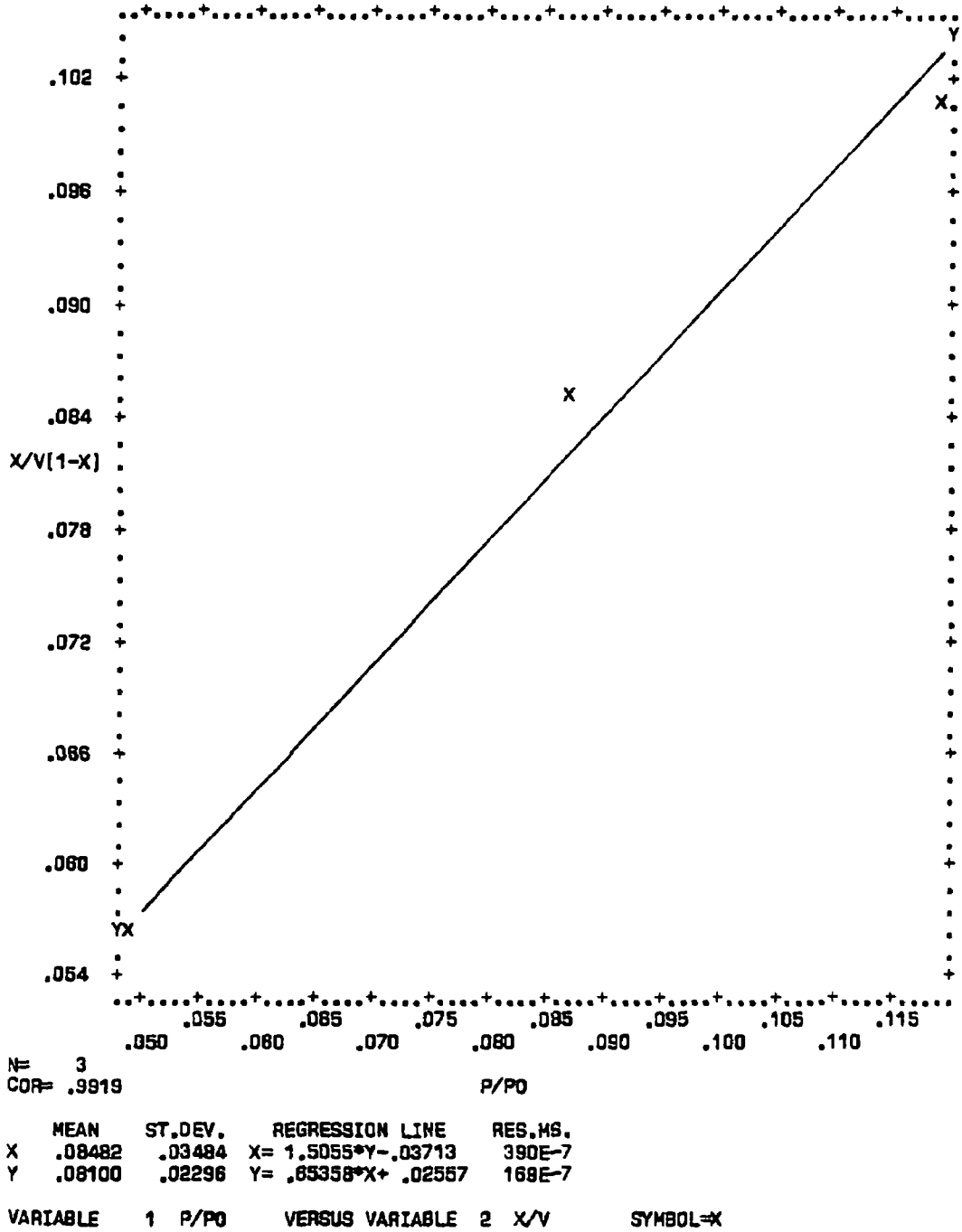
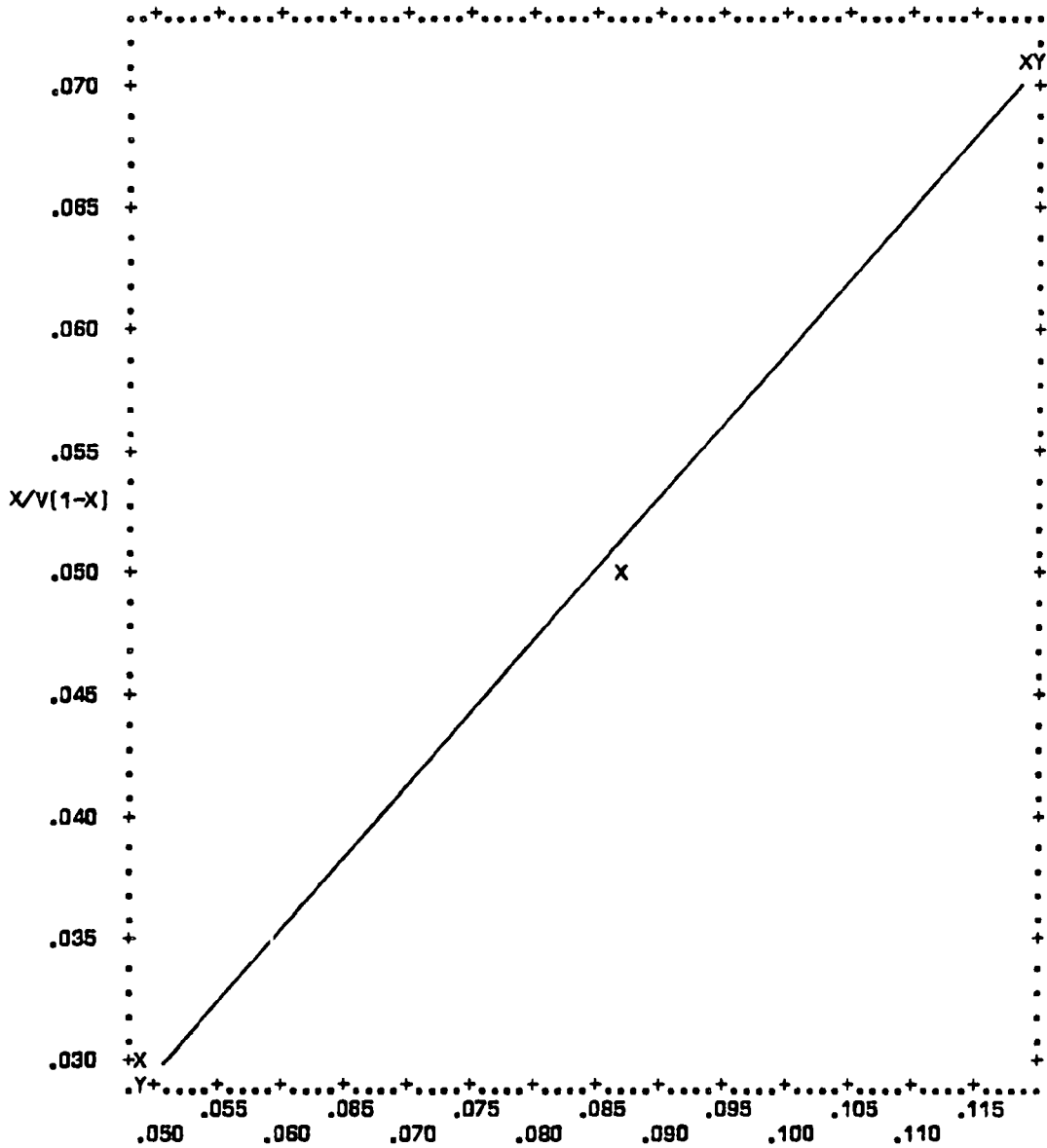


Figure B-43. Plot of BET equation versus relative pressure for Converter A254/0037-A-LL1



N= 3
COR= .9989

P/P0

	MEAN	ST.DEV.	REGRESSION LINE	RES.MS.
X	.08482	.03484	$X = 1.8984 * Y - 315E-6$	545E-8
Y	.05013	.02048	$Y = .58747 * X + 297E-6$	188E-8

VARIABLE 1 P/P0 VERSUS VARIABLE 2 X/V SYMBOL=X

Figure B-44. Plot of BET equation versus relative pressure for Converter A254/0037-A-LL2

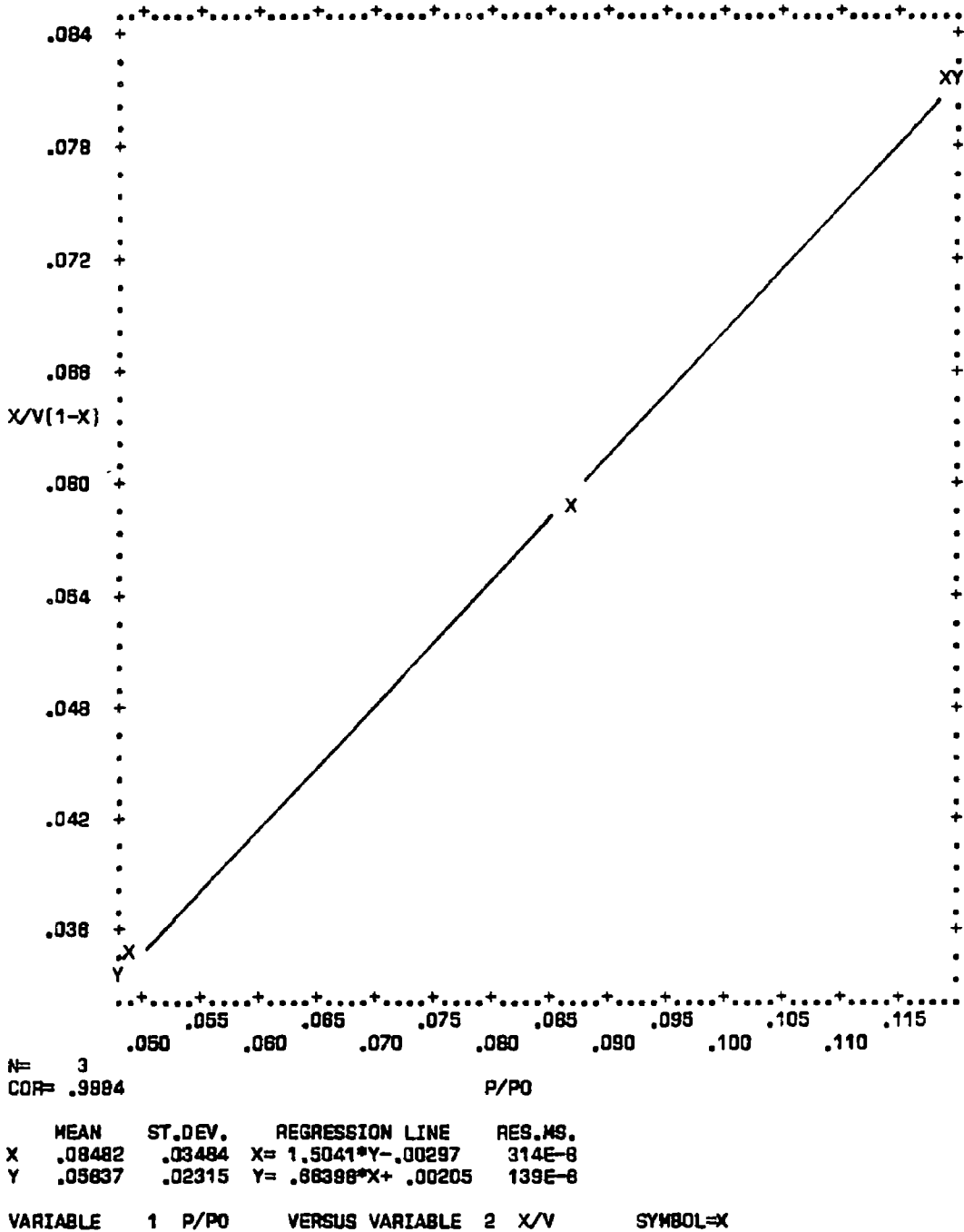
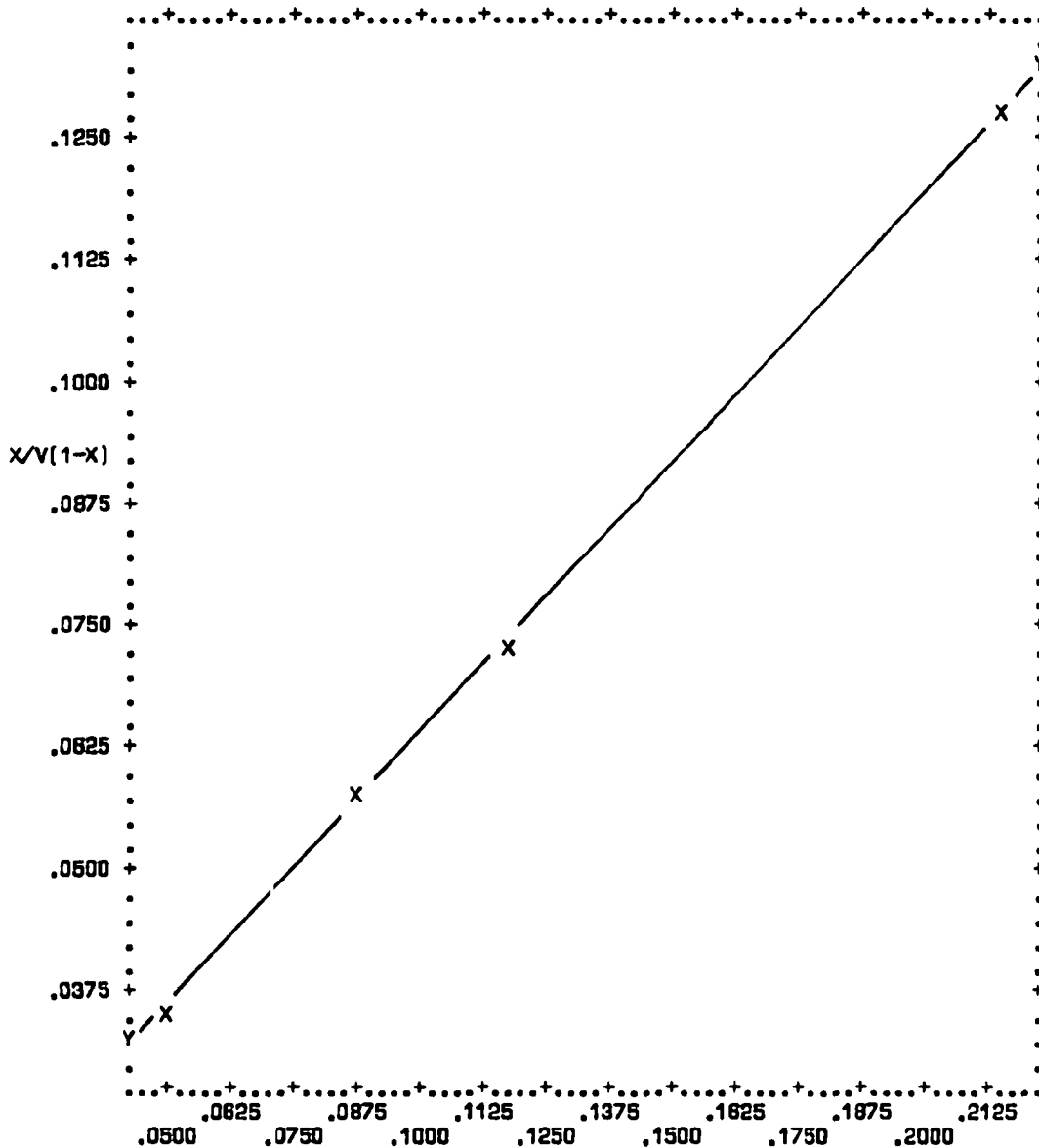


Figure B-45. Plot of BET equation versus relative pressure for Converter A254/0037-A-LL3

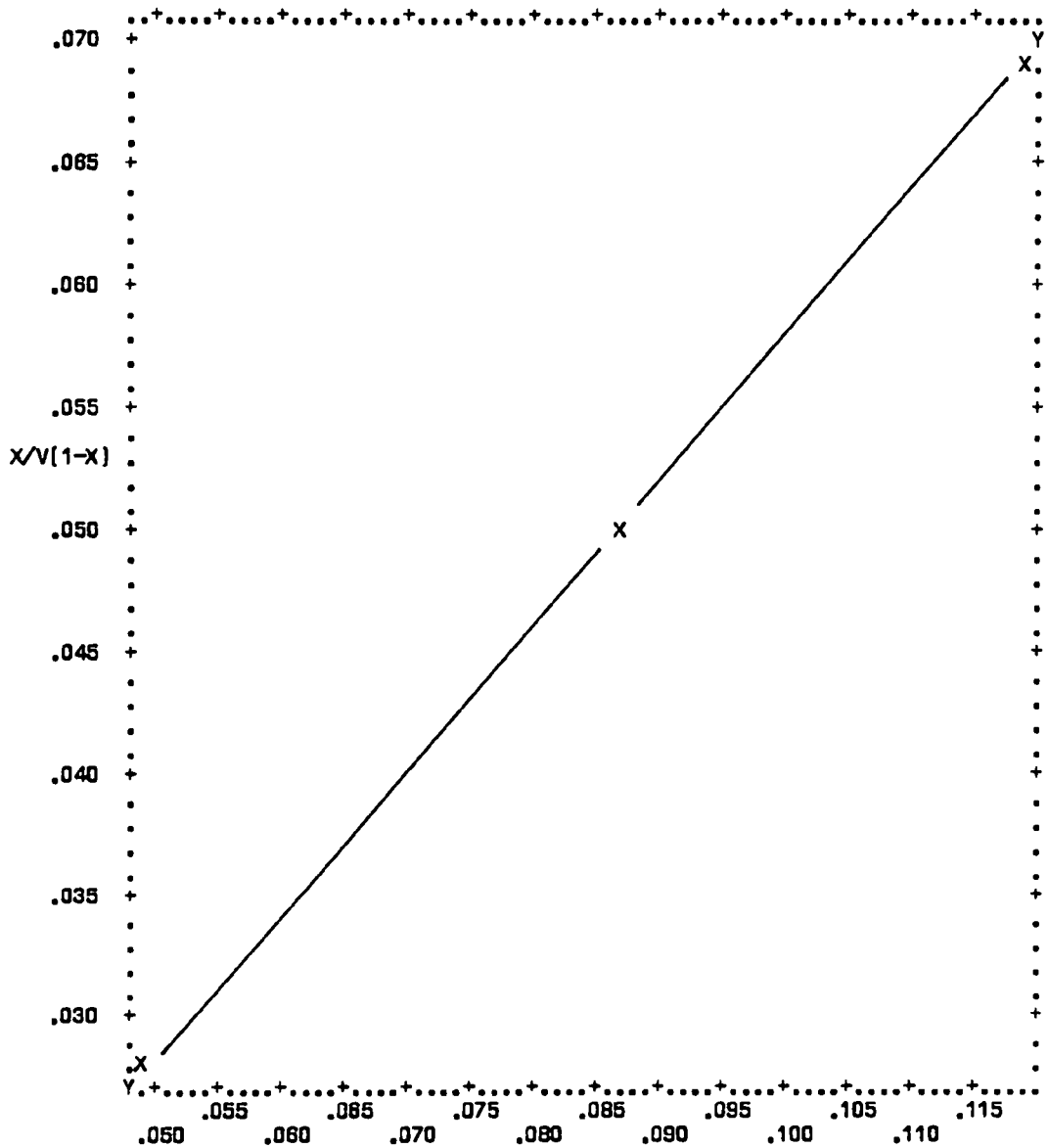


N= 4
 COR= .9993 P/P0

	MEAN	ST.DEV.	REGRESSION LINE	RES.MS.
X	.11751	.07132	$\hat{y} = 1.7938 * Y - .01359$	111E-7
Y	.07309	.03973	$\hat{y} = .55888 * X + .00787$	343E-8

VARIABLE 1 P/P0 VERSUS VARIABLE 2 X/V SYMBOL=X

Figure B-46. Plot of BET equation versus relative pressure for Converter A254/0037-A-LL1 (Powder)



N= 3
COR= .9998 P/P0

	MEAN	ST.DEV.	REGRESSION LINE	RES.MS.
X	.08482	.03484	X= 1.8950*Y+ .00173	762E-9
Y	.04902	.02055	Y= .58879*X-.00101	285E-9

VARIABLE 1 P/P0 VERSUS VARIABLE 2 X/V SYMBOL=X

Figure B-47. Plot of BET equation versus relative pressure for Converter A254/0037-B-UR1

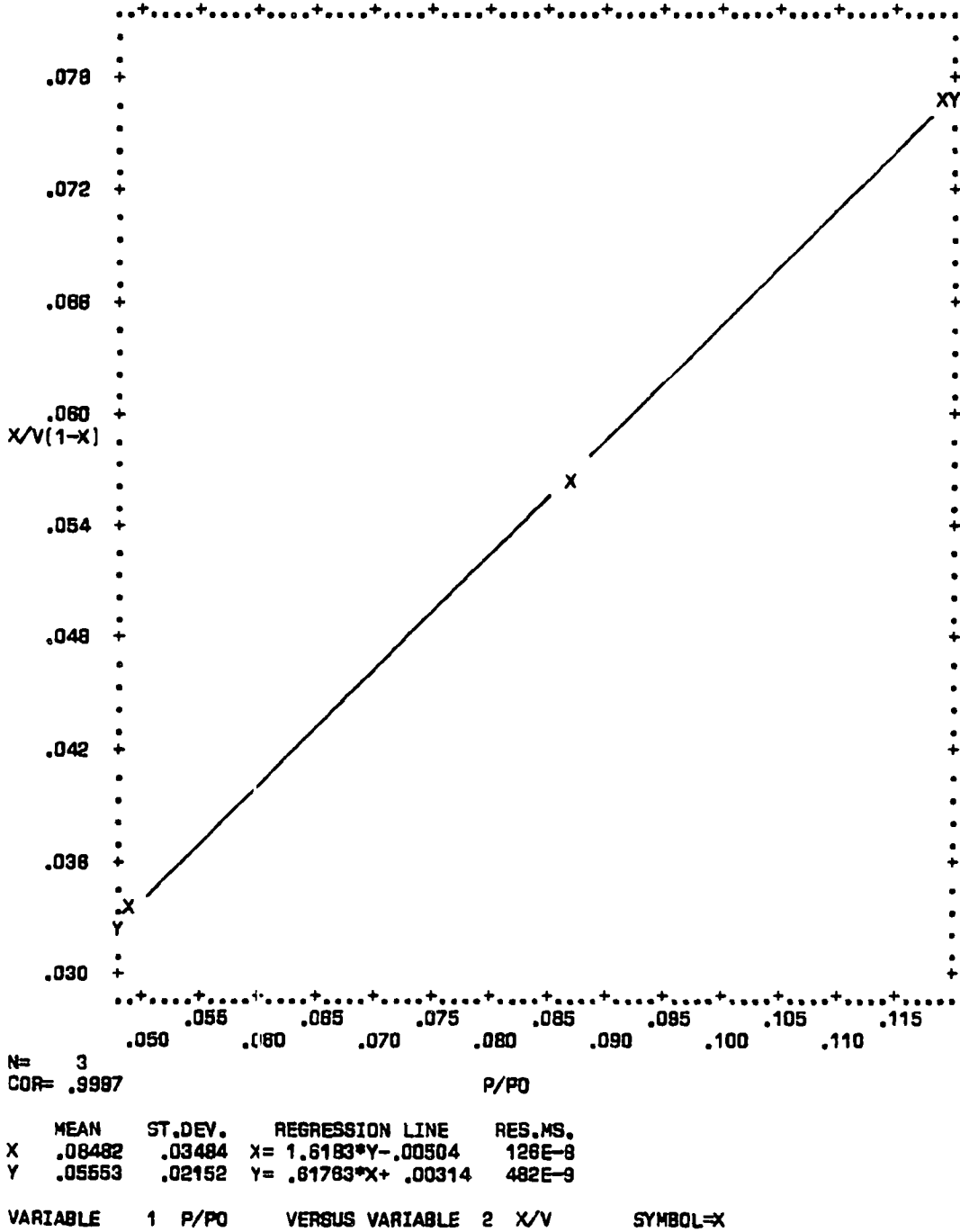
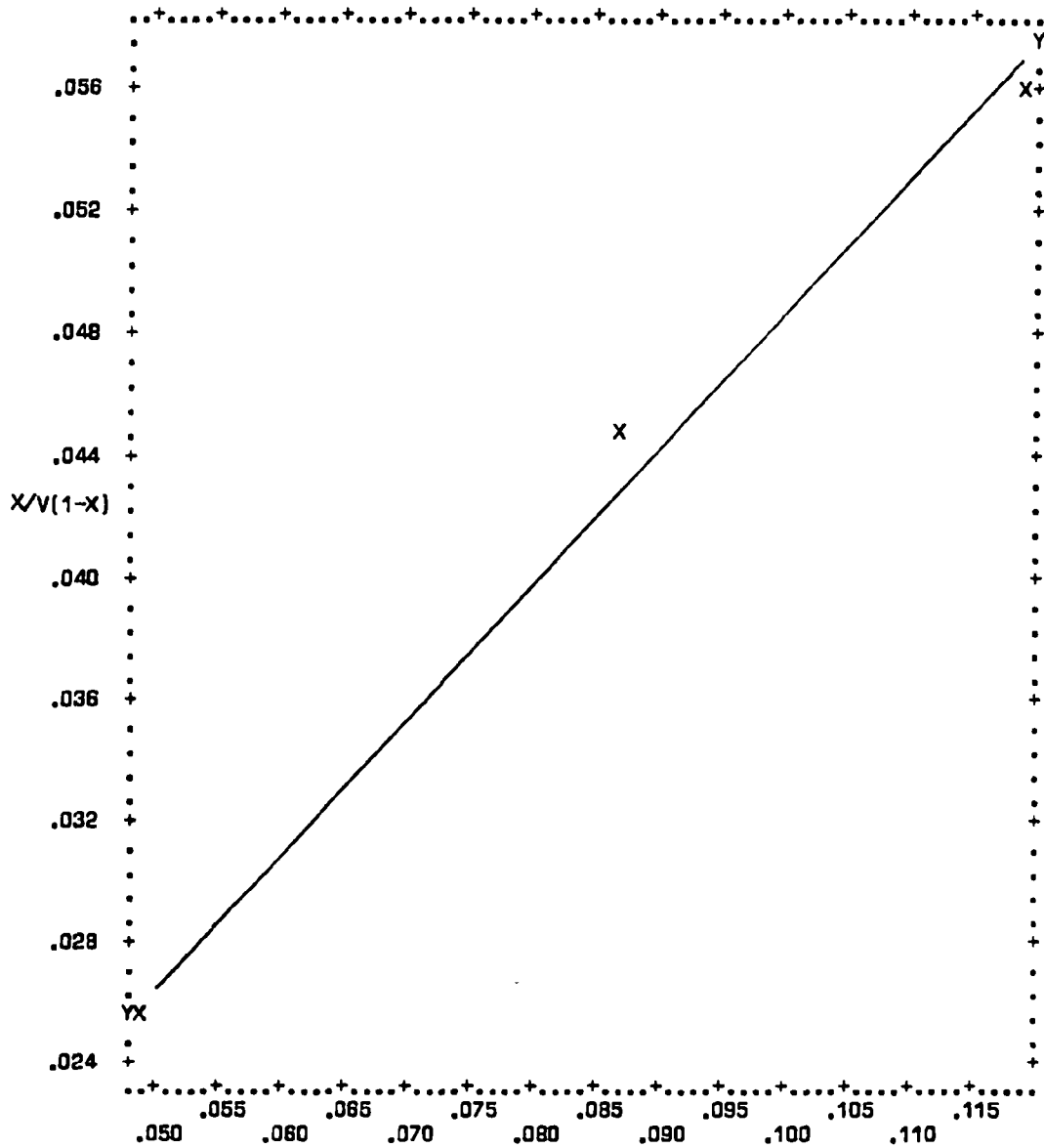


Figure B-48. Plot of BET equation versus relative pressure for Converter A254/0037-B-UR2

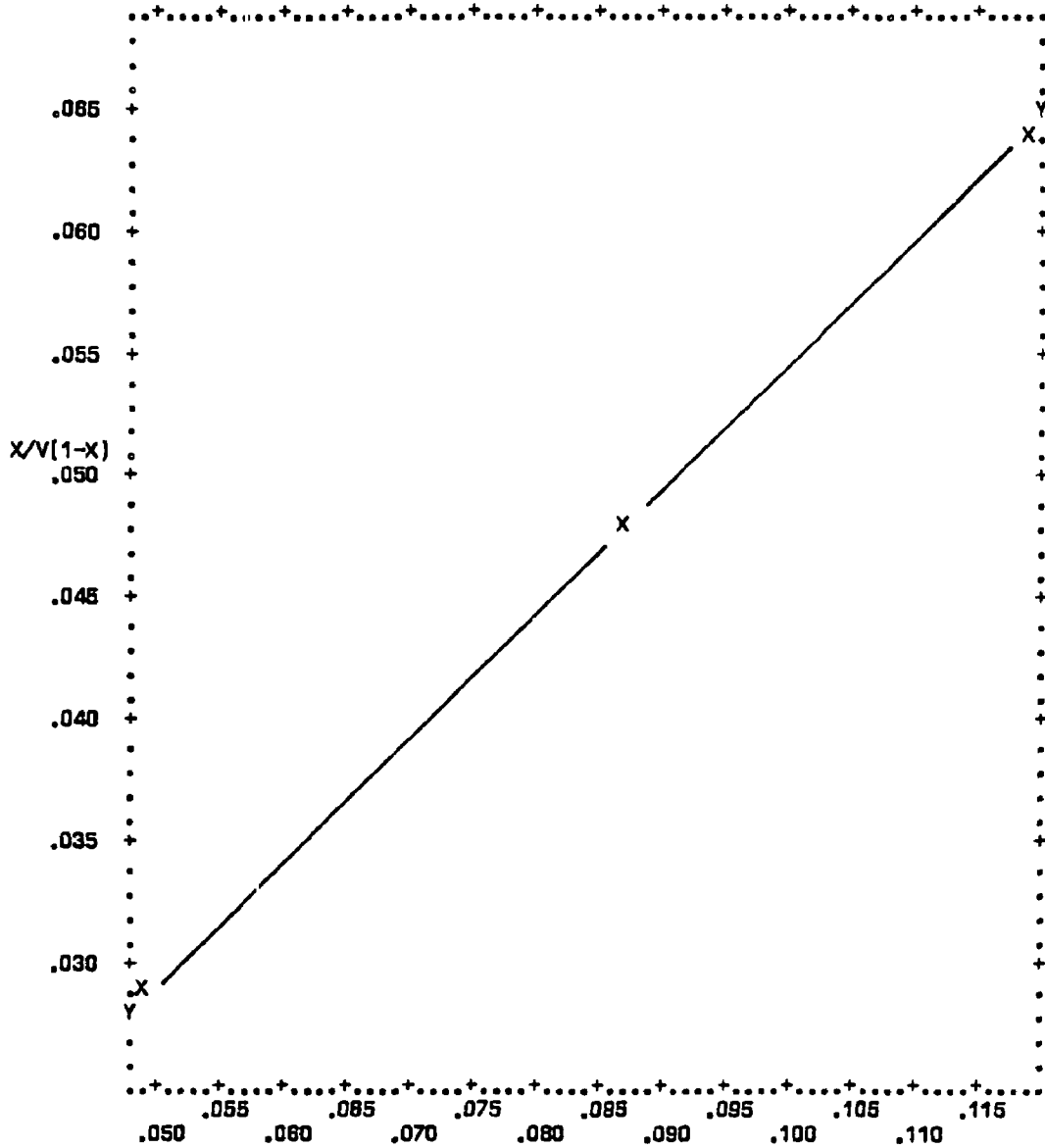


N= 3
 COR= .9980

	MEAN	ST.DEV.	REGRESSION LINE	RES.MS.
X	.08482	.03484	$X = 2.2188*Y - .00852$	198E-7
Y	.04207	.01584	$Y = .44706*X + .00415$	394E-8

VARIABLE 1 P/P0 VERSUS VARIABLE 2 X/V SYMBOL=X

Figure B-49. Plot of BET equation versus relative pressure for Converter A254/0191-A-LL1

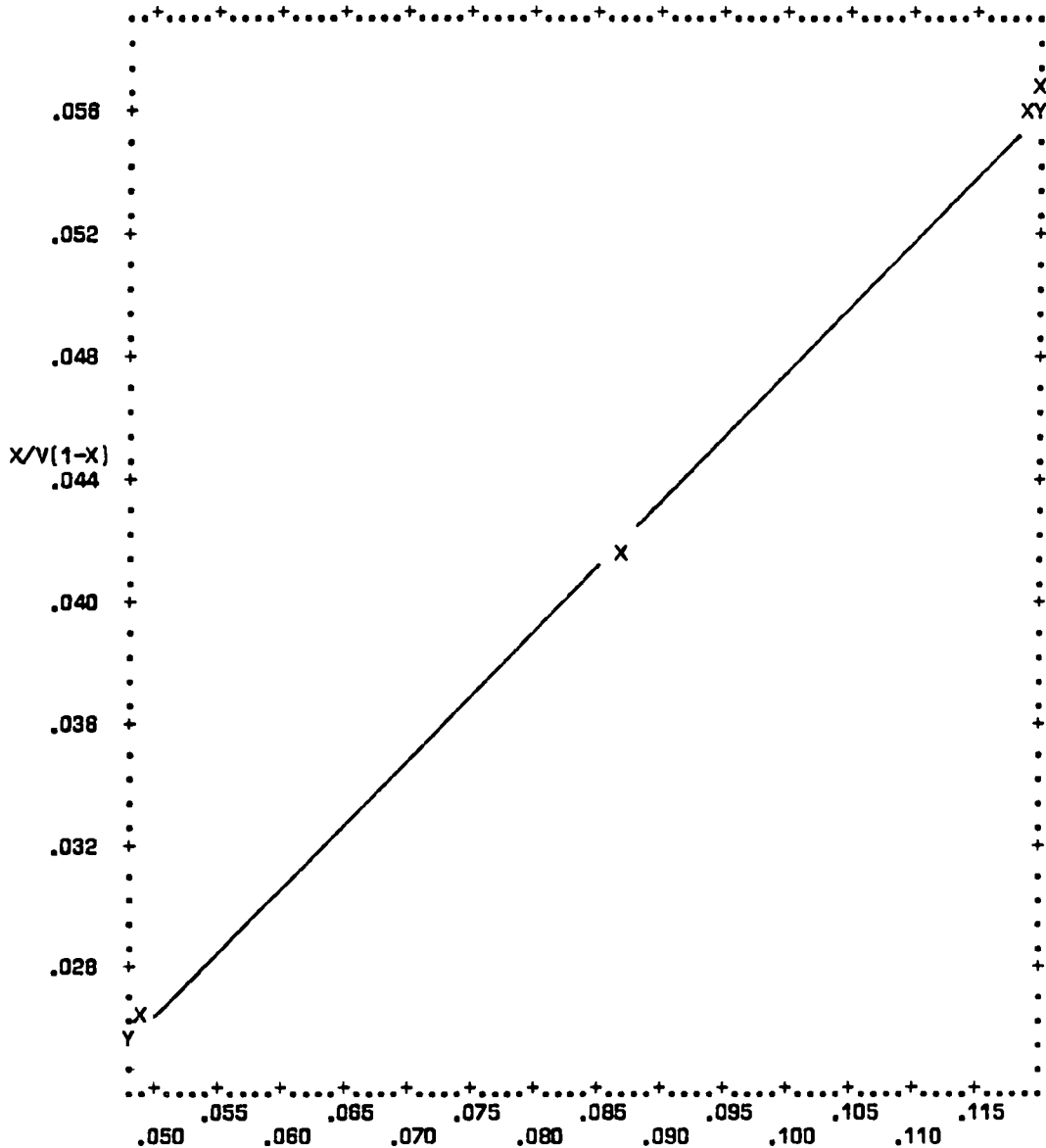


N= 3
COR= 1.000

	MEAN	ST.DEV.	REGRESSION LINE	RES.MS.
X	.08482	.03484	X= 1.9592*Y-.00723	55E-9
Y	.04898	.01778	Y= .51040*X+ .00389	14E-9

VARIABLE 1 P/P0 VERSUS VARIABLE 2 X/V SYMBOL=X

Figure B-50. Plot of BET equation versus relative pressure for Converter A254/0191-A-LL2

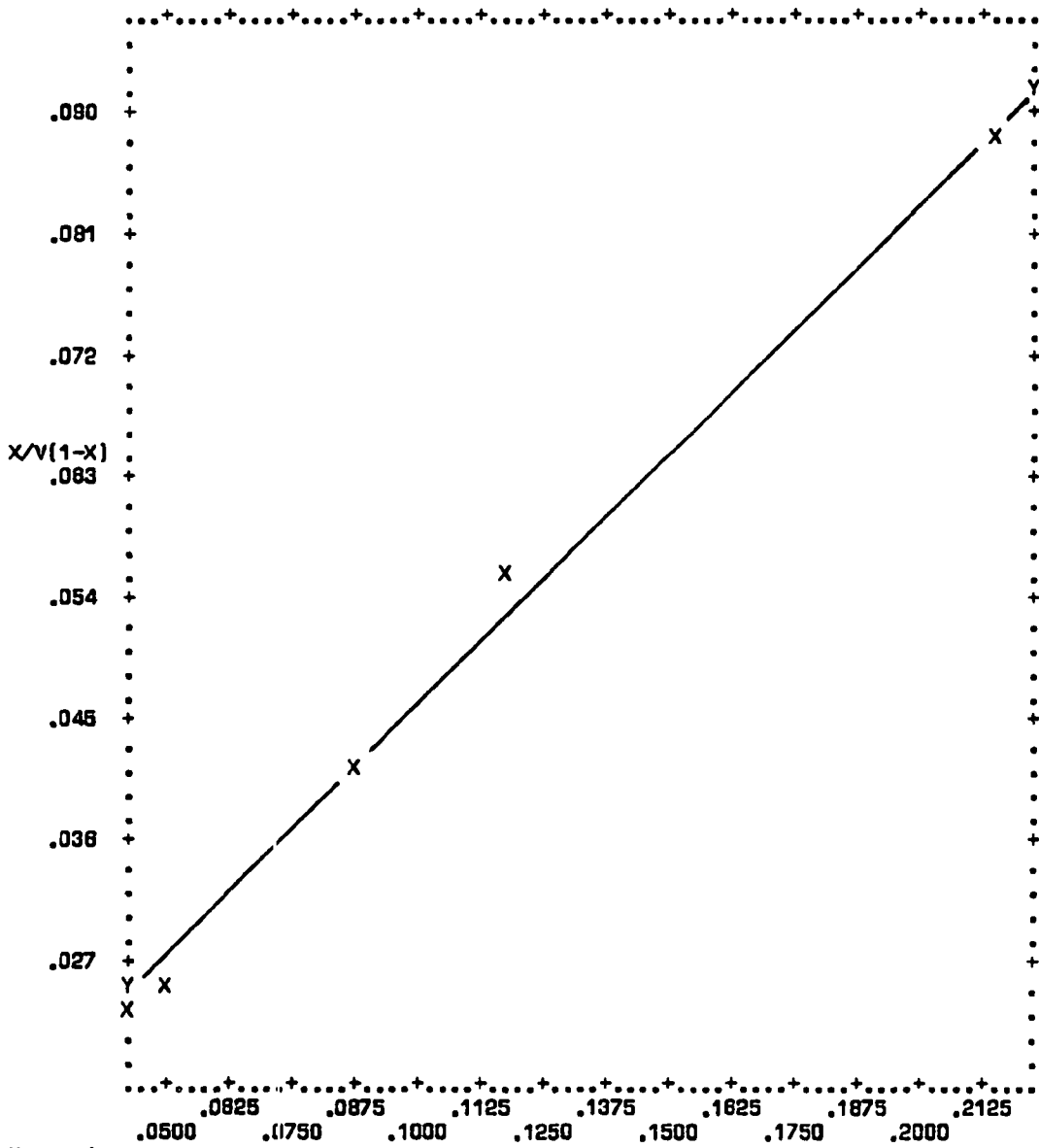


N= 3
COR= .9996

	MEAN	ST.DEV.	REGRESSION LINE	RES.MS.
X	.08481	.03484	X= 2.3359*Y-.01176	173E-8
Y	.04134	.01491	Y= .42779*X+ .00508	316E-9

VARIABLE 1 P/P0 VERSUS VARIABLE 2 X/V SYMBOL=X

Figure B-51. Plot of BET equation versus relative pressure for Converter A254/0191-LL3



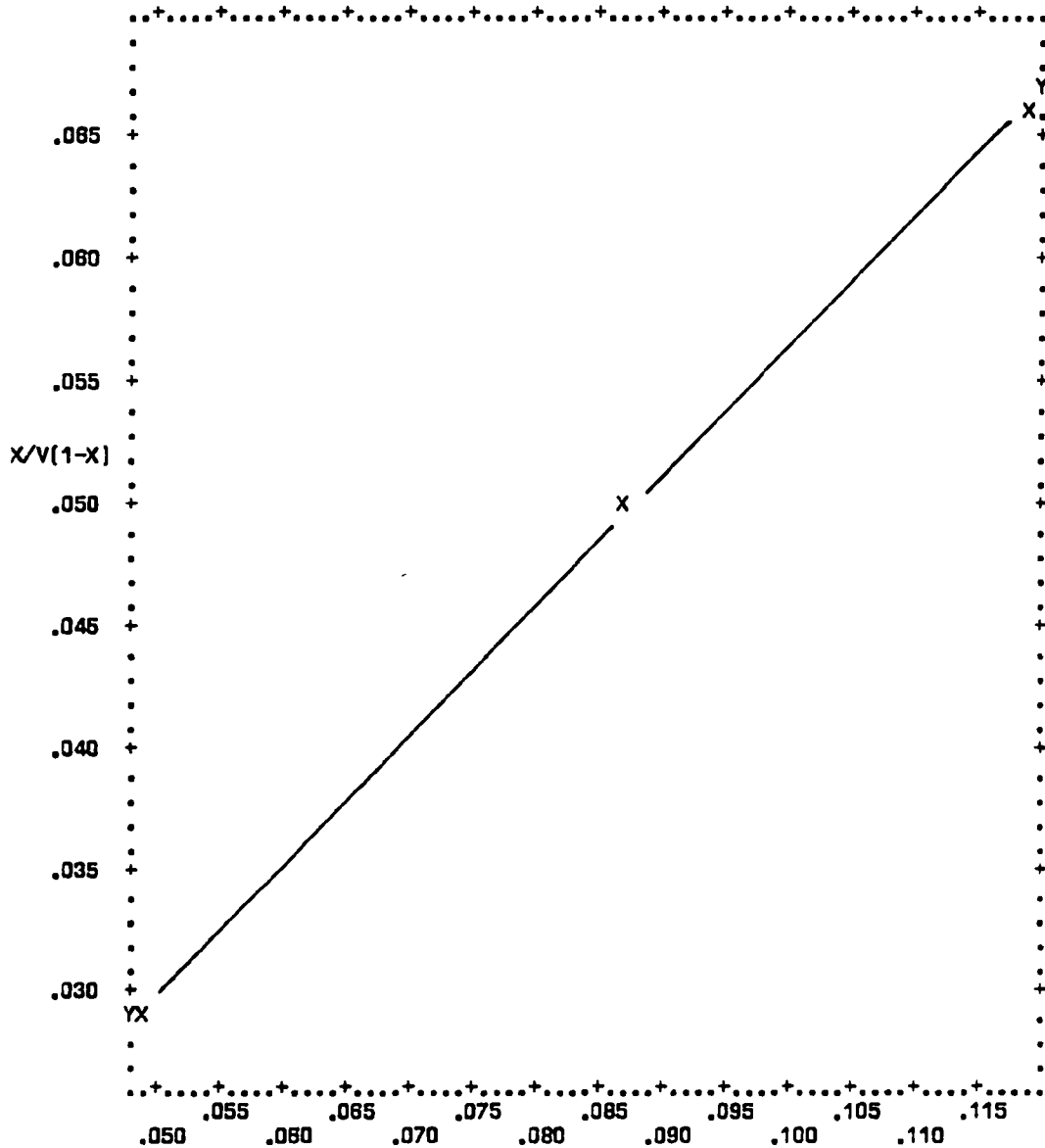
N= 4
COR= .9980

P/P0

	MEAN	ST.DEV.	REGRESSION LINE	RES.MS.
X	.11752	.07132	$X = 2.8481*Y - .02172$	302E-7
Y	.05256	.02887	$Y = .37598*X + .00837$	429E-8

VARIABLE 1 P/P0 VERSUS VARIABLE 2 X/V SYMBOL=X

Figure B-52. Plot of BET equation versus relative pressure for Converter A254/0191-A-LL1 (Powder)



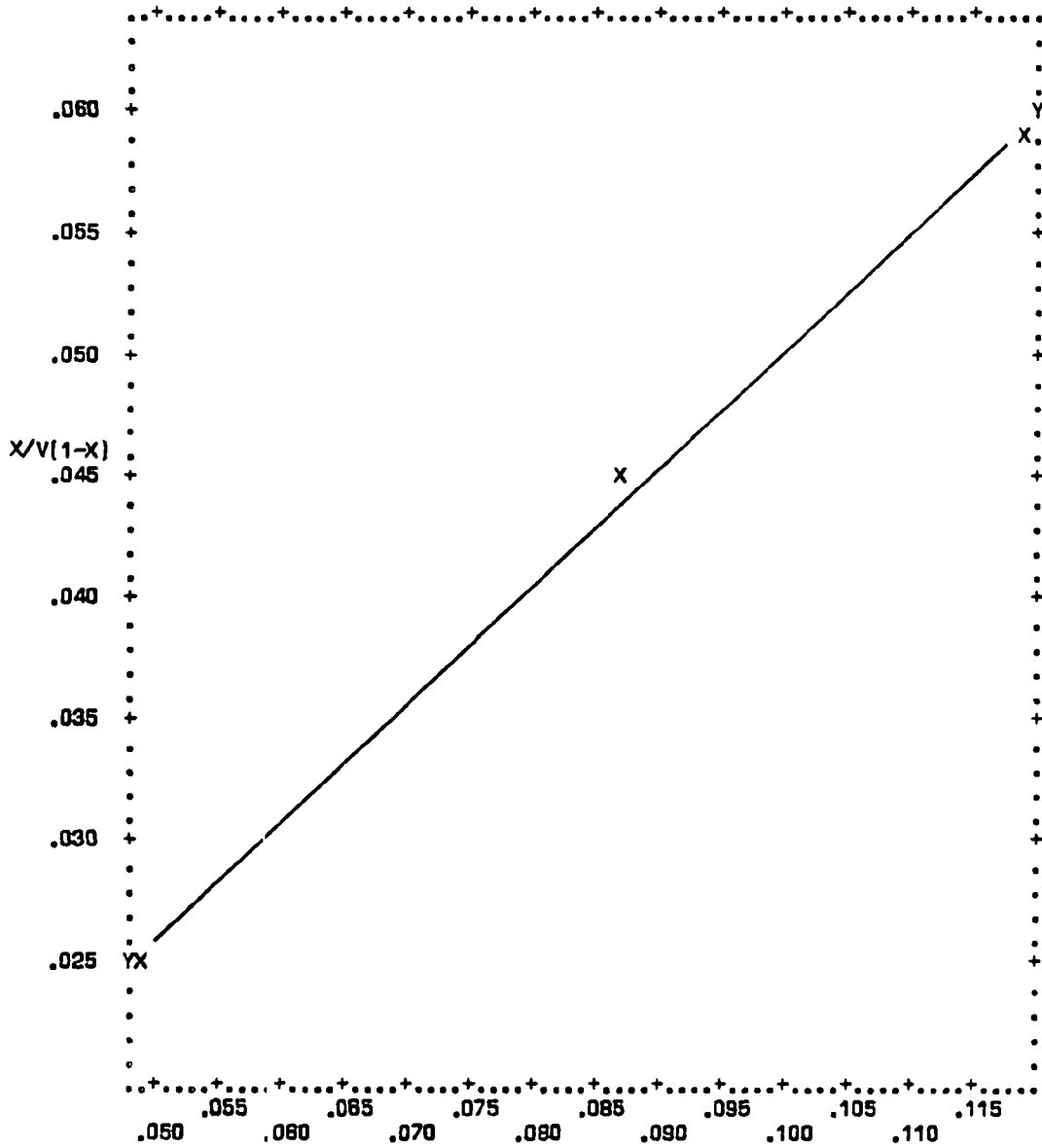
N= 3
COR= .9998

P/P0

	MEAN	ST.DEV.	REGRESSION LINE	RES.MS.
X	.06482	.03484	X= 1.8581*Y-.00521	678E-9
Y	.04846	.01875	Y= .53803*X+ .00282	198E-9

VARIABLE 1 P/P0 VERSUS VARIABLE 2 X/V SYMBOL=X

Figure B-53. Plot of BET equation versus relative pressure for Converter A254/0191-B-UR1



N=	3			
COR=	.9998		P/P0	
	MEAN	ST.DEV.	REGRESSION LINE	RES.MS.
X	.08482	.03484	X= 2.0231*Y-.00224	198E-8
Y	.04303	.01721	Y= .48388*X+ .00114	479E-9
VARIABLE	1	P/P0	VERSUS VARIABLE 2	X/V
				SYMBOL=X

Figure B-54. Plot of BET equation versus relative pressure for Converter A254/0191-B-UR2

APPENDIX C

**ELEMENTAL CONCENTRATIONS OF METALS AND POISONS
FOR REAR BISCUITS BY X-RAY FLUORESCENCE**

RUN DESCRIPTION: AUCAT1 - AUTO CATALYST SWRI
 DATE OF XRAY ANALYSIS: 04/30/87
 SAMPLE TYPE: BRIQUETTE
 SITE ID: N/A
 MISCELLANEOUS INFO: NONE
 SAMPLE SEQUENCE NO.: 1
 SAMPLE ID: A221/0198-B-LL

ELEMENT	DEFN LIM	MASS %	2-SIGMA	
NA	D	.201577E-01	.04206	+- .382057E-01
MG		.189356E-02	4.76499	+- .237119
AL		.228116E-01	20.8927	+ 1.74554
SI		.730753E-02	17.7585	+- .863887
P		.258743E-03	.115019	+- .666537E-03
S		.16524E-02	.147776	+- .783974E-02
CL	X	.936456E-03	-.16422E-02	+- .990382E-03
F		.213093E-03	.221616E-01	+- .114958E-02
CA		.175494E-03	.242356	+- .122542E-01
TI		.150198E-03	.110024	+- .55954E-02
V		.498078E-03	.248302E-02	+- .543275E-03
CR		.107058E-02	.574011E-02	+- .139238E-02
MN		.487141E-03	.416485E-02	+- .672823E-03
FE		.427653E-03	.368426	+- .185978E-01
CO	X	.302105E-03	.248994E-03	+- .289707E-03
NI		.252936E-03	.305474E-02	+- .320243E-03
CU		.254321E-03	.93415E-03	+- .254936E-03
ZN		.244119E-03	.249725E-01	+- .131272E-02
SE	X	.253876E-03	-.637752E-03	+- .23803E-03
BR	X	.183108E-02	-.170802E-02	+- .183369E-02
SR	X	.416501E-02	-.147434E-02	+- .416696E-02
MO	X	.580382E-02	-.44001E-02	+- .580908E-02
CD	D	.188275E-03	.546035E-03	+- .307418E-03
SN	X	.107553E-02	.827267E-03	+- .104028E-02
SB	X	.504788E-03	-.642742E-05	+- .47575E-03
BA	X	.469185E-03	.391651E-03	+- .455728E-03
CE		.179627E-02	.107101E-01	+- .204323E-02
PT		.675297E-03	.419372E-02	+- .700685E-02
HG	X	.70006E-03	-.690435E-03	+- .65634E-03
PB		.707413E-03	.405042E-01	+- .220635E-02

TOTAL DETECTED BY XRF = 44.5613

RUN DESCRIPTION: AUCAT1 - AUTO CATALYST SWRT
 DATE OF XRAY ANALYSIS: 04/30/87
 SAMPLE TYPE: BRIQUETTE
 SITE ID: N/A
 MISCELLANEOUS INFO: NONE
 SAMPLE SEQUENCE NO.: 3
 SAMPLE ID: A221/0310-B-LL

ELEMENT	DETN	LIM	MASS %	Z-SIGMA
NA	D	.243355E-01	.270463E-01	+- .321454E-01
MG		.228857E-02	4.80155	+- .240971
AL		.273151E-01	20.2535	+- 1.0137
SI		.828424E-02	18.0233	+- .902139
P		.283685E-03	.652729E-01	+- .406711E-01
S		.181202E-02	.164057	+- .867205E-02
CL	X	.105726E-02	-.161345E-02	+- .111213E-02
K		.240956E-03	.230581E-01	+- .120034E-02
CA		.197896E-03	.755099E-01	+- .392023E-02
TI		.159796E-03	.115915	+- .589542E-02
V		.545244E-03	.227951E-02	+- .578477E-03
CR		.995394E-03	.522012E-02	+- .13058E-02
MN		.518509E-03	.719535E-02	+- .83701E-03
FE		.447821E-03	.348564	+- .176095E-01
CO	X	.318191E-03	-.129671E-03	+- .297727E-03
NI		.268355E-03	.220463E-02	+- .304129E-03
CU		.257641E-03	.116116E-02	+- .262603E-03
ZN		.245334E-03	.314127E-01	+- .163054E-02
SE	X	.296781E-03	-.247663E-02	+- .29383E-03
BR	X	.247967E-02	-.658591E-02	+- .250195E-02
SR	X	.575585E-02	-.008499	+- .57727E-02
MO	X	.788817E-02	-.23286E-02	+- .78903E-02
CD	X	.211397E-03	.118436E-03	+- .322595E-03
SN	X	.121328E-02	-.489868E-03	+- .112517E-02
SB	X	.570904E-03	-.141099E-03	+- .532762E-03
BA	X	.506728E-03	.238958E-03	+- .485861E-03
CE		.191917E-02	.217753E-01	+- .255819E-01
PT	X	.784401E-03	-.124759E-02	+- .730046E-03
HG	X	.820811E-03	-.796048E-02	+- .824386E-03
PB		.828066E-03	1.24333	+- .062266

TOTAL DETECTED BY XRF = 45.2124

RUN DESCRIPTION: AUCAT1 - AUTO CATALYST SWRI
 DATE OF XRAY ANALYSIS: 04/30/87
 SAMPLE TYPE: BRIQUETTE
 SITE ID: N/A
 MISCELLANEOUS INFO: NONE
 SAMPLE SEQUENCE NO.: 10
 SAMPLE ID: A280/0005L-B

ELEMENT	DETN	LIM	MASS %	Z-SIGMA
NA		.205591E-01	.751819E-01	+- .295265E-01
MG		.001935	4.91991	+- .246374
AL		.231234E-01	17.8837	+- .095101
SI		.734122E-02	18.4027	+- .911096
P		.262408E-03	.802835E-01	+- .40211E-01
S		.167458E-02	.132292	+- .709516E-02
CL	X	.950765E-03	-.638776E-03	+- .10083E-02
I		.216487E-03	.022252	+- .11549E-02
CA		.176364E-03	.898378E-01	+- .462869E-01
TI		.148437E-03	.116503	+- .59191E-02
V		.51224E-03	.263052E-02	+- .559508E-03
CR		.970492E-03	.568574E-02	+- .131584E-02
MN		.492184E-03	.155736E-01	+- .124474E-02
FE		.432557E-03	.381483	+- .192491E-01
CO	X	.303927E-03	.924692E-04	+- .388273E-03
NI		.247699E-03	.179396E-02	+- .274913E-03
CU		.253897E-03	.232959E-01	+- .289933E-03
ZN		.250254E-03	.646118E-01	+- .328332E-02
SE	X	.258086E-03	-.668849E-03	+- .243019E-03
BR	X	.188014E-02	-.186851E-02	+- .188307E-02
SR	X	.428264E-02	-.21578E-02	+- .428527E-02
MO	X	.58899E-02	-.416799E-02	+- .589468E-02
CD	X	.190598E-03	-.442742E-04	+- .297192E-03
SN	X	.109495E-02	.533917E-03	+- .105407E-02
SB	X	.529733E-03	.673364E-04	+- .501195E-03
BA		.467232E-03	.225124E-02	+- .52229E-03
CE		.183201E-02	.122844E-01	+- .002116
PT		.689569E-03	.483687E-02	+- .726971E-03
HG	X	.713118E-03	-.149141E-02	+- .66664E-03
PB		.71943E-03	.126914	+- .646164E-02

TOTAL DETECTED BY XRF = 44.3431

RUN DESCRIPTION: AUCAT1 - AUTO CATALYST SWRI
 DATE OF XRAY ANALYSIS: 04/30/87
 SAMPLE TYPE: BRIQUETTE
 SITE ID: N/A
 MISCELLANEOUS INFO: NONE
 SAMPLE SEQUENCE NO.: 11
 SAMPLE ID: A220/0400-B

ELEMENT	DETN	LIM	MASS %	2-SIGMA
NA	.203599E-01		.671774E-01	+- .293468E-01
MG	.193899E-02		4.54569	+- .230652
AL	.023294		20.9691	+- 1.04736
SI	.74277E-02		17.9359	+- .897752
P	.262256E-03		.628733E-01	+- .343429E-01
S	.167378E-02		.934772E-01	+- .523009E-02
CL	X	.947587E-03	-.224375E-02	+- .100214E-02
F		.216317E-03	.700612E-01	+- .353005E-02
CA		.170956E-03	.830352E-01	+- .423755E-02
TI		.16093E-03	.363384	+- .182648E-01
V		.550421E-03	.530792E-02	+- .683777E-03
CR		.893808E-03	.993665E-02	+- .155476E-02
MN		.479581E-03	.476186E-02	+- .698828E-03
FE		.424651E-03	.348949	+- .176261E-01
CO	X	.301198E-03	.26313E-03	+- .291064E-03
NI		.259071E-03	.552883E-02	+- .420672E-03
CU		.260714E-03	.976886E-03	+- .261576E-03
ZN		.249756E-03	.355787E-01	+- .183894E-02
SE	X	.268453E-03	-.147185E-01	+- .000756
BR	X	.193444E-02	-.271857E-02	+- .193981E-02
SR	X	.441203E-02	-.171879E-02	+- .441419E-02
MO	X	.609663E-02	-.351426E-02	+- .610029E-02
CD	X	.190723E-03	-.804652E-04	+- .287036E-03
SN	X	.106954E-02	.158667E-03	+- .101473E-02
SB	X	.5239E-03	-.481142E-03	+- .474788E-03
BA		.502362E-03	.218175E-02	+- .549171E-03
CE		.195377E-02	.133701E-01	+- .22519E-02
PT		.705595E-03	.996677E-01	+- .512628E-02
HG	X	.728722E-03	-.178723E-02	+- .681098E-03
PB		.741671E-03	.111156	+- .568269E-02

TOTAL DETECTED BY XRF = 44.8781

RUN DESCRIPTION: AUCAT1 - AUTO CATALYST SWRI
 DATE OF XRAY ANALYSIS: 04/30/87
 SAMPLE TYPE: BRIDUETTE
 SITE ID: N/A
 MISCELLANEOUS INFO: NONE
 SAMPLE SEQUENCE NO.: 6
 SAMPLE ID: A230/0649-B

ELEMENT	DETN	LIM	MASS %	NETSIGMA
NA	X	.226321E-01	.414515E-02	+- .302091E-01
MG		.212052E-02	4.73483	+- .257458
AL		.250857E-01	19.7167	+- .276837
SI		.770482E-02	18.1691	+- .909423
P		.269379E-03	.375982E-01	+- .264411E-02
S		.171838E-02	.128869	+- .694037E-02
CL	X	.975095E-03	-.260087E-02	+- .102717E-02
F		.221159E-03	.684632E-01	+- .345065E-02
CA		.167548E-03	.806483E-01	+- .416801E-02
TI		.163828E-03	.375051	+- .188484E-01
V		.587353E-03	.384988E-02	+- .660780E-03
CR		.109389E-02	.637283E-02	+- .143616E-02
MN		.535344E-03	.371275E-02	+- .691471E-03
FE		.570303E-03	.820769	+- .412339E-01
CO	X	.341531E-03	-.576341E-04	+- .320945E-03
NI		.285544E-03	.787091E-02	+- .541822E-03
CU	D	.280466E-03	.35797E-03	+- .269414E-03
ZN		.274784E-03	.144979E-01	+- .816993E-03
GE	X	.290537E-03	-.126298E-02	+- .274204E-03
BR	X	.215584E-02	-.28475E-02	+- .216117E-02
SR	X	.490323E-02	-.146919E-02	+- .490521E-02
MO	X	.668865E-02	-.211067E-02	+- .669067E-02
CD	X	.195153E-03	-.239759E-03	+- .285361E-03
BN	X	.103549E-02	.882292E-03	+- .101419E-02
SB	X	.491484E-03	.206571E-03	+- .472380E-03
BA		.51556E-03	.312956E-02	+- .59556E-03
CE		.206526E-02	.806257	+- .412719E-01
PT		.758076E-03	.920659E-01	+- .476957E-02
HG	X	.778352E-03	-.501076E-03	+- .790772E-03
PB		.797367E-03	.221047E-01	+- .14113E-02

TOTAL DETECTED BY XRF = 45.29.14

RUN DESCRIPTION: AUCAT1 - AUTO CATALYST SWR1
 DATE OF XRAY ANALYSIS: 04/30/87
 SAMPLE TYPE: BRIQUETTE
 SITE ID: N/A
 MISCELLANEOUS INFO: NONE
 SAMPLE SEQUENCE NO.: 7
 SAMPLE ID: A230/0734-B

ELEMENT	DETN	LIM	MASS %	2-SIGMA
NA	D	.022983	.273679E-01	+- .311236E-01
MG		.002155	4.71158	+- .236501
AL		.025519	20.1188	+- 1.00694
SI		.780963E-02	18.1027	+- .906107
P		.271822E-03	.475028E-01	+- .315737E-01
S		.173412E-02	.104401	+- .577548E-02
CL	X	.933762E-03	-.36278E-03	+- .104221E-01
F		.223024E-03	.656881E-01	+- .331241E-02
CA		.179431E-03	.871227E-01	+- .449262E-02
TI		.164748E-03	.361345	+- .181635E-01
V		.577676E-03	.495521E-02	+- .69159E-03
CR		.105924E-02	.717465E-02	+- .146351E-02
MN		.572668E-03	.333883E-02	+- .700891E-03
FE		.583379E-03	.824106	+- .041404
CO	X	.345105E-03	-.917111E-04	+- .323687E-03
NI		.284254E-03	.607008E-02	+- .464714E-03
CU		.28301E-03	.162352E-02	+- .297694E-03
ZN		.279222E-03	.174804E-01	+- .961998E-03
SE	X	.296517E-03	-.104772E-02	+- .278658E-03
BR	X	.220714E-02	-.295393E-02	+- .221272E-02
SR	X	.501832E-02	-.145333E-02	+- .502029E-02
MO	X	.681655E-02	-.176142E-02	+- .681831E-02
CD	X	.196804E-03	-.13707E-03	+- .291923E-03
SN	D	.12194E-02	.141045E-02	+- .11144E-02
SB	X	.545716E-03	-.657978E-03	+- .489367E-03
RA		.514422E-03	.162419E-02	+- .539235E-03
CE		.204492E-02	.978713	+- .498943E-01
PT		.772185E-03	.10619	+- .547305E-02
HG	X	.797036E-03	-.516532E-03	+- .748407E-03
PB		.815326E-03	.587414E-02	+- .856016E-03

TOTAL DETECTED BY XRF = 45.5851

RUN DESCRIPTION: AUCAT1 - AUTO CATALYST SWRI
 DATE OF XRAY ANALYSIS: 04/30/87
 SAMPLE TYPE: BRIDQUETTE
 SITE ID: N/A
 MISCELLANEOUS INFO: NONE
 SAMPLE SEQUENCE NO.: 8
 SAMPLE ID: A246/0092-B

ELEMENT	NETN LIM	MASS %	± SIGMA
NA D	.219277E-01	.574254E-01	+- .304543E-01
MG	.20578E-01	3.85567	+- .194665
AL	.252088E-01	24.7726	+- 1.21557
SI	.796093E-02	15.4711	+- .77456
P	.266171E-03	.024488	+- .194841E-01
S	.170955E-02	.5612	+- .283674E-01
CL X	.980038E-03	-.224615E-02	+- .10327E-02
I	.222885E-03	.404317E-01	+- .205471E-02
CA	.170727E-03	.519932E-01	+- .273682E-02
TI	.186917E-03	.327196	+- .164575E-01
V D	.822607E-03	.183913E-02	+- .80951E-03
CR	.122903E-02	.744353E-02	+- .161623E-02
MN	.550998E-03	.648128E-02	+- .840854E-03
FE	.451795E-03	.478732	+- .241299E-01
CO X	.330308E-03	-.152142E-04	+- .211133E-03
NI	.276412E-03	.95149E-02	+- .609435E-03
CU X	.272276E-03	-.448001E-03	+- .25216E-03
ZN	.268121E-03	.864035E-02	+- .541881E-03
SE X	.288798E-03	-.204556E-02	+- .280412E-03
BR X	.212171E-02	-.307431E-02	+- .212799E-02
SR	.486705E-02	.173954E-01	+- .49464E-02
MO X	.669253E-02	-.131534E-02	+- .669404E-02
CD X	.196412E-03	-.44405E-04	+- .295033E-03
BN D	.104579E-02	.173806E-02	+- .106112E-02
SB X	.48613E-03	.259891E-03	+- .467903E-03
BA	.583259E-03	.772934	+- .389507E-01
CE X	.267478E-02	-.119127E-01	+- .236508E-01
PT	.752518E-03	.171704	+- .872353E-02
HG X	.775283E-03	-.192556E-02	+- .724371E-03
PB	.794207E-03	.018471	+- .12565E-02

TOTAL DETECTED BY XRF = 46.177 *

RUN DESCRIPTION: AUCAT1 - AUTO CATALYST SWRI
 DATE OF XRAY ANALYSIS: 04/30/87
 SAMPLE TYPE: BRIQUETTE
 SITE ID: N/A
 MISCELLANEOUS INFO: NONE
 SAMPLE SEQUENCE NO.: 4
 SAMPLE ID: A240/0007-B-LL

ELEMENT	DETN	LIM	MASS %	2-SIGMA
NA	D	.219351E-01	.048752	+- .303424E-01
MG		.205713E-02	4.24024	+- .212904
AL		.248757E-01	22.4227	+- 1.12209
SI		.78027E-02	16.6828	+- .835128
P		.26692E-03	.101295	+- .587678E-02
S		.170983E-02	.358777	+- .182814E-01
CL	X	.975518E-03	-.289701E-02	+- .102814E-02
I		.2214E-03	.356563E-01	+- .181744E-02
CA		.178475E-03	.705113E-01	+- .366247E-02
TI		.174901E-03	.364354	+- .183141E-01
V		.584541E-03	.448092E-02	+- .680503E-03
CR		.107355E-02	.820918E-02	+- .154814E-02
MN		.527627E-03	.906082E-02	+- .94789E-03
FE		.530128E-03	.392247	+- .198026E-01
CO	D	.32532E-03	.497581E-03	+- .317036E-03
NI		.285018E-03	.104985	+- .533649E-02
CU	D	.279615E-03	.502605E-03	+- .27074E-03
ZN		.273167E-03	.512965E-01	+- .262719E-02
SE	X	.284915E-03	-.103216E-02	+- .267915E-03
BR	X	.210212E-02	-.26506E-02	+- .210693E-02
SR	X	.47807E-02	-.142122E-02	+- .478263E-02
MO	X	.651379E-02	-.141279E-02	+- .651535E-02
CD	X	.19525E-03	.154789E-04	+- .295774E-03
LN	X	.111207E-02	-.649678E-03	+- .102266E-02
SB	X	.536789E-03	-.546718E-03	+- .484706E-03
BA		.535087E-03	.273366E-02	+- .596429E-03
CE		.203425E-02	.701896	+- .360685E-01
PT		.74143E-03	.660635E-01	+- .348243E-02
HG	X	.766971E-03	-.966344E-03	+- .718072E-03
FB		.784044E-03	.398886E-01	+- .220999E-02

TOTAL DETECTED BY XRF = 45.7069

RUN DESCRIPTION: AUCAT1 - AUTO CATALYST SWRI
 DATE OF XRAY ANALYSIS: 04/30/87
 SAMPLE TYPE: BRIQUETTE
 SITE ID: N/A
 MISCELLANEOUS INFO: NONE
 SAMPLE SEQUENCE NO.: 2
 SAMPLE ID: A240/0270-B-LL

ELEMENT	DETN	LIM	MASS %	2-SIGMA
NA	D	.230214E-01	.469377E-01	+- .313488E-01
MG		.215619E-02	3.38178	+- .189977
AL		.270952E-01	27.2414	+- 1.35305
SI		.852961E-02	13.7747	+- .689796
P		.275394E-03	.217341	+- .117014E-01
S		.176854E-02	.298602	+- .0153
CL	X	.101325E-02	-.212533E-02	+- .106637E-02
F		.230041E-03	.340495E-01	+- .173931E-02
CA		.184914E-03	.952361E-01	+- .490156E-02
TI		.168115E-03	.311425	+- .156694E-01
V		.587886E-03	.510342E-02	+- .706933E-03
CR		.11304E-02	.664489E-02	+- .149536E-02
MN		.571213E-03	.224734E-01	+- .164038E-02
FE		.589781E-03	.371922	+- .187973E-01
CO	X	.346125E-03	.172319E-03	+- .329699E-03
NI		.307705E-03	.127741	+- .647892E-02
CU		.301287E-03	.242361E-02	+- .334094E-03
ZN		.290089E-03	.714769E-01	+- .363729E-02
SE	X	.303748E-03	-.138938E-02	+- .287049E-03
BR	X	.232545E-02	-.329761E-02	+- .233193E-02
SR	X	.530237E-02	-.119535E-02	+- .530422E-02
MO	X	.721172E-02	.676599E-03	+- .721305E-02
CD	X	.202829E-03	.985276E-04	+- .309325E-03
SN	X	.11568E-02	-.315768E-03	+- .107829E-02
SB	X	.562513E-03	-.440369E-03	+- .513449E-03
BA		.52216E-03	.260602E-02	+- .581829E-03
CE		.206782E-02	1.1948	+- .607154E-01
Pt		.795886E-03	.940623E-01	+- .48785E-02
HG	X	.817101E-03	-.111842E-02	+- .764592E-03
PB		.834755E-03	.140446	+- .716307E-02

TOTAL DETECTED BY XRF = 47.4411

RUN DESCRIPTION: AUCAT1 - AUTO CATALYST SWRI
 DATE OF XRAY ANALYSIS: 04/30/87
 SAMPLE TYPE: BRIQUETTE
 SITE ID: N/A
 MISCELLANEOUS INFO: NONE
 SAMPLE SEQUENCE NO.: 1
 SAMPLE ID: A254/0037-B

ELEMENT	DETN	LIM	MASS %	2-SIGMA
NA	D	.232126E-01	.569765E-01	+- .324219E-01
MG		.216244E-02	3.61891	+- .181903
AL		.254631E-01	20.5577	+- 1.02889
LI		.756962E-02	13.5061	+- .676258
P		.248131E-03	.348893E-01	+- .244436E-02
S		.160333E-02	1.00933	+- .507314E-01
CL	X	.927552E-03	-.179154E-02	+- .977577E-03
F		.210467E-03	.046475	+- .235276E-02
CA		.172297E-03	.068959	+- .35774E-02
TI		.265052E-03	.24552	+- .123678E-01
V	X	.748457E-03	-.100272E-02	+- .690913E-03
CR		.143902E-02	.148187E-01	+- .213399E-02
MN		.686156E-03	.616519E-02	+- .897412E-03
FE		.744595E-03	.114499	+- .593956E-02
CO	D	.283578E-03	.308914E-03	+- .2741E-03
NI	D	.238765E-03	.704516E-03	+- .239135E-03
CU	X	.232864E-03	-.579264E-04	+- .218799E-03
ZN		.229735E-03	.105716E-01	+- .612328E-03
SE	X	.244432E-03	-.194256E-02	+- .239427E-03
BR	X	.203331E-02	-.681392E-02	+- .20626E-02
SR	X	.463394E-02	-.823245E-02	+- .465311E-02
MO	X	.64075E-02	-.212357E-01	+- .649571E-02
CD	D	.185502E-03	.280545E-03	+- .290752E-03
SN	X	.106153E-02	-.21099E-03	+- .9929E-03
SB	X	.500975E-03	-.440857E-03	+- .454889E-03
BA	X	.747265E-03	-.660791E-03	+- .691889E-03
CE		.335964E-02	.83077	+- .425405E-01
PT		.631103E-03	.149615	+- .760499E-02
HG	X	.648189E-03	-.203309E-02	+- .604435E-03
PB		.667627E-03	.94707E-02	+- .835755E-03

TOTAL DETECTED BY XRF = 40.2821

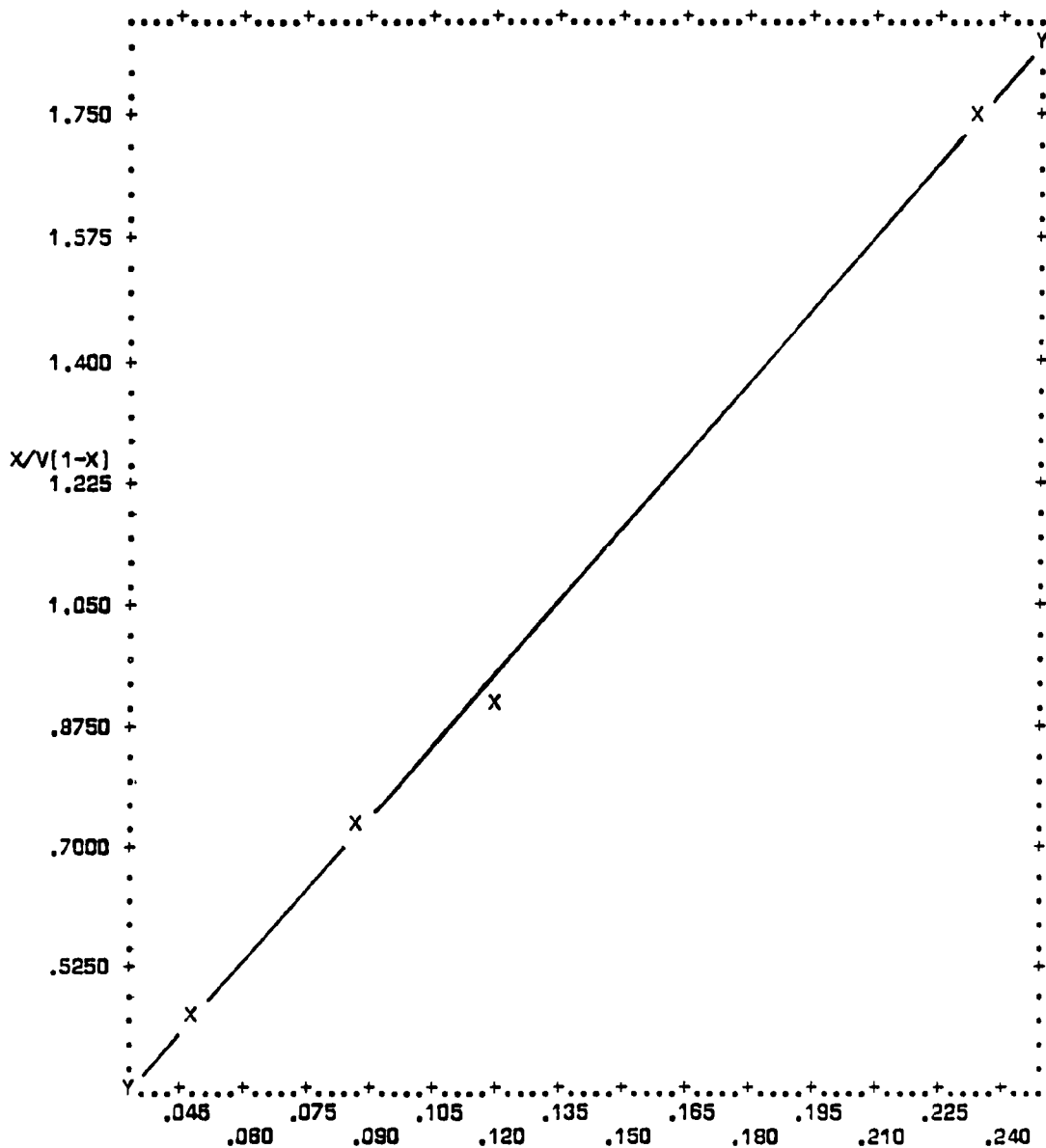
RUN DESCRIPTION: AUCAT1 - AUTO CATALYST SWRI
 DATE OF XRAY ANALYSIS: 04/30/87
 SAMPLE TYPE: BRIQUETTE
 SITE ID: N/A
 MISCELLANEOUS INFO: NONE
 SAMPLE SEQUENCE NO.: 7
 SAMPLE ID: A254/0191-B

ELEMENT	DETN	LIM	MASS %	1-SIGMA
NA	D	.236185E-01	.388776E-01	+- .324494E-01
MG		.21979E-02	3.37741	+- .167836
AL		.260666E-01	21.5494	+- 1.07847
SI		.773349E-02	12.5509	+- .628515
P		.248918E-03	.311464E-01	+- .334041E-01
S		.160688E-02	.908222	+- .456777E-01
CL	X	.928729E-03	-.221421E-02	+- .977772E-03
F		.210697E-03	.432863E-01	+- .219399E-02
CA		.17076E-03	.051683	+- .271319E-02
TI		.270869E-03	.2326	+- .117214E-01
V	X	.774827E-03	-.112888E-02	+- .714808E-03
CR		.156335E-02	.158694E-01	+- .226029E-02
MN		.707276E-03	.23845E-02	+- .756214E-03
FE		.77353E-03	.10747	+- .559504E-02
CO	X	.293817E-03	-.541653E-04	+- .275935E-04
NI	X	.244282E-03	.11351E-03	+- .232232E-03
CU	X	.237003E-03	.310309E-04	+- .22386E-03
ZN		.232074E-03	.979236E-02	+- .577091E-03
SE	X	.244541E-03	-.178941E-02	+- .237232E-03
BR	X	.207318E-02	-.724691E-02	+- .210504E-02
SR	X	.472368E-02	-.91504E-02	+- .474678E-02
MO	X	.64925E-02	-.221265E-01	+- .658689E-02
CD	X	.185612E-03	.142998E-03	+- .135338E-03
BN	X	.105373E-02	-.707171E-03	+- .965707E-03
SB	X	.498693E-03	-.978856E-04	+- .466271E-03
BA	X	.76784E-03	-.164834E-02	+- .695986E-03
CE		.353422E-02	.977396	+- .499637E-01
PT		.642423E-03	.152587	+- .775501E-02
HG	X	.650963E-03	-.152375E-02	+- .607033E-03
PB		.668348E-03	.220629E-01	+- .134088E-02

TOTAL DETECTED BY XRF = 40.0731

APPENDIX D

**BET EQUATION VERSUS RELATIVE PRESSURE
FOR QUALITY ASSURANCE STANDARDS**



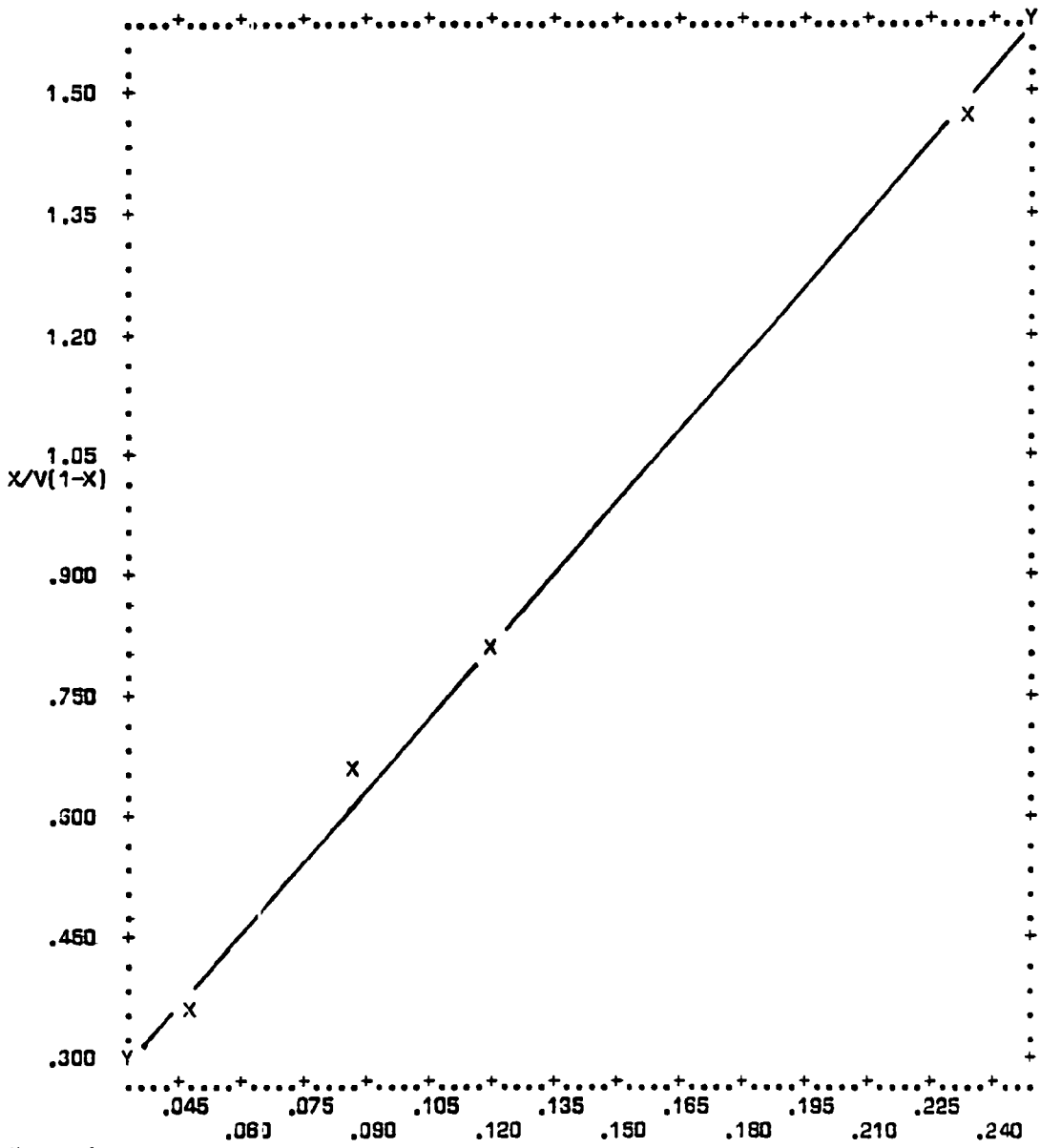
N= 4
COR= .9994

P/P0

	MEAN	ST.DEV.	REGRESSION LINE	RES.MS.
X	.12179	.07968	X= .14269*Y-.01687	120E-7
Y	.97176	.55808	Y= 6.9994*X+ .11929	589E-6

VARIABLE 1 P/P0 VERSUS VARIABLE 2 X/V SYMBOL=X

Figure D-1. Plot of BET equation versus relative pressure for Zinc Oxide 0.62±0.04



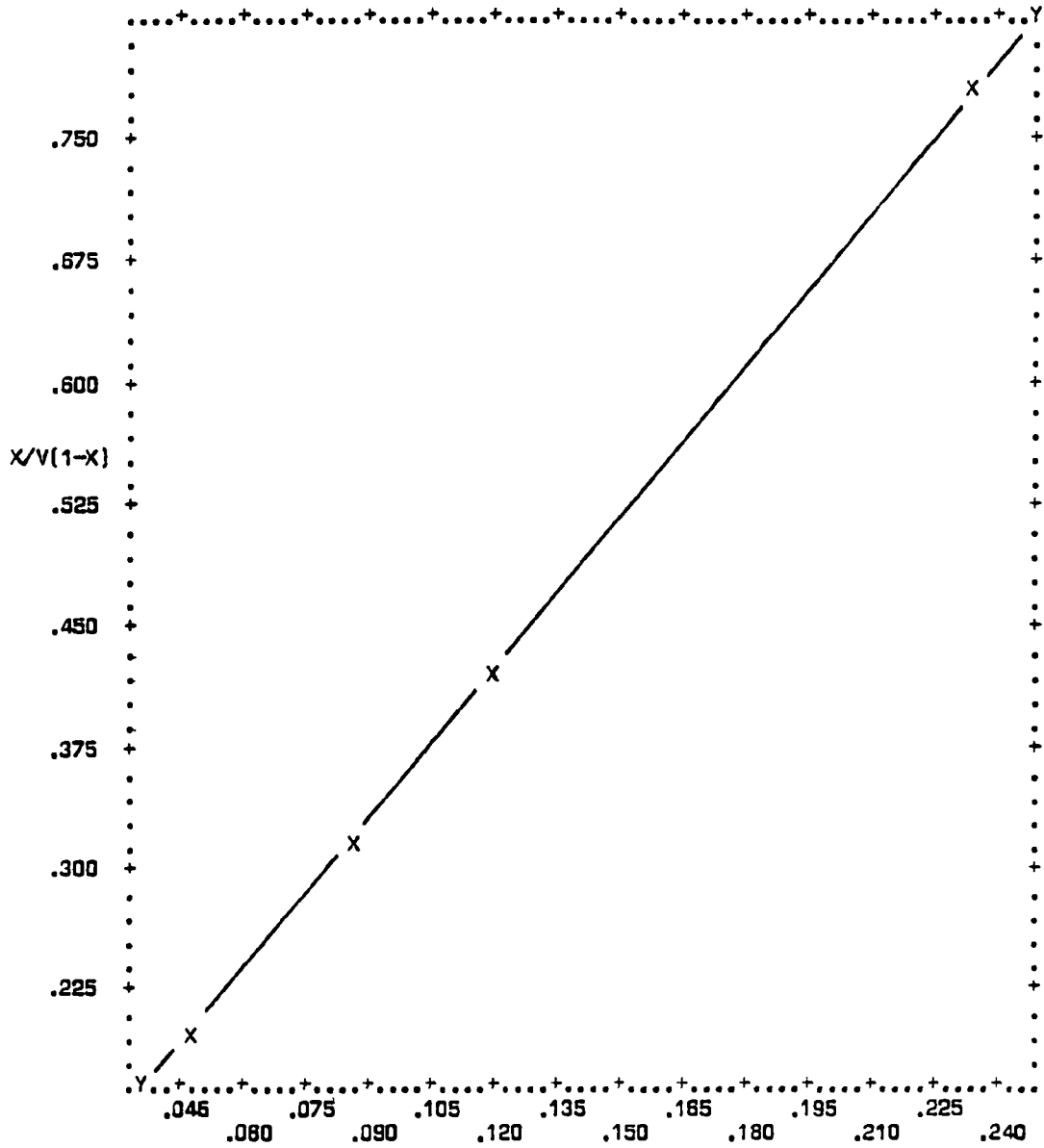
N= 4
COR= .9984

P/P0

	MEAN	ST.DEV.	REGRESSION LINE	RES.MS.
X	.12178	.07967	X= .17000*Y-.01924	305E-7
Y	.82955	.48792	Y= 5.8837*X+ .11548	.00105

VARIABLE 1 P/P0 VERSUS VARIABLE 2 X/V SYMBOL=X

Figure D-2. Plot of BET equation versus relative pressure for Alpha Alumina 0.78 NBS

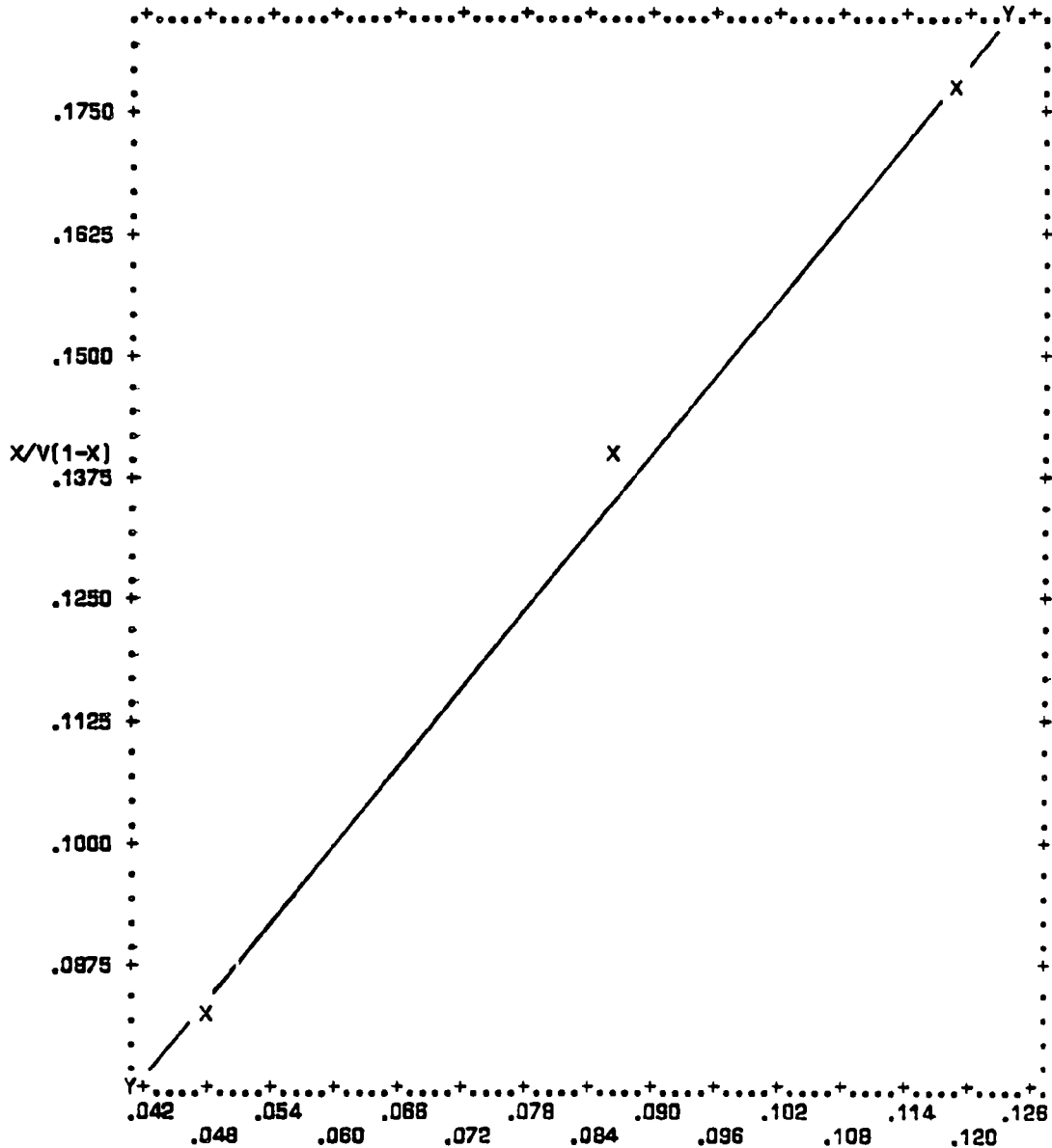


N= 4
COR= 1.000

	MEAN	ST.DEV.	REGRESSION LINE	RES.MS.
X	.12178	.07987	X= .32159*Y-.01600	249E-9
Y	.42844	.24774	Y= 3.1095*X+ .04978	241E-8

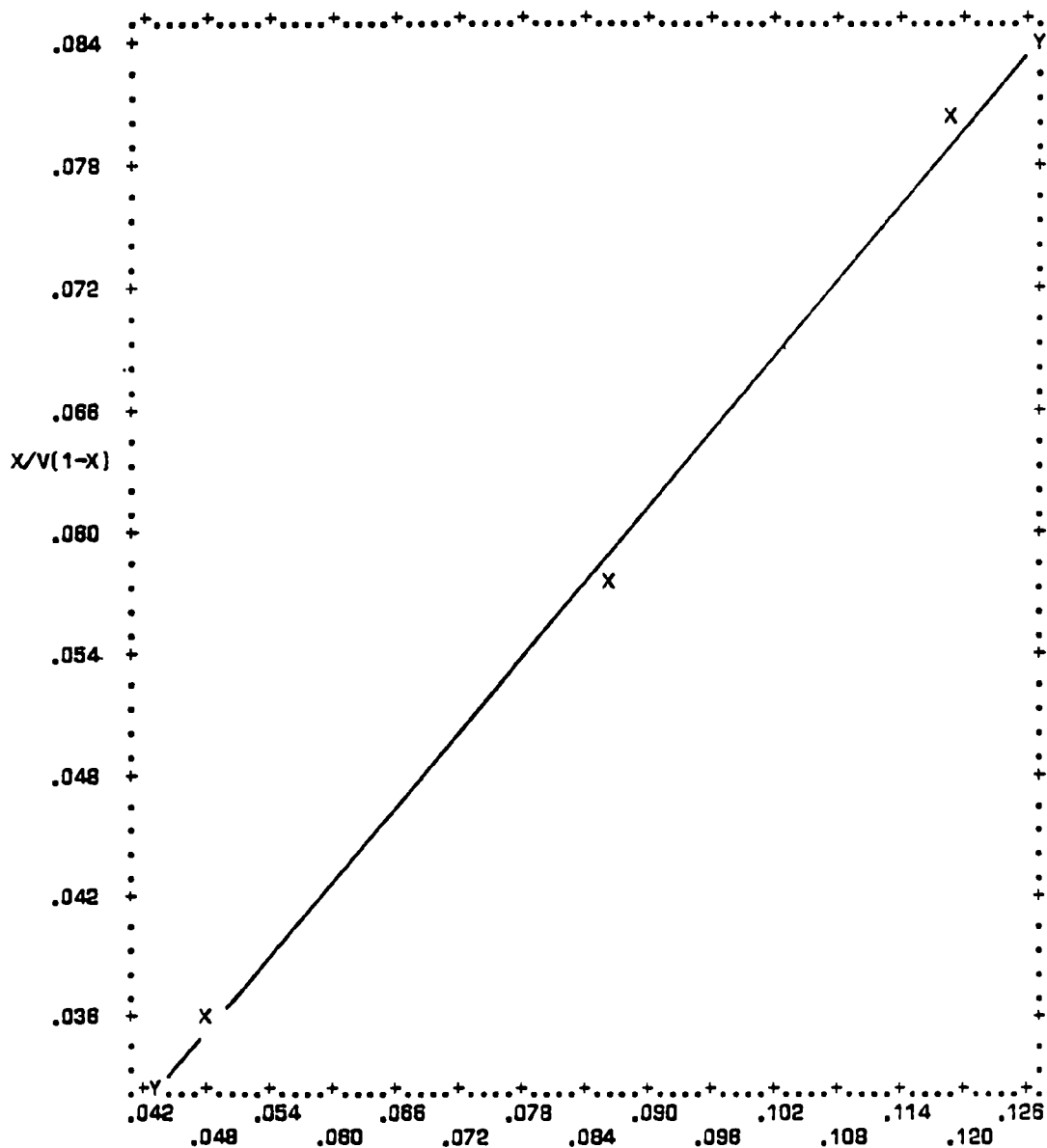
VARIABLE 1 P/PO VERSUS VARIABLE 2 X/V SYMBOL=X

Figure D-3. Plot of BET equation versus relative pressure for Alumina 1.39±0.12



N=	3			
COR=	.9979		P/P0	
	MEAN	ST.DEV.	REGRESSION LINE	RES.MS.
X	.08482	.03514	X= .74584*Y-.01459	105E-7
Y	.13308	.04704	Y= 1.3358*X+.02006	187E-7
VARIABLE	1 P/P0	VERSUS	VARIABLE 2 X/V	SYMBOL=X

Figure D-4. Plot of BET equation versus relative pressure for Alumina 3.04 ± 0.25



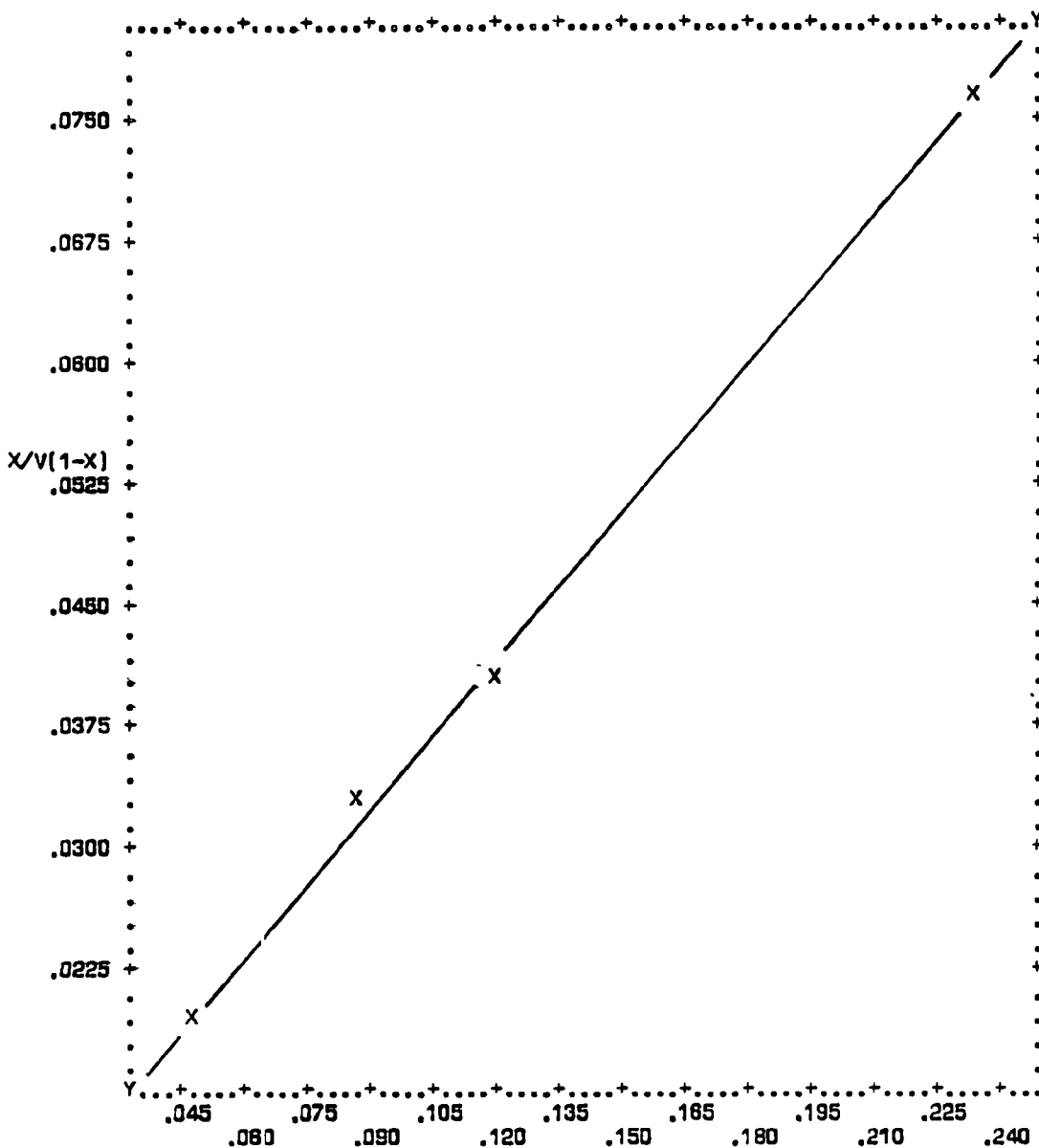
N = 3
COR = .9974

P/P0

	MEAN	ST.DEV.	REGRESSION LINE	RES.MS.
X	.08462	.03514	X = 1.8081*Y - .00884	128E-7
Y	.05811	.02179	Y = .61861*X + .00577	492E-8

VARIABLE 1 P/P0 VERSUS VARIABLE 2 X/V SYMBOL=X

Figure D-5. Plot of BET equation versus relative pressure for Titanium Dioxide 7.05±0.7

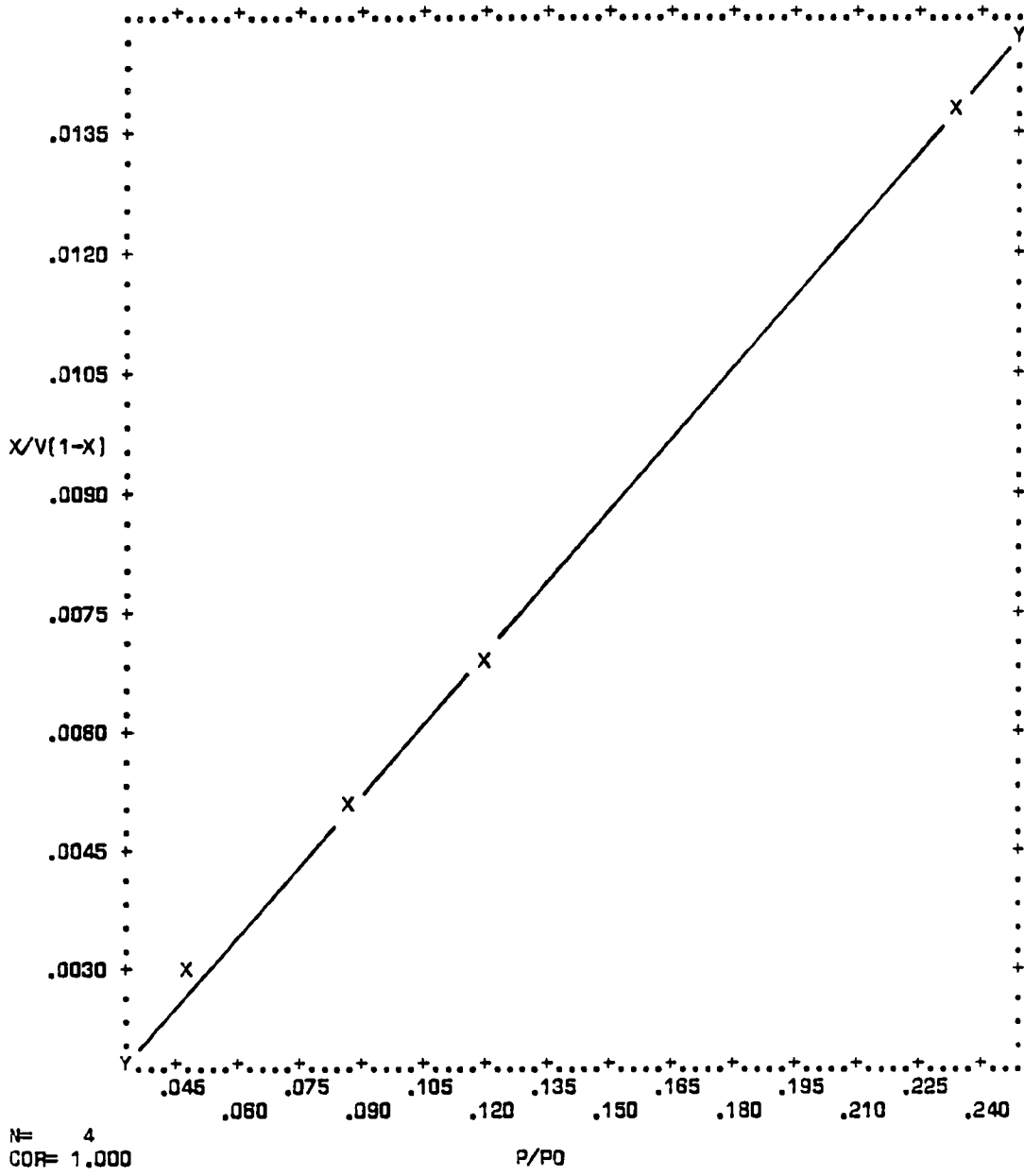


N= 4
 COR= .9994

	MEAN	ST.DEV.	REGRESSION LINE	RES.MS.
X	.12179	.07988	X= 3.2683*Y-.01722	116E-7
Y	.04253	.02437	Y= .30560*X+ .00531	108E-8

VARIABLE 1 P/P0 VERSUS VARIABLE 2 X/V SYMBOL=X

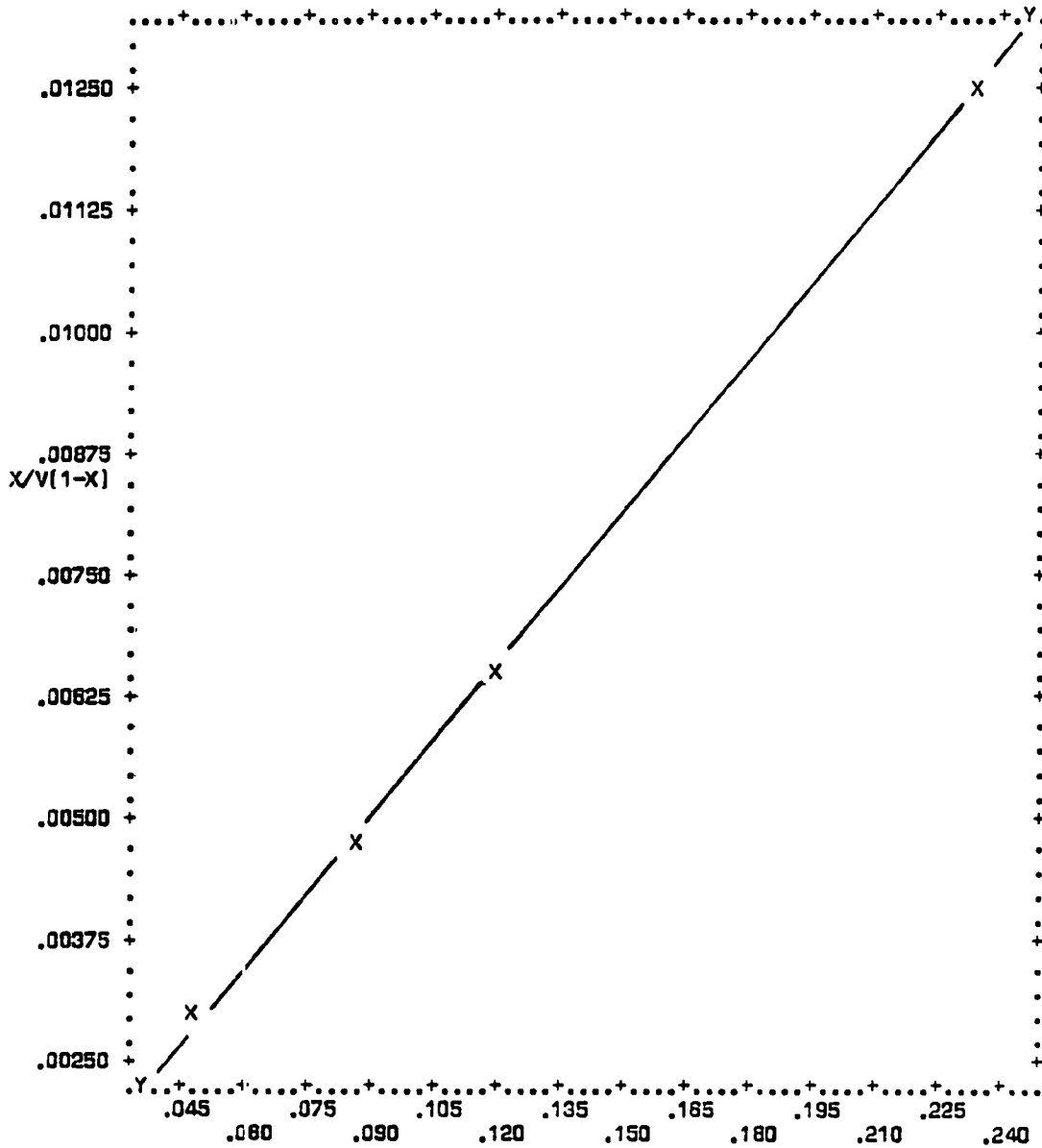
Figure D-6. Plot of BET equation versus relative pressure for Alumina 14.0±0.6



	MEAN	ST.DEV.	REGRESSION LINE	RES.MS.
X	.12178	.07987	X= 16.791*Y+ 509E-6	580E-9
Y	.00722	.00474	Y= .05955*X-299E-7	21E-10

VARIABLE 1 P/PO VERSUS VARIABLE 2 X/V SYMBOL=X

Figure D-7. Plot of BET equation versus relative pressure for Graphitized Carbon Black 71.3 NBS



N= 4
COR= .9989

P/P0

	MEAN	ST.DEV.	REGRESSION LINE	RES.MS.
X	.12177	.07967	X= 19.036*Y-.00819	192E-8
Y	.00872	.00418	Y= .05252*X+ 327E-6	53E-10

VARIABLE 1 P/P0 VERSUS VARIABLE 2 X/V SYMBOL=X

Figure D-8. Plot of BET equation versus relative pressure for Alumina 81.4±6.2

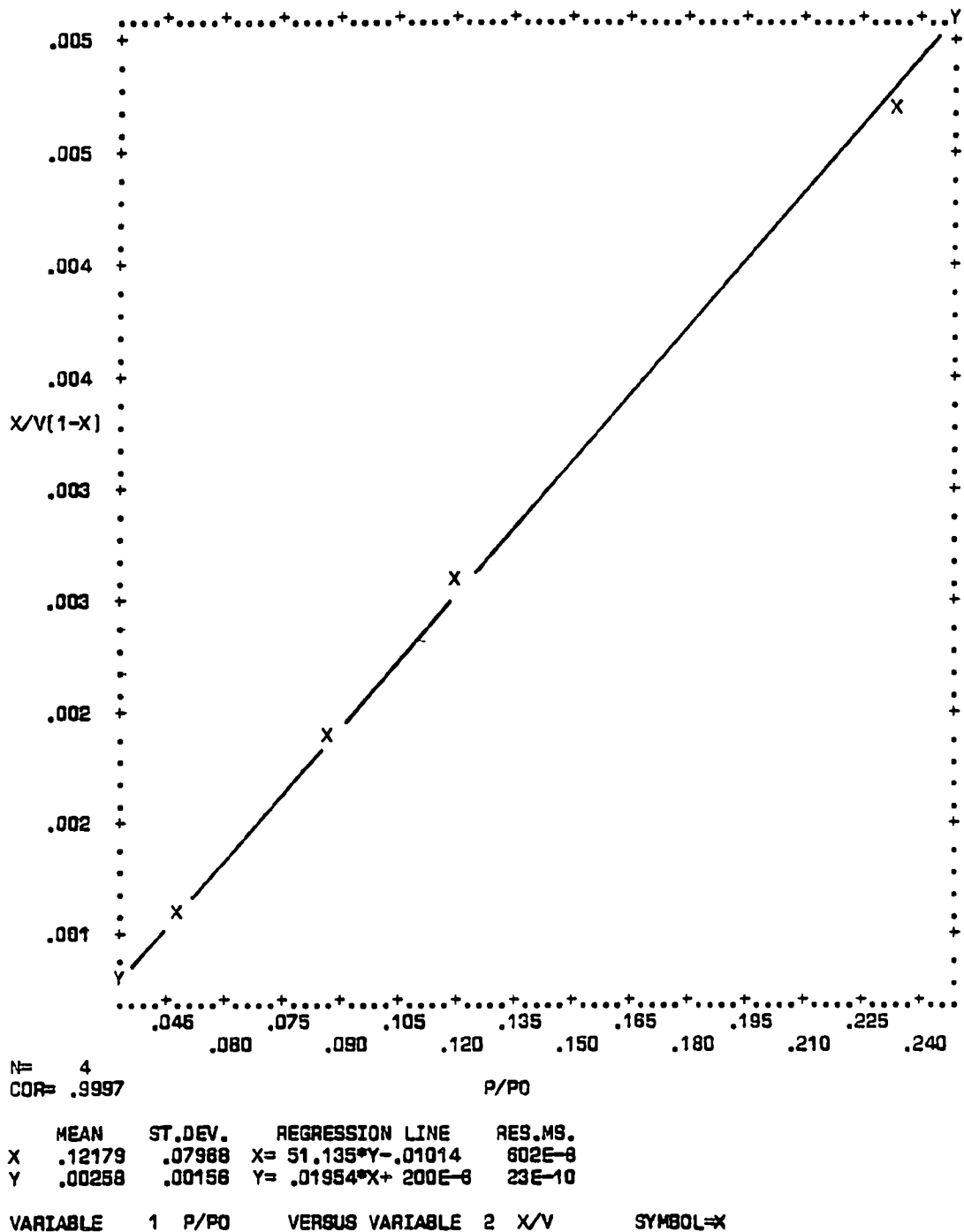
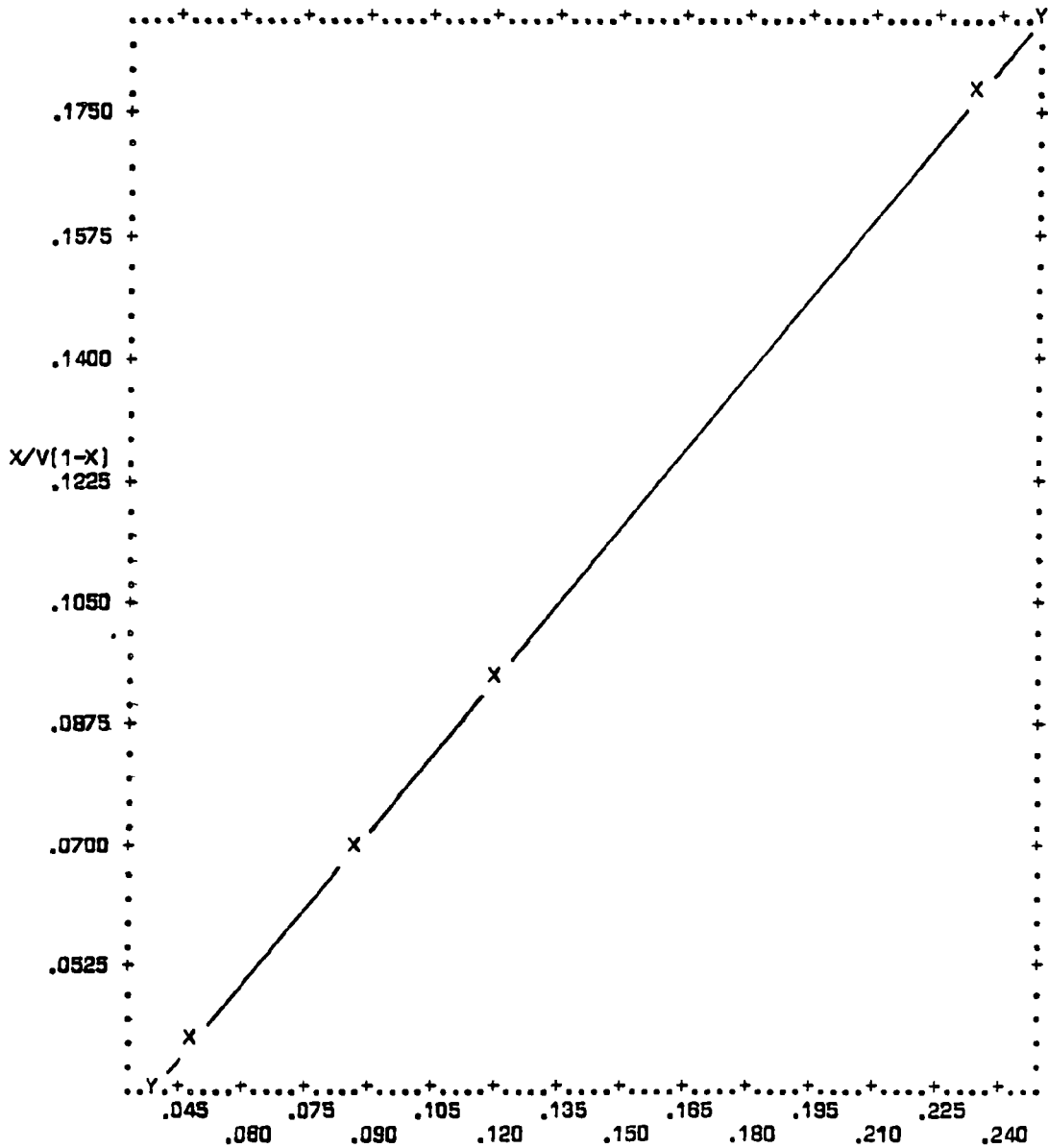


Figure D-9. Plot of BET equation versus relative pressure for Alumina 265±11

APPENDIX E

**BET EQUATION VERSUS RELATIVE PRESSURE
FOR CORRELATION SAMPLES**

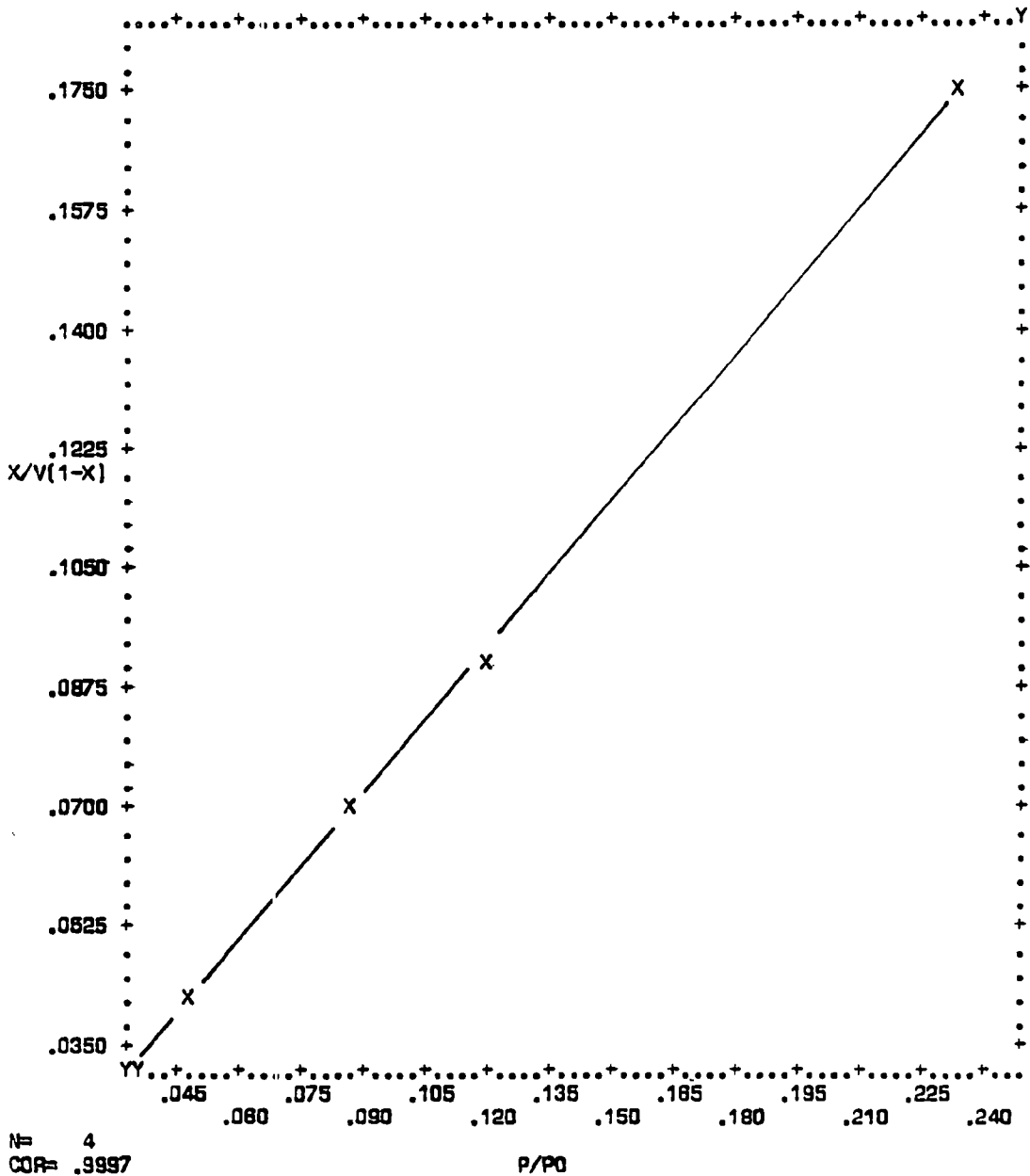


N= 4
COR= 1.000

	MEAN	ST.DEV.	REGRESSION LINE	RES.MS.
X	.12178	.07987	X= 1.3488*Y-.00721	203E-9
Y	.09858	.05902	Y= .74081*X+ .00534	112E-9

VARIABLE 1 P/P0 VERSUS VARIABLE 2 X/V SYMBOL=X

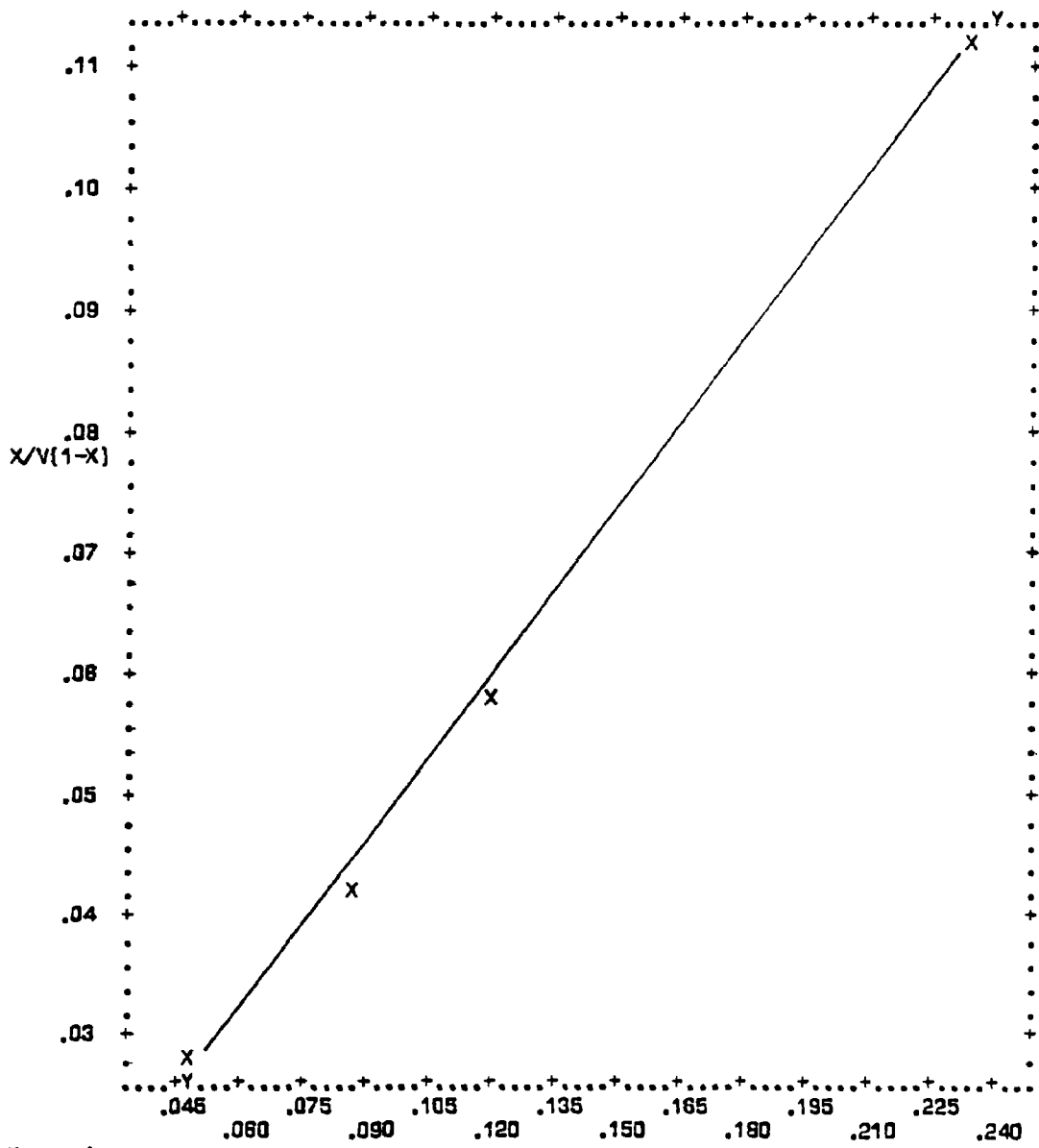
Figure E-1. Plot of BET Equation Versus Relative Pressure for Converter A221/0447-A (Powder Sample)



	MEAN	ST.DEV.	REGRESSION LINE	RES.MS.
X	.12176	.07986	$X = 1.3829*Y - .00833$	588E-8
Y	.09407	.05758	$Y = .72267*X + .00808$	297E-8

VARIABLE 1 P/P0 VERSUS VARIABLE 2 X/V SYMBOL=X

Figure E-2. Plot of BET Equation Versus Relative Pressure for Converter A221/0447-B (Powder Sample)



N= 4
 COR= .9982

	MEAN	ST.DEV.	REGRESSION LINE	RES.MS.
X	.12178	.07987	X= 2.1894*Y-.00790	342E-7
Y	.05978	.03888	Y= .45931*X+ .00384	725E-8

VARIABLE 1 P/P0 VERSUS VARIABLE 2 X/V SYMBOL=X

Figure E-3. Plot of BET Equation Versus Relative Pressure for Converter A220/0810-1-A (Powder Sample)

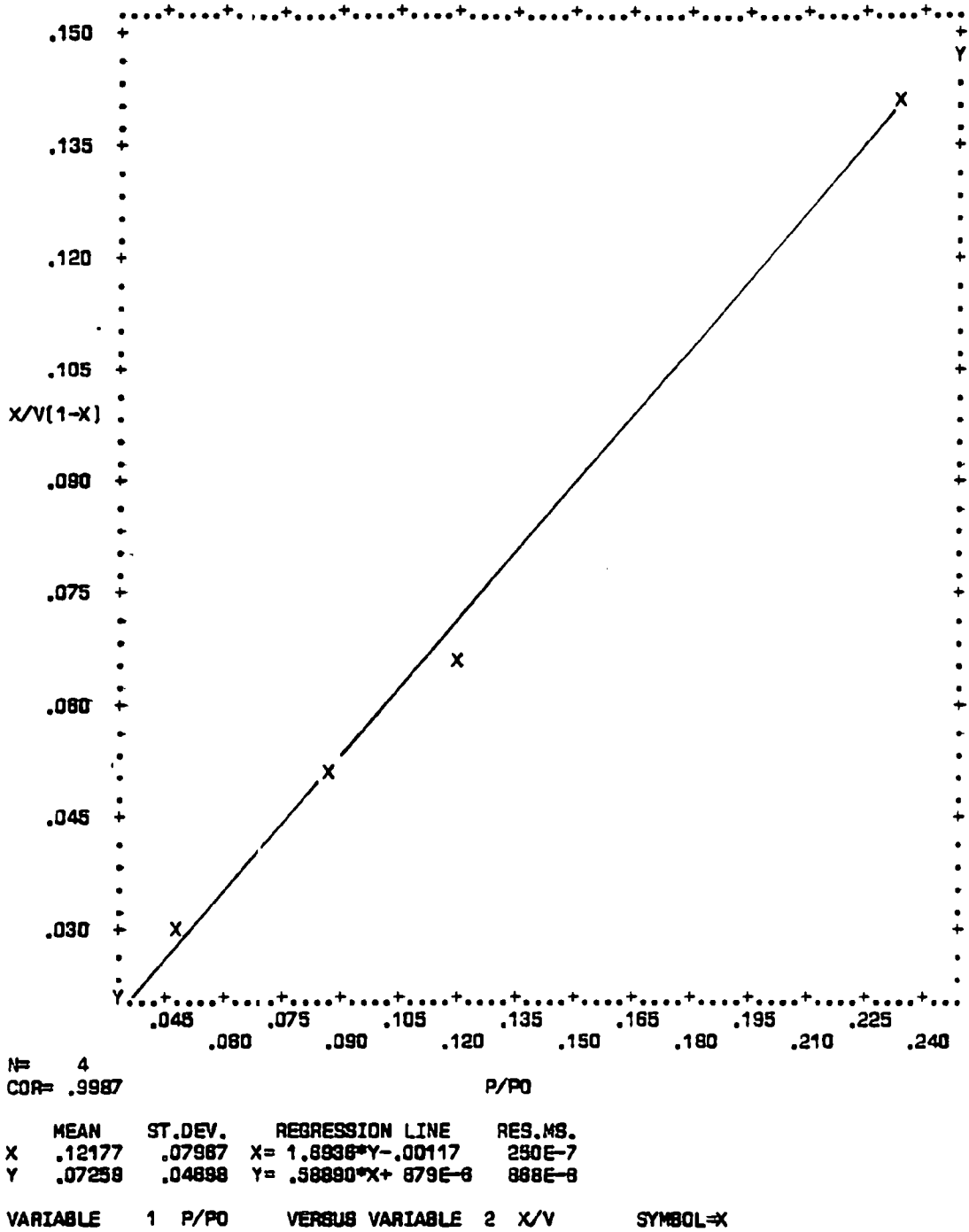
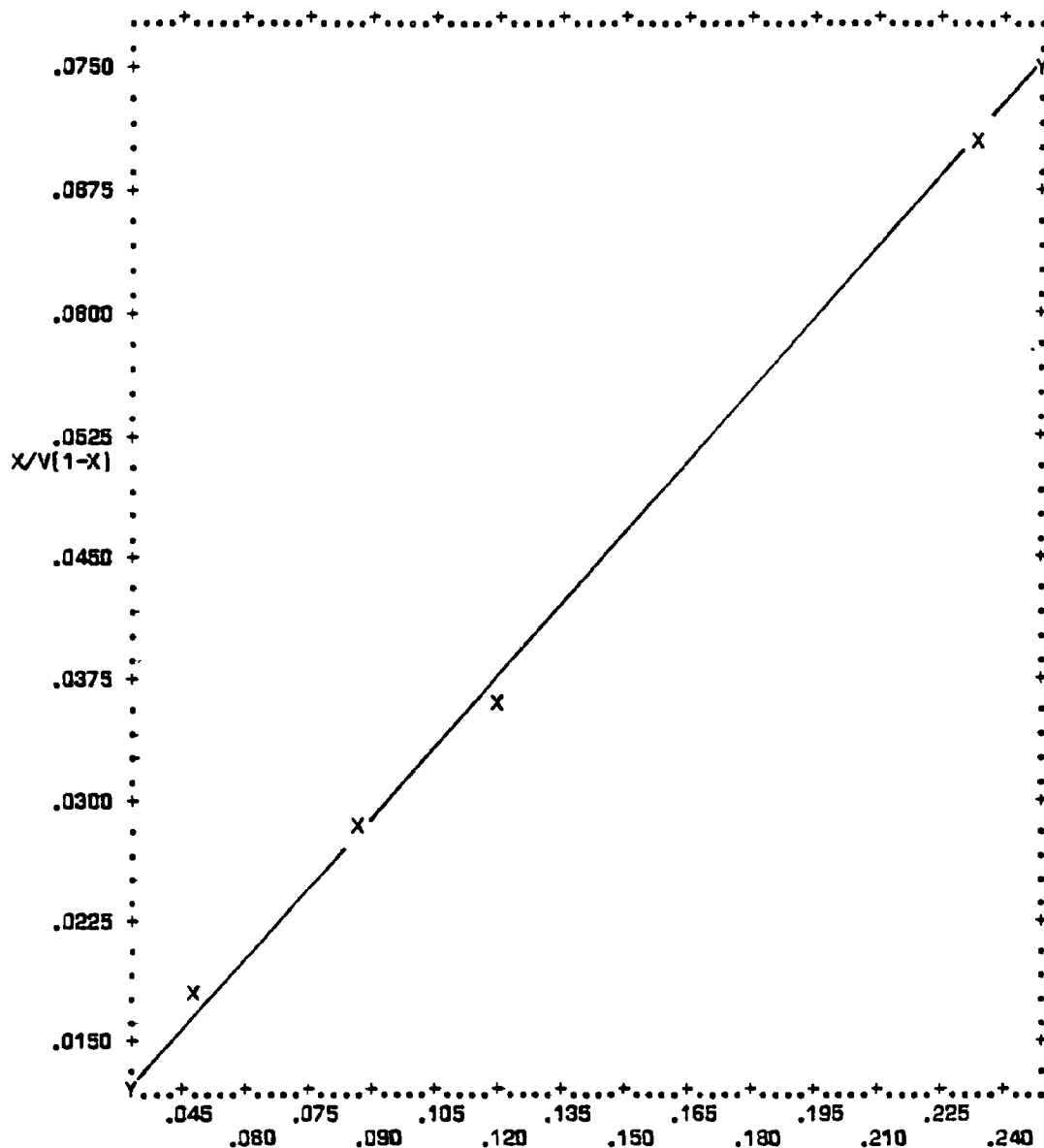


Figure E-4. Plot of BET Equation Versus Relative Pressure for Converter A220/0810-1-B (Powder Sample)

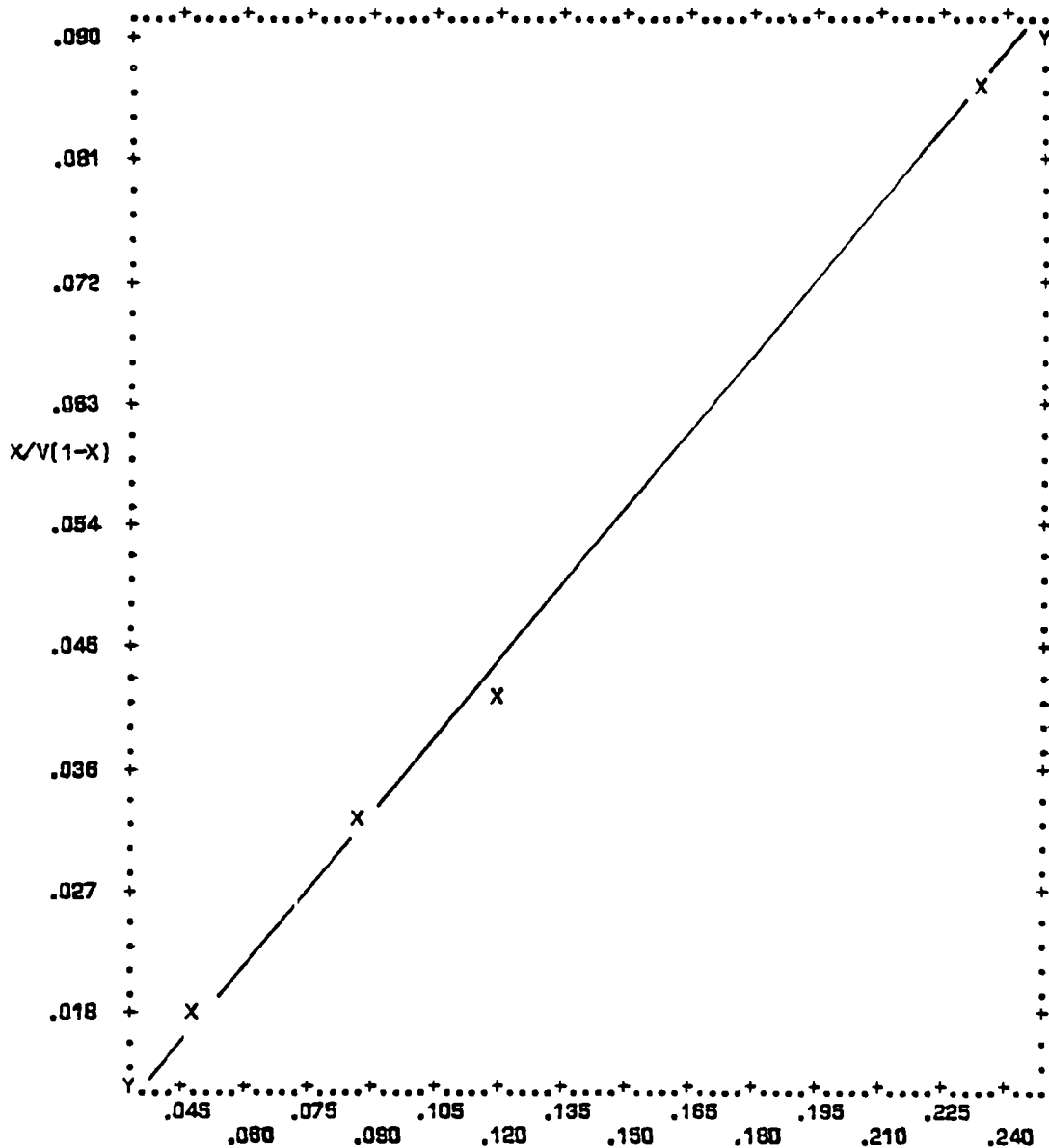


N= 4
 COR= .9995

	MEAN	ST.DEV.	REGRESSION LINE	RES.MS.
X	.12178	.07988	X= 3.4599*Y-.01082	102E-7
Y	.03833	.02302	Y= .28872*X+ .00317	850E-9

VARIABLE 1 P/P0 VERSUS VARIABLE 2 X/V SYMBOL=X

Figure E-5. Plot of BET Equation Versus Relative Pressure for Converter A230/0177X-A (Powder Sample)



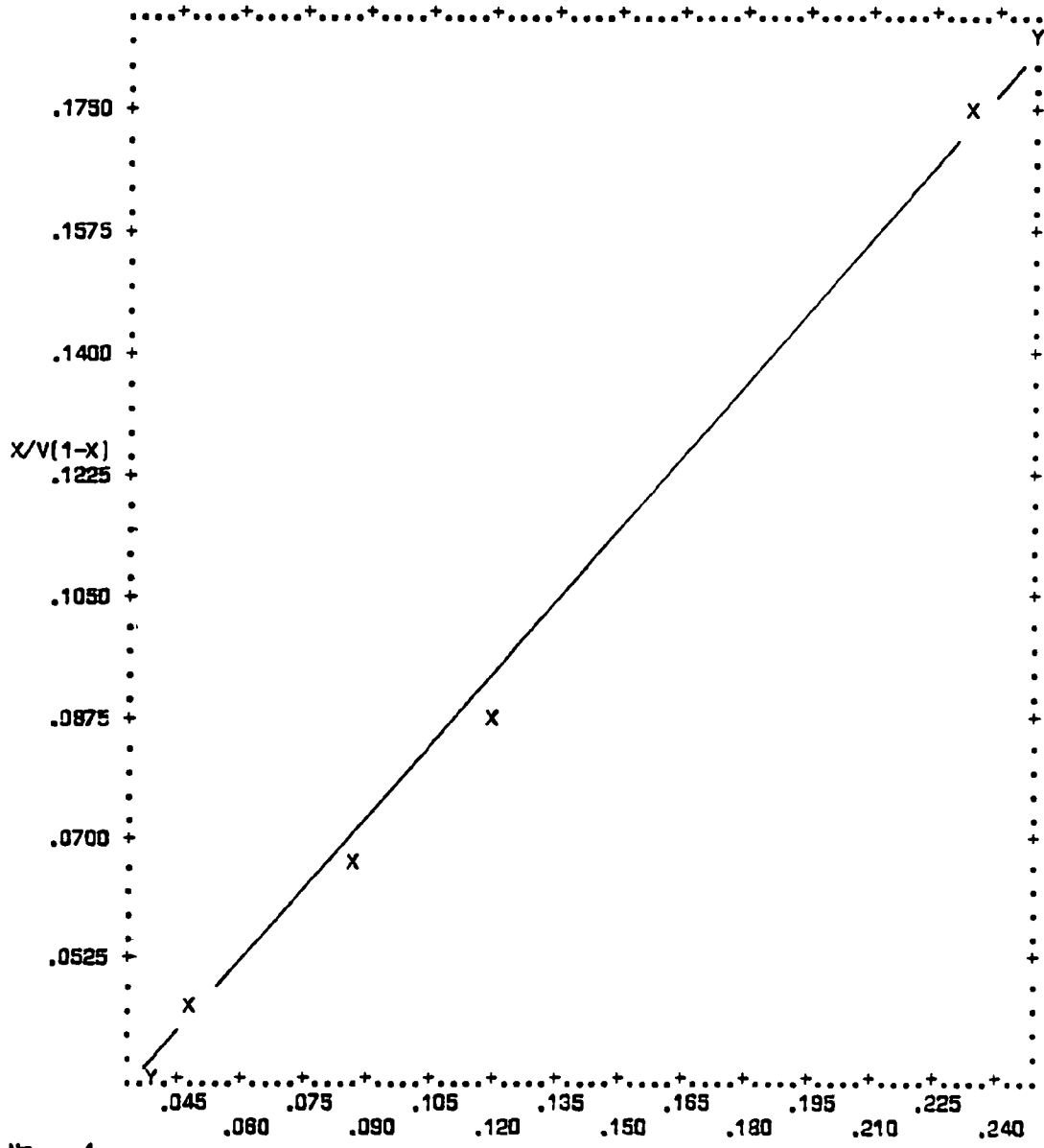
N= 4
COR= .9988

P/P0

	MEAN	ST.DEV.	REGRESSION LINE	RES.MS.
X	.12178	.07967	$X = 2.7572 * Y - .00136$	257E-7
Y	.04488	.02888	$Y = .36171 * X + 813E-8$	337E-8

VARIABLES 1 P/P0 VERSUS VARIABLE 2 X/V SYMBOL=X

Figure E-6. Plot of BET Equation Versus Relative Pressure for Converter A230/0177X-B (Powder Sample)



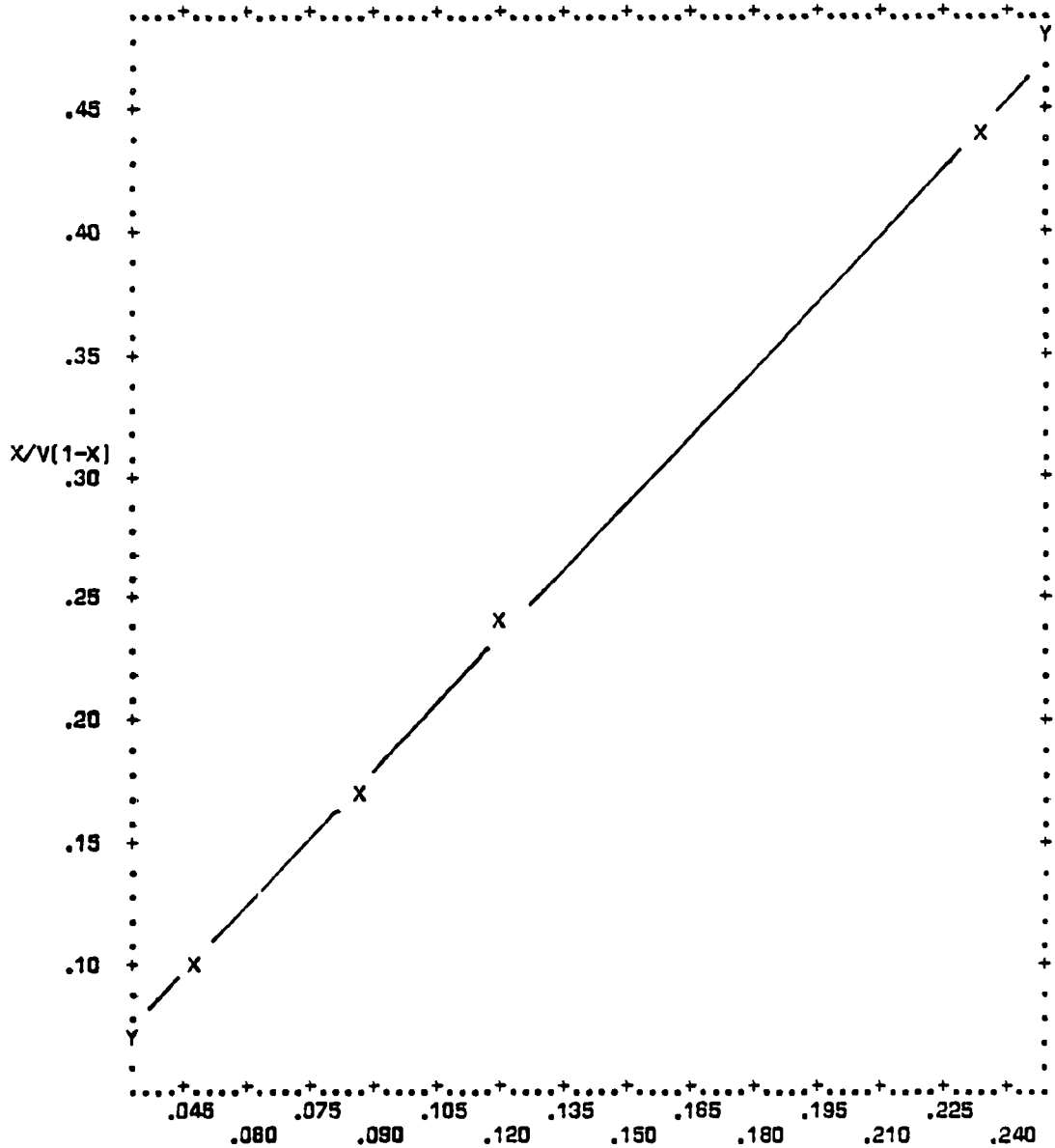
N= 4
COR= .9977

P/P0

	MEAN	ST.DEV.	REGRESSION LINE	RES.MS.
X	.12177	.07967	X= 1.3907*Y-.00860	434E-7
Y	.09367	.05716	Y= .71581*X+ .00691	223E-7

VARIABLE 1 P/P0 VERSUS VARIABLE 2 X/V SYMBOL=X

Figure E-7. Plot of BET Equation Versus Relative Pressure for Converter A155/0941-1-A (Powder Sample)



N= 4
COR= .9998

P/P0

	MEAN	ST.DEV.	REGRESSION LINE	RES.MS.
X	.12179	.07988	$X = .53748*Y - .00838$	372E-8
Y	.23848	.14823	$Y = 1.8598*X + .01198$	129E-7

VARIABLE 1 P/P0 VERSUS VARIABLE 2 X/V SYMBOL=X

Figure E-8. Plot of BET Equation Versus Relative Pressure for Converter A155/0941-2-A (Powder Sample)

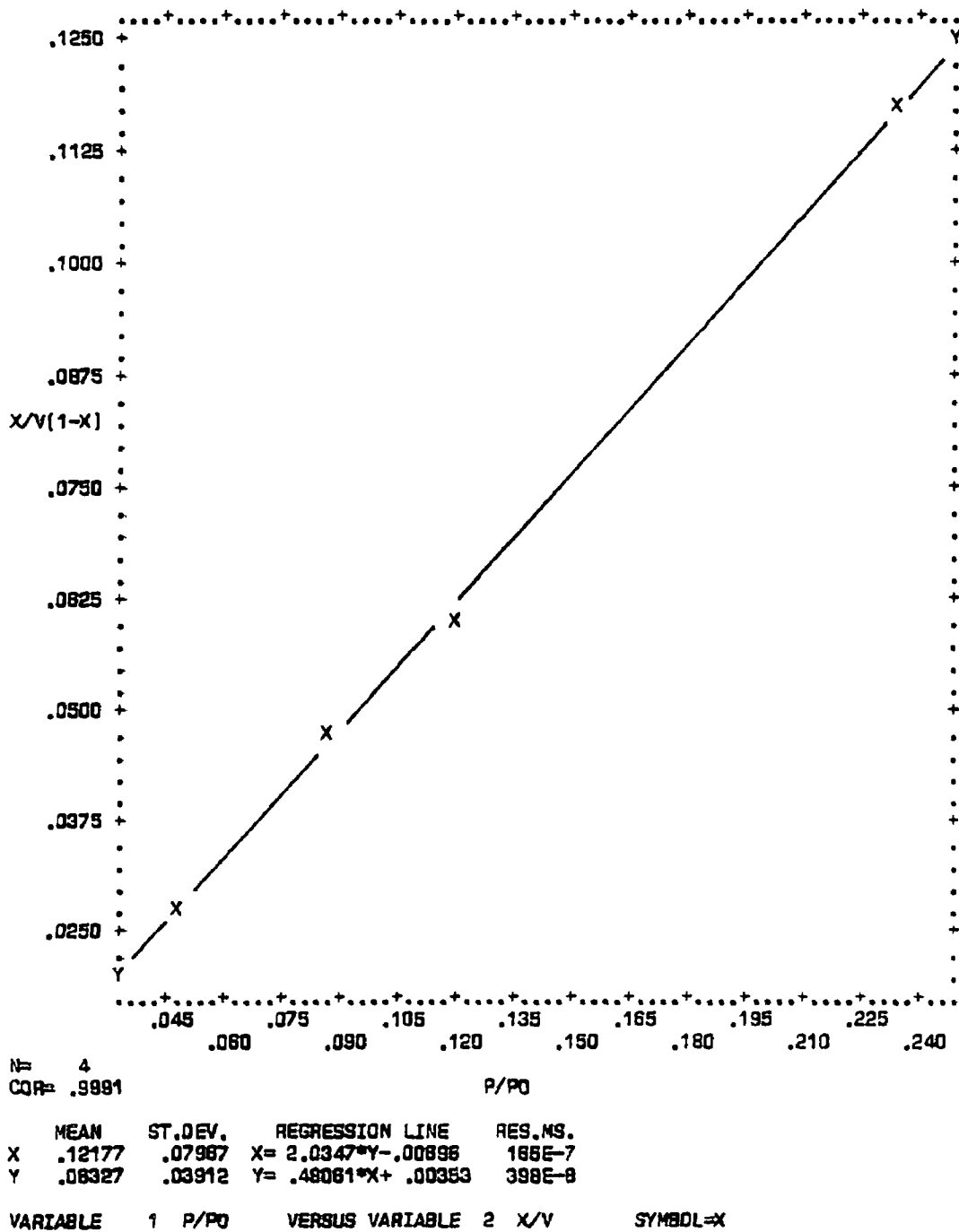


Figure E-9. Plot of BET Equation Versus Relative Pressure for Converter A240/0141L-B (Powder Sample)

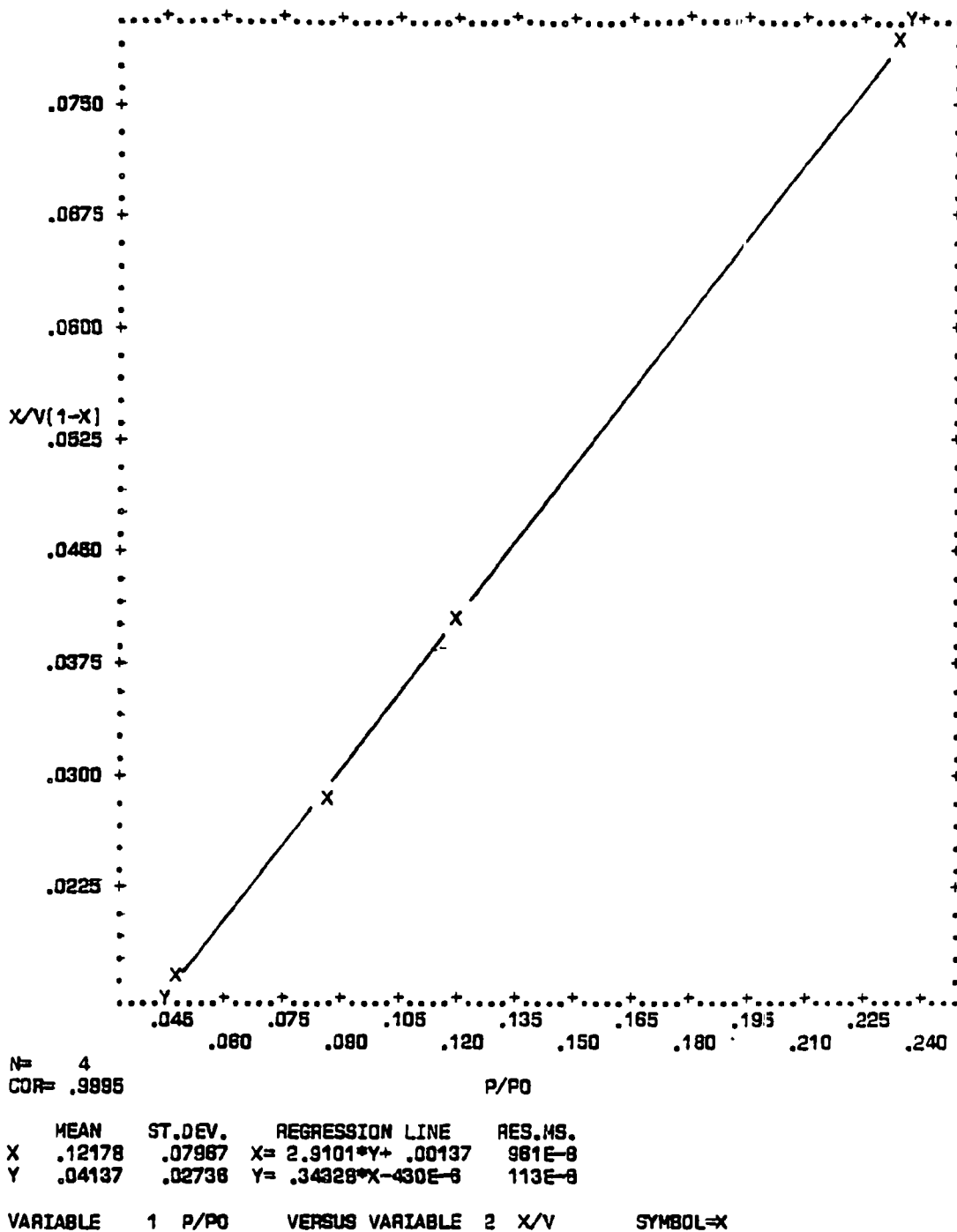


Figure E-10. Plot of BET Equation Versus Relative Pressure for Converter A240/0334L-A (Powder Sample)